Cooperative Research Centre for Coastal Zone, Estuary & Waterway Management

Technical Report 74

Chlorophyll and suspended sediment assessment in a macrotidal tropical estuary adjacent to the Great Barrier Reef

Spatial and temporal assessment using remote sensing

V. Brando
A. Dekker
A. Marks
Y. Qin
k. Oubelkheir

June, 2006

CSIRO

CRC for Coastal Zone
Estuary & Waterway Management

Chlorophyll and suspended sediment assessment in a macrotidal tropical estuary adjacent to the Great Barrier Reef: spatial and temporal assessment using remote sensing

V. Brando, A. Dekker, A. Marks, Y. Qin & K. Oubelkheir

CSIRO Land and Water, Canberra

CRC for Coastal Zone
Estuary & Waterway Management

Chlorophyll and suspended sediment assessment in a macrotidal tropical estuary adjacent to the Great Barrier Reef: Spatial and temporal assessment using remote sensing

Written by:

V. Brando
A. Dekker
A. Marks
Y. Qin
K. Oubelkheir

Published by the Cooperative Research Centre for Coastal Zone, Estuary and Waterway Management (Coastal CRC)

Indooroopilly Sciences Centre
80 Meiers Road
Indooroopilly Qld 4068
Australia

www.coastal.crc.org.au

National Library of Australia Cataloguing-in-Publication data

Chlorophyll and suspended sediment assessment in a macrotidal tropical estuary adjacent to the Great Barrier Reef: Spatial and temporal assessment using remote sensing

QNRM06352

ISBN 1 921017 71 6 (print and online)

Acknowledgments

This project was funded by the Coastal CRC.

We are grateful to Dr Edward King and Dr Matt Paget at CSIRO Marine and Atmospheric Research in Canberra for their support in the distributed processing of the MODIS archive on the CMAR data processing cluster.

Dr Barbara Robson and Dr Ian Webster provided the model maps for comparison with the remote sensing maps and contributed their modelling insight on the possible causes of mismatches between the remote sensing maps and the biogeochemical model outputs.

We acknowledge the Great Barrier Reef Marine Park Authority, CRC Reef Research Centre and the Australian Institute of Marine Science for the provision of the Great Barrier Reef long-term chlorophyll monitoring dataset.

Table of contents

List of figures

List of tables

Executive summary

Introduction

This report presents the results of the Coastal CRC remote sensing project in the Fitzroy River estuary and Keppel Bay carried out in 2004–2006, focussing on daily satellite images (collected by the moderate resolution imaging spectrometer, MODIS). Two years (2003–2004) of daily MODIS satellite data were processed to determine total suspended matter, chlorophyll and dissolved organic matter using unique regional algorithms. These satellite-based map products were then compared with the Fitzroy Estuary–Keppel Bay biogeochemical model outputs of total suspended matter and chlorophyll in order to initiate the process of data-assimilation of remote sensing information and modelling work for the Fitzroy estuary. The aim of this data-assimilation work will be to provide the managers of the Fitzroy system with accurate information as well as a predictive capacity for assessing and managing the environmental state of the estuary as an effect of management actions in the catchment and the river.

The range of total suspended matter and chlorophyll concentrations estimated from remote sensing and predicted from the biogeochemical model were similar, which is a strong indication that these two information sources are accurate.

However, when comparing the spatial distribution of the chlorophyll and total suspended matter from the remote sensing images and from the model, the agreement varied across the year 2004 from almost none to high. This indicates that, most likely, the biogeochemical model (or its underlying hydrodynamic model) needs to be adapted to better represent the distribution of chlorophyll and suspended matter shown in the remote sensing images, as the patterns observed in remote sensing images are real, whereas the model outputs are predictions.

These results are unique for Australia and even internationally this kind of work in a macrotidal tropical estuary has never been published. The outcomes of this project will allow the application of remote sensing of coastal waters in Australia to become increasingly relevant as a contribution to sophisticated estuarine management.

Aim of the project

The original aim of the activity 'Production of single and multi-date total suspended sediment and chlorophyll concentration maps for the Fitzroy estuary' was to provide image maps and error assessment statistics of single and multi-date total suspended sediment (TSM) concentration, chlorophyll (CHL), and coloured dissolved organic matter (CDOM) for the Fitzroy Estuary (FE) and Keppel Bay (KB) using satellite image data from the MODIS sensor. These maps were to be used by the Coastal CRC's Fitzroy Agricultural Contaminants project as input to and validation of models of the loads of sediments, nutrients and other contaminants that move through the Fitzroy estuary and offshore during summer flow events.

The main stages of this activity were intended to include:

- The scoping of model/data fusion requirements
- Assessment of MODIS global algorithms accuracy for the FE–KB
- Implementation of MODIS processing chain (standard algorithms)
- Delivery of preliminary set of TSM, CHL and CDOM maps
- Model/data fusion and quality control/assurance for TSM, CHL and CDOM maps.

However, a result of this research was that the global water quality information products based on global algorithms provided by NASA did not represent actual regional water quality conditions of Fitzroy Estuary–Keppel Bay. The main reason is that the global algorithm presumes chlorophyll is the dominant optically active variable, whereas in the Fitzroy Estuary–Keppel Bay system, suspended matter and coloured dissolved organic matter are the optically dominant variables in the water column. The reliance of the global NASA algorithms on the dominance of chlorophyll for water colour meant there was no simple solution available (such as adapting the NASA global algorithms) for adapting these products. Therefore, effort was redirected into developing new water quality algorithms for MODIS that were robust and applicable to hundreds of images (as typically captured over one year by one satellite sensor such as MODIS) in the Fitzroy Estuary–Keppel Bay aquatic ecosystem. Care was taken to ensure that the algorithms developed could be applied elsewhere in Australian coastal waters into the future. Thus the basis for these new regional algorithms is generic for Australian waters.

Therefore, the main stages of this project became:

- Assessment of MODIS global algorithms accuracy for FE–KB
- Implementation of MODIS processing chain (standard algorithms)
- Development of a new generation of region-specific algorithms for the FE–KB system applicable to large satellite datasets of the MODIS sensors and easily adaptable to other sensors (past, current and future)
- An initial comparison of one year's (2004) worth of outputs from the biogeochemical model with MODIS satellite imagery–derived maps of total suspended matter and chlorophyll.

Main results

Optical complexity of the Fitzroy Estuary–Keppel Bay system

The results of the optical characterisation of the Fitzroy Estuary–Keppel Bay system show that land-derived material originating in the estuary mixes with more typically oceanic material incoming from the northern and eastern sides of Keppel Bay. Changes in the characteristics of the suspended particulate assemblages (mineral, detrital and plankton composition and size) and the dissolved components lead to changes in the optical properties of the system.

The high spatial and temporal variability in optical properties observed in the FE–KB is a critical result for the application of remote sensing algorithms to similar complex coastal systems.

The new regional algorithm for processing MODIS data to chlorophyll and suspended matter using the matrix inversion method

The standard global algorithms provided by NASA for chlorophyll and total suspended matter (and coloured dissolved organic matter) produced through the standard SEADAS processing system are unreliable in complex coastal waters such as the Fitzroy Estuary–Keppel Bay system.

To process MODIS/Aqua images to chlorophyll, total suspended matter and coloured dissolved organic matter, the CSIRO developed and implemented a different type of algorithm that can cope with the significant variability in the optical properties encountered in these waters. This matrix inversion method (MIM) is robust and suitable for processing large numbers (hundreds or thousands) of images.

Remote sensing data from satellites such as MODIS is often from the same time of day; it is susceptible to prevailing cloudiness conditions and is therefore, non-uniformly distributed throughout the year. Satellite images also may have part cloud cover and part visibility, or indeed may have some other errors throughout the scene causing ‘failed ‘ pixels. Nevertheless satellite images are by far the cheapest and most spatially and temporally complete datasets available, when compared against any other measurement method.

Archives of MODIS-like satellite images are available from 1997 onwards from the following satellite sensor systems: from 1997 SeaWiFS, from 1999 onwards MODIS/Terra, and from 2002 onwards both MODIS/Aqua and MERIS. The MIM algorithm can easily be adapted and applied to all these satellite data sets thus giving the climatology of the FE–KB system from 1997 to present. The applicability to multiple sensors is another reason why it was well worth investing so much effort into developing regionally correct algorithms.

Comparing MIM estimates of chlorophyll and suspended matter values and distribution with the biogeochemical model output

The concentration ranges determined from the MODIS/Aqua MIM images and the output of the biogeochemical model are in a high level of agreement. As these two data products are produced independently of each other this is an indication that these two information sources are accurate for concentration assessments, especially as the ranges in the FE–KB system are similar to those measured *in situ*. This could mean a significant shift in the requirements for a monitoring program in the FE–KB system as remote sensing using MODIS or similar sensor data such as SeaWiFS and MERIS for TSM and CHL (and other products such as Secchi disk transparency, turbidity, vertical attenuation of light and coloured dissolved organic matter concentrations) can provide the monitoring data at an unsurpassed temporal and spatial scale.

When the CHL and TSM dynamic in Keppel Bay is dominated by processes occurring at a larger scale, the biogeochemical model (together with its underlying hydrodynamic model) is unable to appropriately recreate the spatial distribution of those processes.

The remote sensing images show how the assumption by the model of low chlorophyll concentration along the coast misrepresents the likely true situation. In some cases there is a significant lobe of chlorophyll-rich water visible in the satellite images, that passes across the top (north) of Curtis Island, travels to the east and then after Curtis Island turns south-east. The model does not show this

pattern although this may be a significant conduit of nutrient-rich waters not returning into Keppel Bay after each tidal cycle. If this is the case, then the nitrogen and phosphorous budget of the FE–KB system to the Great Barrier Reef (GBR) lagoon as calculated by the model will be underestimated.

The biogeochemical model output can be improved (forced/nudged) by the remote sensing–derived information to become more representative of the FE–KB system, in the first instance by improving the boundary conditions or expanding the boundary.

An improved biogeochemical model (with all its output variables) and the 40 (minimum amount) to 100 (maximum current amount) of satellite images per year (with its more limited set of output variables), can in combination give a management-relevant set of water quality indicators for the FE–KB system at a relatively low cost now that both the regional algorithms and the biogeochemical model have been developed.

The satellite images can cover a much larger area than shown here (typically up to 1000 km^2); the biogeochemical model can also become as large as required (although necessarily at a coarser scale). A nested approach of larger scale to finer scale remote sensing and biogeochemical modelling would be appropriate to model and manage much larger parts of the Queensland coast. Such a nested approach would place the FE–KB system into a larger context, required to understand broader-scale issues (such as along-shore, coastal lagoon and even oceanic waters) affecting the FE–KB system. Specifically this research showed that significant amounts of chlorophyll may enter the FE–KB system from the north, whereas in some cases there could be large amounts of export across Curtis Island to the south-east.

Recommendations

The comparison between biogeochemical model outputs and regionally valid satellite images of TSM and chlorophyll is a first step towards data integration of these two sources of information. The next step should be to confirm this preliminary analysis with a more rigorous statistical comparison of the datasets. This will involve the use of advanced geostatistical and temporal statistical methods that can deal with these two very different data sets in their time and space domains. A next step is to incorporate any *in situ* measurements into these two innovative methods. Alternatively the results of these two independent assessment methods can be used to devise an optimum *in situ* sampling program that has a maximum cost–benefit ratio.

The biogeochemical model (together with the underlying hydrodynamic model) has a 24 hour/7days a week/52 weeks a year capacity at almost any desired interval and for many more variables than remote sensing can deliver. However, the concentrations and patterns may not be real or correct. The biogeochemical model has a three-dimensional depth component whereas the remote sensing information is from the top layer of water only, varying from the top 20 cm in the Fitzroy River to the top one or two metres in the estuary to more than five or seven metres deep into the Keppel Bay and GBR waters. Therefore, the biogeochemical model can extrapolate the top layer, remote sensing–based information to the deeper parts of the water column.

It is recommended to expand the comparison of the biogeochemical model output and the satellite image–derived information to all the variables that both methods can determine: not only chlorophyll and TSM but also the optically active CDOM (an inverse tracer of salinity as well as a conservative carbon content component), measurement of cyanobacteria such as *Trichodesmium* and the physically based light variables of turbidity, Secchi disk transparency and the vertical attenuation coefficient of diffuse downwelling light.

It is recommended to begin the process of data assimilation, which is another step of sophistication above data integration. Data assimilation is the process in which the information from remote sensing interacts with the biogeochemical model and vice versa to obtain improved information from both. One example is that the model is forced/nudged/improved to adopt the patterns that remote sensing images demonstrate repeatedly under certain standard conditions. This will lead to better predictions. Another example is to apply boundary conditions from remote sensing to improve the biogeochemical model parameterisation.

The improved biogeochemical model can also improve the remote sensing by understanding what happens under suboptimal remote sensing conditions when large parts of the image are influenced by, for example, bushfire smoke, jet contrails, wind-blown dust, etc. Also, the improved biogeochemical model can aid in establishing where bottom visibility may occur in a remote sensing image (which can then be corrected for this effect). Another example is using the vertical attenuation of light from the satellite images to give a more realistic approximation of the photosynthetically available light in the biogeochemical model.

In the long term, linking quantitative remote sensing and hydrological, biogeochemical and hydrodynamic models for the Fitzroy catchment to estuary through to Keppel Bay would provide the most powerful tool for understanding and managing the entire Fitzroy catchment to Keppel Bay and Great Barrier Reef receiving waters.

1 Introduction

The Fitzroy Estuary and Keppel Bay (FE–KB) system (central Queensland, Eastern Australia) is a macrotidal tropical estuary–coast–open ocean continuum. The Fitzroy River Basin is a large, predominantly agricultural catchment. After the Burdekin River, the Fitzroy River provides the second largest riverine input of sediments and nutrients to the Great Barrier Reef lagoon (Furnas, 2003). Fitzroy River discharge undergoes large variations as a result of seasonal variability in rainfall (Furnas, 2003), usually with its strongest flows through the austral summer, and negligible flows at other times of the year. During the dry season, the FE–KB system is a macrotidally dominated system. Tides range from ~ 1 m (neap tides) to ~ 5 m (spring tides). FE–KB is a shallow system with highly turbid waters in the estuary and clear blue waters offshore in the bay. The large tides cause significant temporal variability at hourly to daily scales.

Prior to the remote sensing research carried out in Phase I (2000–2004) of the Coastal CRC, no quantitative remote sensing of water quality variables had been carried out in the Fitzroy Estuary–Keppel Bay ecosystem. Dekker and Phinn (2005) present the methodology developed and applied to Landsat data for the FE–KB system. Phase I focussed on Landsat imagery as it was useful for both terrestrial and aquatic applications (due to its pixel size of 30 m) and because it was the only source of suitable remote sensing data available before the onset of the ocean colour satellite sensors beginning with SeaWiFS in 1997 and MODIS/Terra in 1999, MODIS/Aqua in 2002 and MERIS in 2002.

However, Landsat has limitations for water quality assessment purposes as its wide spectral bands (leading to coarse colour discrimination) do not allow chlorophyll assessment in coastal waters. Also, the frequency of overpass (once every 16 days) is limited; especially considering that cloud cover often occurs over the FE–KB area. However, quantitative methods (algorithms) were developed for assessing total suspended matter (TSM), and coloured dissolved organic matter (CDOM) as well as Secchi disk transparency for Landsat images spanning the time range of 1988 to 2002, opening the way for retrospective processing of the entire Landsat archive (of over 100 images spanning 1984 to 2004) for this region.

For Phase II, a significant requirement was the availability of chlorophyll (and TSM) images, preferably daily, of the FE–KB system in order to compare these results and, if possible, to integrate these results into the biogeochemical model for the FE–KB system. Thus attention was shifted to the MODIS sensor system

as it has more spectral bands than Landsat (and better positioned spectral bands to assess chlorophyll pigment light absorption), is more sensitive than Landsat, and has daily overpasses for each of the two MODIS sensors (MODIS/Terra since 1999 with an average overpass time at 10:30 and MODIS/Aqua with an average overpass time at 13:30 since 2002).

Remote sensing with sensor systems such as MODIS overcomes the spatial and temporal uncertainties inherent in manual sample collection and, in the longer term, provides cost-effectiveness as much or all of the processing can be automated because the raw satellite image input data is highly standardised.

As more and more coastal and marine water sensors become operational and as their specifications become increasingly sophisticated, it was well worthwhile investing in this area of innovative research as the methodology is generic and can be easily adapted to other sensors.

1.1 About this report

The report is organised as follows:

- Chapter 1 provides a brief general introduction to the Fitzroy Estuary–Keppel Bay (FE–KB) area and to satellite remote sensing, its current status and future, and details the MODIS sensor used in this project.
- Chapter 2 summarises fieldwork undertaken to characterise the optical biogeochemical and ecological processes of the study region—information necessary for validating and redefining algorithms.
- Chapter 3 addresses the issue of poor performance of the standard NASA global MODIS products of chlorophyll and total suspended matter for the FE–KB waters.
- Chapter 4 describes the development of a valid regional MODIS algorithm approach through iterative matrix inversion for the FE–KB study area.
- Chapter 5 applies the developed procedures and products to one year (2003) of MODIS imagery as a demonstration of their utility and shows some time-averaged results for the entire year and for the wet and dry season MODIS images.
- In Chapter 6 we compare the new remote sensing and biogeochemical model products for chlorophyll and total suspended matter on the spatial

and temporal scale. Examples of agreement and disagreement between the two sets of information are described and discussed.

- Chapter 7 concludes by summarising the major findings, discussing the applicability and operational issues of implementing remote sensing as a monitoring tool throughout the GBR. Finally, it evaluates the research work from a number of perspectives.

1.2 Remote sensing for coastal water quality monitoring

1.2.1 Potential

Satellite remote sensing—the collection and interpretation of earth observation imagery from satellites—provides a unique set of capabilities for monitoring the state and trend of the environment. Satellite images are spatially and temporally dense: each pixel, or grain in the image, is a unique measure representing an area of the earth's surface, from a few metres to over one kilometre across, which can be repeatedly measured, as frequently as twice daily.

This capability provides great potential to overcome some of the spatial and temporal uncertainties inherent in monitoring programs that use conventional, manual sample collection techniques. Such monitoring programs can be time-consuming and costly, resulting in sparse spatial and temporal data coverage that often cannot identify the causes of specific events nor ensure a representative coverage of the variability in complex heterogeneous environments like coastal waters.

While routine application of remote sensing monitoring has been implemented in Australian terrestrial (e.g. land-use change and vegetation indices) and clear oceanic environments (e.g. sea surface temperature), its application in optically complex coastal waters has been limited both in Australia and globally. Algorithms are still far from well established for these often turbid waters. In the turbid coastal waters, optical properties depend not only on phytoplankton and its degradation products (phaeophytin) but also on other optically active constituents such as non-algal particulate matter (NAPM, referred to as tripton in this report) and coloured dissolved organic matter (CDOM).

With the introduction in the last few years of high temporal frequency multispectral sensors capable of producing specific coastal water quality products, several large multinational initiatives in Europe and the US are 'operationalising' this satellite image application for monitoring the quality of coastal waters in two ways: firstly by validating and where necessary refining the

algorithms used, and secondly, by developing a variety of multi-date products that meet the needs of coastal managers.

1.2.2 Tropical estuaries applications and user needs

Coastal remote sensing holds great promise for better management and protection of coastal waters by providing a comprehensive monitoring capability that can assist adaptive management of these water ecosystems. One such area of application is the benchmarking of water quality objectives, now a cornerstone of many of the recent catchment and coastal management initiatives being implemented around Australia. The size of Australia's coastline and adjacent coastal waters and the paucity of *in situ* data create an even stronger case for developing operational remote sensing methods.

In Queensland, apart from the research reported here, there are relevant coastal initiatives that are developing the application of remote sensing in coastal waters, these include:

- *Water quality improvement plans* (WQIPs): Under the Coastal Catchment Initiative (CCI) component of the Natural Heritage Trust WQIPs seek to implement adequate and relevant aquatic resource monitoring systems. A key condition for funding under such programs as CCI is the provision of a reasonable assurance that specified concentration and/or load-based targets specified in WQIPs are being achieved. Sediment and nutrient concentrations are recognised as key issues to evaluate in WQIPs. A study was carried out in the Mossman–Daintree area to determine the feasibility of water quality compliance monitoring using MODIS remote sensing images (Stevens *et al.,* submitted).
- *The Great Barrier Reef Water Quality Protection Plan* (Reef Plan): In 2004 the Reef Water Quality Protection Plan was introduced by the Australian and Queensland governments to halt and reverse the decline in water quality of runoff originating from Queensland catchments that may be affecting reef health. Under the Reef Plan a comprehensive reef monitoring program is being implemented. In the near-shore marine monitoring program, MODIS-based measurements of chlorophyll, suspended sediments and the vertical attenuation coefficients of light are seen as a supplementary source for the continuing long-term chlorophyll monitoring program first introduced in 1992. If successful, remote sensing–based near-shore and marine

monitoring may become the prime source of information regarding these three variables.

There are several challenges to be met to achieve operational use of remote sensing–derived products for water quality management purposes. Firstly, if remote sensing–derived information is to be used for environmental management decisions, then definitions of acceptable concentration ranges are needed. Determining such compliance levels is not easy because of the spatial and temporal scales over which ecosystems vary, and because biota do not respond in similar or predictable ways. Many of the criteria developed to date are generic and not applicable to the specific conditions of the GBR lagoon or the FE–KB area with their extremes of episodic river runoff, and/or high resuspension of muds near tidal estuaries adjacent to clear coral reef type oceanic waters. Remote sensing can help address some of these issues as it provides unprecedented insight into spatial distributions and temporal processes.

Another potential remote sensing capacity is to 'alert' or 'capture' incidents such as algal blooms or flood plumes. These applications require fast processing and dissemination of the information products with significant consequences for the underlying information technology infrastructure required.

Defining (or developing) the end-user product requirements for these products, operationalising their delivery and demonstrating the validity and accuracy as well as cost-effectiveness of remote sensing–derived information is required.

Lastly, to date no formal survey of user's requirements for routine remotely sensed water quality monitoring has been conducted in Australia. In a survey of users and their requirements, Phinn *et al.* (2004) found that aerial photography and Landsat Thematic Mapper were the most commonly acquired forms of remotely sensed data and that these are primarily used for habitat mapping rather than water quality assessments. Although monitoring was listed as a concern by many surveyed, little operational monitoring was conducted using remote sensed data. Dissatisfaction with cost and the temporal and spatial resolution of images was expressed by many respondents (a lack of knowledge of the current capabilities as reported here probably led to these assessments by end-users).

Further down the track of operationalisation and implementation, institutional issues of capacity and training of end-users will also need to be addressed.

1.3 Remote sensing: a primer

This section provides background information on the theory of remote sensing applications and technical details of the MODIS sensor and products used in this study. For a comprehensive discussion on all aspects of remote sensing of water quality refer to Dekker *et al.* (2001) and Dekker *et al.* (2005).

1.3.1 Light in water

The colour of natural waters is a complex optical feature, influenced by light scattering and light absorption processes by the water column and of reflectance by the substrate (Figure 1-1). This substrate light reflectance (off seagrass, macro-algae, corals, sand, mud, benthic micro-algae, etc.) is similarly a function of absorption and scattering of light from the substrate materials.

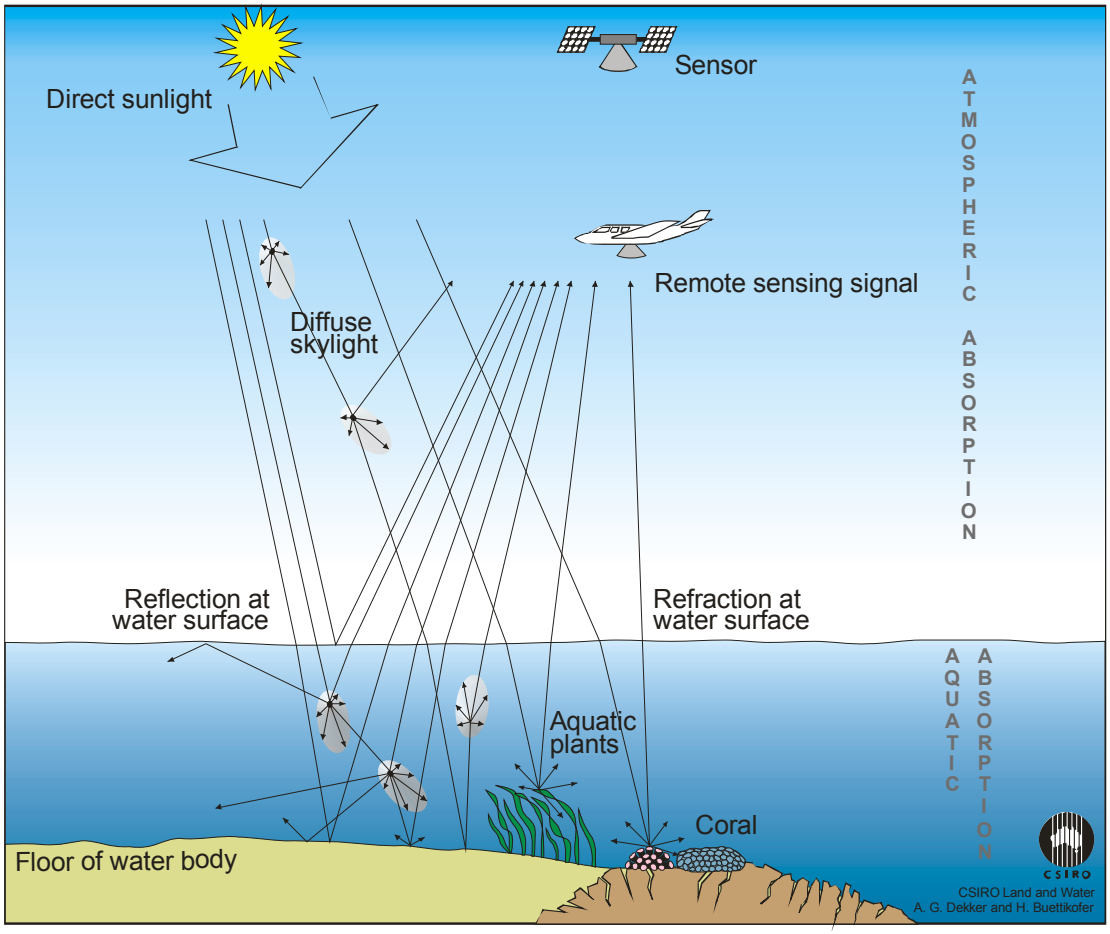

Figure 1-1. Schematic diagram of the various processes that contribute to the signal as measured by a remote sensor in an optically shallow water (left) where the substrate has a significant effect on the water leaving radiance at the water surface or an optically deep water (right) where there is no measurable effect of the substrate on the water leaving radiance. MODIS standard algorithms are designed for optically deep waters

Variations in water colour are determined by the particulate and dissolved substances that absorb and scatter skylight and sunlight that passes through the water surface into the water body. The resultant radiances leaving the water (the colour and intensity) are masked by the direct reflection of sun and skylight at the water surface and by light absorption and scattering processes in the atmosphere. Thus it requires substantial processing of remote sensing data in order to derive valid water quality maps that are corrected for all the unwanted light contributions. An understanding of the radiative transfer in the atmosphere to and through the air–water interface and into the water column is a prerequisite for the testing of existing algorithms as well as for the development of new algorithms for retrieving the concentrations of selected water constituents.

Therefore, the relationship between the optical properties of light absorption and scattering and the concentration of these constituents has to be known for the water column as well as the reflectance properties of the substrate for substrate mapping.

For remote sensing purposes, optically active substances in natural waters can be split into the distinct classes of algal pigments, suspended matter and coloured dissolved organic matter. If the inherent optical properties of these substances are sufficiently well characterised, their contribution to water column colour can be discriminated and their content quantified. For substrates there is currently insufficient information on how the optical properties influence the reflectance of substrate materials; therefore, in practice it is mainly the reflectance of the substrate and not the concentration-dependent absorption and scattering that is determined.

The light exiting the water body is a function of the concentration-specific light absorption and scattering and the actual substance concentrations. Therefore, this water colour contains information about the concentration of these water quality parameters and, if visible at the water surface, the substrate cover. To determine the amounts of different water constituents as well as substrate cover from a remotely sensed signal, a suite of inversion methods are available, ranging from the often used but less precise regression methods through to physics based inverse modelling or inversion methods. These latter approaches are described here as they are more quantitative, reproducible and generic.

Knowing the specific optical properties of the water constituents and of the substrate and modelling the radiative transfer through water and atmosphere as a function of these water constituents enables the simulation of the remotely sensed signal. Once we have accurately simulated the sensor spectra (simulated

spectra as seen by the MODIS satellite sensor) this modelled multispectral sensor signal can be compared with the actual measured multispectral sensor signal, leading to determination of the concentrations of the water constituents and, if visible, the substrate cover.

The range of optical water quality properties measurable in the water column that may be estimated by remote sensing has increased from suspended matter to include properties such as chlorophyll *a*, some cyanobacterial pigments, coloured dissolved organic matter, vertical attenuation coefficients of downwelling and upwelling light, transparency and turbidity. If the water column is sufficiently transparent and the substrate is within the depth where a sufficient amount of light reaches the bottom and is reflected back out of the water body, it has been demonstrated that maps may be made of seagrasses, macro-algae, sand, coral reefs etc. (Dekker *et al.,* 2006).

1.3.2 Measuring and modelling the optical properties of coastal waters

For quantitative assessment of optical water quality variables from remote sensing imagery, it is necessary to describe the relationship between the inherent and apparent optical properties of the water column and the water constituents. The inherent optical properties (IOPs) are the properties of the medium itself regardless of the ambient light field; the IOPs are measured by active (i.e. having their own light source) optical instruments. The radiometric variables are the basic properties of the light that are measured by passive optical instruments (using the sun as the light source). The apparent optical properties are combinations of radiometric variables that can be used as indicators for the colour or transparency of the water—for example, the reflectance or vertical attenuation coefficients.

The water constituents used in this work are chlorophyll, coloured dissolved organic matter and tripton, where tripton is the ‘lifeless‘ or non-algal particulate component of the suspended matter. For the remainder of this report whenever we refer to total suspended matter we are referring to tripton. The reason is that, by necessity, we need to determine both chlorophyll and tripton and coloured dissolved organic matter to fully describe the three components determining the colour of water.

1.3.3 Chlorophyll as an integrative measure of nutrient status

Knowledge of phytoplankton dynamics and distributions in coastal waters is vital to ensure a scientific basis for coherent management of the coastal environment and the human activities which impact on or benefit from it. This section outlines the basis for its application.

1.3.3.1 Phytoplankton

Some 5000 or so different species of phytoplankton exist. They are freely drifting, photosynthesising, microscopic organisms that live in the upper sunlit layers of the ocean. Phytoplankton is the oceanic equivalent of terrestrial plants, forming the basis of virtually all marine food webs. The total phytoplankton biomass outweighs that of all the marine animals (zooplankton, fish, whales, etc.) put together. Phytoplankton productivity is one of the primary forces regulating our planetary climate—for instance via impacts on atmospheric carbon dioxide levels which are closely linked to the oceanic concentrations.

Plankton communities in GBR waters are comprised of oceanic, coastal and benthic taxa. Phytoplankton biomass is overwhelmingly dominated (50% and 80%) by very small phototrophic picoplankton (< 2 µm) such as *Prochlorococcus* and *Synechoccus*. Chlorophytes dominate in oceanic and outer waters, giving way to cyanobacteria in the coastal zone. Coexisting with this ubiquitous community of picoplankters is a diverse but sparse assemblage of oceanic dinoflagellates and coccolithophorids and a cosmopolitan assemblage of diatoms. Table 1-1 provides a summary of the physiological features of some of the phytoplankton species recorded during the field campaigns (see Chapter 2).

Table 1-1. Common phytoplankton species and their physiology

Feature	Cyanobacteria, prochlorophytes and flagellates	Dinoflagellates	Diatoms
Average size (µm)	< 2	2–20	> 20
Doubling time (days)	2–3	1	2–4
Uptake rate	< 0.02	0.05	< 0.05
Diagnostic pigments	Zeaxanthin, Alloxanthin	Peridinin	Fucoxanthin
Common species	*Synechoccus* *Prochlorus*		*Leptocyclindricus* *Cylindrotheca* *Chaetoceros* *Pseudonitzchia*

In low-nutrient ecosystems such as the GBR lagoon, warm water temperatures and abundant light energy support high rates of primary production by phytoplankton and rapid nutrient metabolism and rapid microbial (bacteria, micro-algae, protists) growth occur. The state of water quality is here less determined by static concentrations of suspended sediments, nutrients or pollutants in reef waters than by local or regional dynamic levels of sediment, nutrient or pollutant delivery to affected communities, nutrient uptake and (re-)cycling by phyto- and bacterio-plankton and organic matter production by plankton communities (Furnas, 2003).

1.3.3.2 Chlorophyll as an integrative measure of nutrient status

Chlorophyll is the major photosynthetic pigment found in all phytoplankton species while a number of other accessory pigments (e.g. chlorophylls *a, b, c,* carotenoids and phycobilisomes) are often used diagnostically to differentiate between different classes and genera of phytoplankton (see Table 1-1). Chlorophyll concentration assessment is one of the most frequently employed techniques for assessing phytoplankton standing stock even though pigment composition and concentration may vary depending on phytoplankton species, cell physiology, light intensity, light spectral quality and nutrient availability.

As phytoplankton stocks respond quickly to changes in nutrient availability, measurement of chlorophyll *a* concentration is often considered a proxy indicator of nutrient status. The advantages of monitoring chlorophyll *a* concentrations as compared with nutrient concentrations include:

- *Integration over time*: Phytoplankton assimilate available nutrients over their lifetime, whereas water column inorganic nutrient concentrations are notoriously variable over much shorter time scales.
- *Bio-available nutrients*: Phytoplankton take up only those forms of nutrient that are bio-available. These include organic nitrogen and phosphorus compounds which comprise a major proportion of total nutrient stocks, and are analytically difficult to measure.
- *Sensitivity:* Phytoplankton respond rapidly to pulsed nutrient inputs that might otherwise go undetected by regular nutrient sampling.
- *Ease of collectio*n: Chlorophyll *a* samples require minimal processing and storage in the field and are not easily contaminated.
- *Cost*: Chlorophyll *a* is cheap in comparison to the analysis of a full suite of dissolved nutrients.

- *Detectability:* Remote sensing can detect chlorophyll concentrations but cannot detect nutrient concentrations such as phosphorous and nitrogen directly.

1.3.4 Total suspended sediment, light and Secchi depth

1.3.4.1 Conceptual basis

Several measures of water column or benthos light availability are in use: turbidity (TURB), suspended matter (TSM), vertical light attenuation (K_d) and Secchi disk transparency (SD). They are all interrelated, however, if defined in the optical physics sense. Algal pigments, suspended matter and coloured dissolved organic matter (and the pure seawater component) all scatter and absorb light as a function of their specific absorption and scattering and as a function of their concentrations (note that coloured dissolved organic matter should not scatter light, only absorb it). The resultant effects on the light penetration into the water column and to the substrate are described in the turbidity, vertical light attenuation coefficient (K_d) and Secchi disk transparency. Thus algal pigments, suspended matter and coloured dissolved organic matter (and the pure seawater component) determine the underwater light field. Subsequently turbidity, K_d and Secchi disk transparency are a function of these optically active components.

As discussed at the start of this chapter the two main processes that determine the fate of light in water are the absorption and the scattering of light. The scattering of light needs to be further split into a forward and backward scattering component. It is the backscattered light that is measured by a field spectro-radiometer or by a remote sensor (see Figure 1-1). In these terms we can explain the three descriptors of turbidity, K_d and Secchi disk transparency.

Turbidity is a poorly defined term as it depends on the measurement method used. When measuring how much light passes through a tube, turbidity is a measure of loss of light by absorption and by (back) scattering; when measured by emitting a laser beam and measuring the scattering at an angle, turbidity measures the scattering particles only and does not measure absorption of light. For this reason (i.e. lack of standardisation) and because it is also sometimes used as a proxy for the better defined vertical attenuation coefficient (K_d), we do not advise the use of turbidity.

Vertical attenuation (K_d) is a clear, quantifiable measure of the attenuation of light with depth in a water column due to the combined effects of absorption and

backscattering of light. K_d allows the exact calculation of the amount of light available for photosynthesis, which turbidity does not. If K_d can be measured spectrally it can provide information on the relative contribution of algal pigments, suspended matter and coloured dissolved organic matter to photosynthesis.

Secchi disk transparency is in essence a two-way vertical attenuation reading of light travelling to the disk and then upward again to the observer. As it is human observer-based and therefore susceptible to human error and bias (e.g. eye adaptation to light strength), it is not very accurate. However, Secchi disks are cheap and easy to use and large data sets are available, and it is therefore a handy measure to take (even more so as it is not subject to equipment failure as often as more sophisticated equipment can be).

Total suspended matter is a gravimetric measure of the particle load per volume unit of a size that does not pass through a filter (usually a 0.7 µm glass fibre filter with an effective pore size of 0.45 µm). Suspended matter is composed of algae (pigments and cell material), dead organic matter and mineral matter. These three components interact with light very differently. Algae absorb light through their photo-harvesting pigments, and (much less) through their other cell material; algae also scatter light, mostly in the forward direction (if they are transparent). Some algal species such as coccoliths have a highly scattering cell material. Dead organic matter is usually brown-coloured (and thus absorbs blue to blue-green light effectively) and it scatters light. Mineral matter is usually light-coloured and a strong scatterer.

Suspended matter plays an important role in water quality management since it is related to total primary production of both pelagic and benthic photosynthetic organisms and to fluxes of heavy metals, organic micro-pollutants and other anthropogenic materials. Synoptic information on suspended matter at a regular frequency is difficult to obtain from the routine *in situ* monitoring network since suspended matter is (like chlorophyll) a spatially non-homogeneous parameter. This problem can be circumvented entirely by integrated use of remote sensing data, *in situ* data and biogeochemical and hydrodynamic water quality models.

In general, on the Queensland eastern coast, suspended sediment concentrations show a clear cross-shelf gradient with higher concentration in near-shore water regardless of season or latitude. This clearly reflects the greater influence of wind- and wave-forced sediment resuspension on shallow coastal waters. During floods, massive amounts of suspended sediment (either from land erosion or that were collecting upstream and in the deltas) are released into the GBR lagoon area. Once in the lagoon it will disperse or

settle out. In the case of sedimentation near-shore it will be resuspended often. In general, the coastal waters in the FE–KB region show significant gradients from very high TSM loads inshore to low TSM in clear ocean water kilometres to tens of kilometres offshore. In managing the FE–KB, or indeed the entire GBR lagoon, a crucial issue is to understand the variations in TSM occurring as a function of land use and climate-induced weather patterns. As the TSM is so highly variable remote sensing offers a solution to whole of ecosystem scale monitoring of TSM.

1.3.5 Optical models

There are two modelling approaches to determine the relationship between the inherent and apparent optical properties of the water column and the water constituents: the analytical modelling and the radiative transfer modelling methods.

Radiative transfer numerical models (e.g. Hydrolight: see Mobley, 1994) compute radiance distributions and related quantities (irradiances, reflectances, diffuse attenuation functions, etc.) in the water column as a function of the water constituent light absorption and scattering properties, the sky and air–water interface conditions, and the bottom boundary conditions (i.e. substrate reflectance).

The analytical model is a simplification of the full radiative transfer equations, based on a set of given assumptions. Analytical models have the advantage that, due to their relative simplicity, they can be solved quickly. This is important in a remote sensing application where a model must be evaluated at every pixel of an image. Typically each image may have four million pixels (= 2000 km^2). Two images are obtained each day by the MODIS/Terra and MODIS/Aqua sensors and thus a year's worth of data is typically 365 * 2 * 4 000 000 = approximately three gigabytes of pixel data to process.

An analytical model for water quality retrieval relates the subsurface irradiance reflectance R(0-), to the water constituent concentrations. Several models for coastal and inland waters were investigated as summarised by Dekker *et al.* (2001). They are very similar to an analytical solution of the irradiance transfer equations given by Aas (1997):

$$R(0-) = f\frac{b_b}{a+b_b}, \quad f = \frac{1}{1+\bar{\mu}_d/\bar{\mu}_u} \qquad \text{(Eqn 1-1)}$$

where *a* is the total absorption coefficient, b_b is the total backscattering coefficient; *f* is the anisotropy factor of the downwelling light field (allowing for varying sun angles and sun and skylight relative distributions of incoming light); and $\bar{\mu}_d$ and $\bar{\mu}_u$ are the average cosines of the downwelling and upwelling light field, respectively. All variables in the equation are spectral but the wavelength dependency was omitted for readability. In the general case, the absorption and backscattering coefficients are the sum of the contributions of N constituents and a constant coefficient for pure water:

$$a = a_0 + \sum_{j=1}^{N} a_j^* C_j \; ; \; b_b = b_{b0} + \sum_{j=1}^{N} b_{bj}^* C_j \qquad \text{(Eqn 1-2)}$$

where a_0 and b_{b0} are determined by the absorption and backscattering of pure water, a^*_j and b_{bj}^* are the specific inherent optical properties (SIOPs) of j^{th} constituent with concentration C_j.

In the present study an analytical model for water quality retrieval which relates the subsurface irradiance reflectance to the water constituent concentrations was adopted as described in Equations 1-1 and 1-2. MODIS algorithms are based on normalised water-leaving radiances nLw: these are related to the R values in Equation 1-1, through a simple transformation.

1.3.5.1 Optical measurements

In order to understand the colour of water as measured by a remote sensor it is necessary to identify the contributions of each of the separate components (algae, non-algal particulate matter [tripton] and CDOM) to light absorption, light scattering and light backscattering; the inherent optical properties (IOPs). Of more relevance to algorithms are the concentration-specific inherent optical properties (SIOPs), where the light absorption or scattering of each component is divided by its concentration to arrive at the specific inherent optical property. These SIOPs are concentration-independent and may be used in simulations as it is then possible to multiply the SIOPs by any concentration range to arrive at simulated IOPs which are related to R or nLw (see Equations 1-1 and 1-2). If the SIOPs in a remote sensing image do not vary, one algorithm can be applied to the entire image to retrieve concentrations of optically active substances. This is the essential premise for all global algorithms that the average SIOPs apply all over the world.

As Figures 2-2 and 2-3 and Table 2-1 in the following chapter illustrate, the specific absorptions at the sites show significant variability. This is a first indication that standard algorithms that assume an average SIOP set to be valid will not be accurate in such a highly variable water composition within one MODIS image. Thus new regionally valid algorithms need to be developed to deal with this variability as already proposed in Dekker and Phinn (2005) to deal with a similar variability in SIOPs found previously in Port Curtis and the Fitzroy Estuary.

1.3.5.2 The need for a spectral library related to optical water quality remote sensing in a region

The monitoring method developed for this study required knowledge on the specific inherent optical properties of the FE–KB system. The various fieldworks carried out in this area produced a concentration-independent typology of the measured water masses ranging from Fitzroy River water through mixed estuarine waters to clearer coral reef waters. Unfortunately it was not possible to sample a river flood plume during the study period. Thus our current *in situ* data is biased towards a dry season situation.

Once a representative set of the seasonal and weather event–induced changes in the optical properties (but not concentration differences) is available, no more fieldwork is required in future as our forward inverse bio-optical model can permutate any combination of concentrations that is possible in nature. Thus currently, only if water type conditions occur that were not yet measured (e.g. an extreme Fitzroy River flood plume carrying much eroded sediment directly into Keppel Bay) will our method need an additional fieldwork or sampling.

After the initial investment in obtaining a representative set of specific inherent optical properties, the fieldwork and laboratory analysis cost price of this type of information will therefore drastically reduce as the necessity for fieldwork is eliminated. Computer-based MODIS image processing is the work left to be done. Once this processing is fully parameterised and automated the cost per image will be very low and will have a high benefit-to-cost ratio.

1.4 MODIS features and utility

1.4.1 Sensor capability

MODIS, the moderate resolution imaging spectroradiometer, is a multispectral instrument carried on two polar-orbiting satellites, Terra and Aqua, launched as part of the NASA Earth Observation Sensor (EOS) mission. With a 2330 km-wide viewing swath, MODIS sees every point on the globe at least once every two days in 36 discrete spectral bands, at 1 km resolution or better, simultaneously measuring land, ocean and atmosphere at the same resolution.

The Terra and Aqua formation allows MODIS to provide unprecedented spatial and temporal coverage allowing a complete electromagnetic picture of the globe every two days. MODIS-Terra (MODIS-T) launched in December 1999 provides an equatorial morning overpass at around 10.30 AM, while MODIS-Aqua (MODIS–A) launched in May 2002 provides an afternoon overpass at around 13.30 PM.

Working in tandem to see the same area of the Earth in the morning and the afternoon, the two satellites help to ensure the measurement accuracy of MODIS and other instruments by optimising cloud-free remote sensing and minimising any optical effects, like shadows or glare, that are unique to morning or afternoon sunlight. Having morning and afternoon sensors also permits investigation of changes that occur over the course of the day, such as the build-up or dissipation of clouds and changes in sea temperature or tidal conditions.

1.4.2 Standard MODIS products

The multispectral capacity of MODIS allows for a range of products to be derived. For example, global ocean products include sea surface temperature (SST), concentrations of chlorophyll, pigment, total suspended solids, fluorescence, light absorptions and primary productivity. Atmosphere products include aerosols, atmospheric water vapour, clouds and cloud masks and atmospheric profiles from 20 layers.

Table 1-2 overviews the nomenclature often used in remote sensing to facilitate discussion on the applied level of processing of the sensor data from raw counts at the sensor at the top of the atmosphere, through various levels of corrections to arrive at the desired information of a water quality constituent, a water column depth estimate or a substrate cover type.

Table 1-2. MODIS data levels

Note that the MODIS 500 m resolution data only has four wide spectral bands and the MODIS 250 m data only has two wide spectral bands. Only the 1000 m resolution data has spectral bands suitable for water quality monitoring other than suspended matter and turbidity.

Level of processing	Scale of pixel (size in m or km)	Description of general product
Top of atmosphere at satellite sensor:		
Level 0	250, 500, 1000 m	Raw digital counts at sensor No geocorrection
Level 1A	250, 500, 1000 m	Radiances (calculated from Level 0) at sensor No geocorrection
Level 1B	250, 500, 1000 m	Radiances at sensor geolocated
Atmospheric and water surface effects correction:		
Level 2	1 km	36 ocean and coastal \water products (daytime) and four sea surface temperature products (daytime and night-time)
Level 3	4.63 km 4.89 km or 39 km, or 1 degree global grid	Temporal and spatial binned data of the Level 2 products
Level 4		Global ocean primary productivity products

Typically, processing level indications run from level 0 to level 4, with many sublevels distinguished.

Level 0 to level 1B data are satellite sensor data as measured at the sensor above the atmosphere.

- Level 0 data is a level that only the sensor engineers deal with in general. These are the detector unprocessed values (photon counts) that correspond to the radiance (light) measured.
- Level 1A and especially level 1B data of radiance (or light intensity) are often of interest to remote sensing scientists as this is the core optical data that can be processed into geophysical data by expert science groups. Radiometrically calibrated radiance or reflectance data with associated geolocation information (Level 1B) are the input to retrieve 'higher levels' of information such as chlorophyll concentration or suspended solid concentrations (Level 2 products).

Level 2 data are sensor radiance data corrected for atmospheric effects (thus as if the light was measured at the water surface or just below the water surface level). Level 2 data products are the geophysical values for each pixel derived from level 1B radiance counts by applying the sensor calibration, atmospheric corrections and bio-optical algorithms.

Level 3 products consist of temporal and spatial composites of level 2 products. Level 3 products are the best way to synthesise the large quantities of observations that satellite sensors provide and may thus enhance their usefulness. From a practical point of view they are the only products that can be stored and manipulated by users examining regional scale applications except for situations such as harmful algal bloom monitoring or river flood plume mapping purposes.

Level 4 products are derived from (a combination of) level 2 or 3 products using algorithms to derive properties such as primary productivity in the upper layer of the ocean.

For example the chlorophyll products can occur as both a level 2 and a level 3 product containing ocean chlorophyll *a* pigment concentration for coastal (Case 1) and oceanic (Case 2) waters. The chlorophyll products are produced at level 2 at 1 km resolution, daily, as a composite 8-day mean, as a monthly mean, and at level 3 as a yearly mean at 8 km resolution. Valid data exist only for ocean cloud-free pixels and the 8-day composite will be an average of cloud-free acquisitions for each ocean pixel.

1.4.3 MODIS standard algorithms: NASA and SEADAS

MODIS-based coastal and ocean products may be processed operationally by two methods:

- NASA's MODIS adaptive processing system (MODAPS) for the data acquired from February 2000 to February 2004.
- For data acquired after February 2004 processed from Level 1B to Level 2 using a NASA-provided software package which aligns the processing for SeaWiFS with that for MODIS: the SEADAS package.

Currently SEADAS version 4.9 is the most up-to-date. New releases occur roughly every 6 to 12 months as more and more validation data becomes available to improve the algorithms. In SEADAS the following algorithms are relevant to this study.

1.4.3.1 Global MODIS total suspended matter algorithm

The MODIS total suspended matter algorithm, known as *TSM Clark,* is an exponential algorithm based on taking the logarithm of the dark blue band (nLw_1) plus the second blue band (nLw_2) divided by the green band (nLw_4) with fitted coefficients a_i. This algorithm compensates (to a degree) for CDOM and CHL variations in these bands, but not sufficiently for terrestrial-derived fluvial or coastal resuspended non-algal suspended matter.

$$TSM = 10^{\sum_{i=0}^{5} a_i x^i}$$

Where $x = \log(nLw_1 + nLw_2 / nLw_4)$

and a_i = {0.490330, -2.712882, 3.412666, -8.336478, 12.111023, -5.961926}.

1.4.3.2 Global MODIS chlorophyll algorithms

Several algorithms were developed by various groups in the USA prior to MODIS being launched. These algorithms were implemented and subsequently updated as experience with the results increased. Table 1-3 published by Blondeau-Patissier *et al.* (2004), details the nomenclature of the various MODIS chlorophyll algorithms that can be produced using the SEADAS processing package. We have tested these algorithms on real MODIS data for FE–KB (a few match-up points between *in situ* and MODIS data) and on simulated data for FE–KB waters (allowing us to analyse the general behaviour of these algorithms).

Table 1-3. Global MODIS chlorophyll estimation algorithms

MODAPS parameter name	MODIS-MODAPS ATBD and parameter number	SEADAS product name	Algorithm principle	Ocean water	Clear coastal water	Comments
**		Chl_OC4v4	Empirical ratios	Y	Y	
Chlor_MODIS	MOD-19 Param. 14	Chl_Clark	Empirical ratios	Y	N	Not suitable for coastal
Chlor_a_2	MOD-21 Param. 26	Chl_OC3	Empirical Ratios	Y	Y	Overestimation of CHL in coastal waters
Chlor_a_3	MOD-21 Param.27	Chl_Carder	Semi-analytical	N	Y	Needs adapting to each specific SIOP domain: Best at CHL< 2µg L^{-1}

** SeaWiFS OC4-v4 is not produced by MODAPS but is available in SEADAS and may thus be applied to MODIS data (CHL=chlorophyll).

1.4.4 Delivery of MODIS data

NASA provides operational processing of the daily coverage of the MODIS data to different levels of calibration (correction and aggregation). The Global Environmental Services Data Administration and Archiving Center (GES-DAAC) is responsible for the distribution of the level 1 data, and the higher levels of all ocean and atmosphere products (and products are distributed through the Land Processes (LP) DAAC, and the snow and ice products are distributed though the National Snow and Ice Data Center (NSIDC) DAAC).

While most MODIS data products are archived and distributed in the Hierarchical Data Format–Earth Observing System (HDF—EOS 2.7) format, the ocean binned (averaged in time) products and primary productivity products (level 4) are in the native HDF4 format. MODIS level 1 and level 2 data are of the HDF–EOS swath type and are packaged in files representing five minutes of MODIS viewing (scenes of approximately 2000 by 2330 km). Files for levels 3 and 4 are global products at daily, weekly, monthly or yearly resolutions. Apart from the ocean binned and level 4 products, these are in HDF-EOS grid type, and the maps are in the cylindrical equidistant projection with a rectangular grid.

1.4.4.1 Remote Sensing of chlorophyll

Satellite remote sensing measurements of chlorophyll concentrations rely on the absorption and scattering characteristics of phytoplankton and the way these optical properties affect the underwater light field and the reflectance (R_{rs}) or radiance (nLw) values measured by the satellite sensor. Information on chlorophyll concentration is obtained by using appropriate algorithms that relate measurements of remote sensing reflectance spectra either directly to chlorophyll concentration (empirical algorithms), or to optical properties of phytoplankton and other optically active materials in the water (semi-analytical algorithms, based on radiative transfer and theoretical relationships).

Satellite estimations of surface concentration of chlorophyll *a* and associated pigments have contributed significantly in gaining a better understanding of the temporal and spatial variations of phytoplankton biomass and biological activity in the world's oceans and the role of phytoplankton in the climate system.

1.4.4.2 Remote sensing of TSM, turbidity, Kd and Secchi disk transparency

The three variable components that determine the colour of water are CDOM, algal pigments (usually expressed as chlorophyll concentration) and total suspended matter (TSM). TSM can be determined empirically with remote sensing by determining a relationship between scattering in the green, red or nearby infrared and the TSM concentration. The MODIS TSM algorithm by Clark is less straightforward as it has a lot of normalisations in the equation, making it robust for ocean conditions but less applicable to coastal waters.

The other three measures (turbidity, Kd and Secchi disk transparency) are a function of the combined effects of CDOM, chlorophyll (and associated pigments) and TSM. Empirical algorithms can be developed but they will be site-specific and circumstance-specific.

Improved algorithm approaches are discussed In the recommendations in Chapter 7.

2 Optical characterisation and water quality in the Fitzroy Estuary–Keppel Bay region

2.1 Study area and fieldwork description

The Fitzroy Estuary and Keppel Bay (FE–KB) system (central Queensland, Eastern Australia) is a macrotidal tropical estuary–coast–open ocean continuum. The Fitzroy River basin is a large, predominantly agricultural catchment. After the Burdekin River, the Fitzroy River provides the second-largest riverine input of sediments and nutrients to the Great Barrier Reef lagoon (Furnas, 2003). Fitzroy River discharge undergoes large variations as a result of seasonal variability in rainfall (Furnas, 2003), usually with its strongest flows through the austral summer, and negligible flows at other times of the year. During the dry season, the FE–KB system is a macrotidally dominated system. Tides range from ~ 1 m (neap tides) to ~ 5 m (spring tides). FE–KB is a shallow system with highly turbid waters in the estuary and clear blue waters offshore in the bay. The large tides cause significant temporal variability.

The main questions we address here are: (i) to what extent does the variability in particle assemblage characteristics shape the inherent optical properties in the near-surface layer over various spatial and temporal scales and, inversely, (ii) how can these optical properties measured by *in situ* profiling devices with a high spatial and temporal resolution be used to describe the distribution of biogeochemical properties (concentration, composition and size).

2.1.1 Sampling

To validate and parameterise a new regional MODIS algorithm over a range of water quality and optical water properties, field sampling was undertaken twice during the dry season. These two cruises follow and augment the database of optical properties of the FE–KB already sampled twice in January and June 2002 (Dekker & Phinn, 2005).

Optical and biogeochemical properties of the FE–KB system were sampled twice during the dry season: first, during an 8-day cruise on 5–12 September 2003 and second, during a 4-day cruise on 15–18 August 2004. During both cruises, discrete samples were collected for analysis together with *in situ* continuous optical measurements.

While the 2003 survey aimed to describe the spatial variability in optical and biogeochemical properties throughout the study region, the 2004 survey examined the effect of tidal phase on these properties at three fixed sites (A, B and C) repeatedly sampled over a 12–24 hours cycle during the spring tides (Figure 2-1). Discharge from the Fitzroy River was insignificant during both surveys and for several months preceding them. At each of these sites, water quality and optical measurements were made throughout the water column. When possible, sampling was conducted to coincide with the MODIS overpasses.

In situ optical measurements of spectral absorption, scattering and backscattering coefficients—hyperspectral radiance and irradiance—were made with instrumentation described in detail in Oubelkheir *et al.* (2006).

Discrete water samples were taken in surface and bottom water at each site for later laboratory analysis of the discrete optical and biogeochemical parameters described in Section 2.2. Oubelkheir *et al.* (2006) and Radke *et al.* (2006) summarise the purpose of these measurements and give a brief description of the methods used.

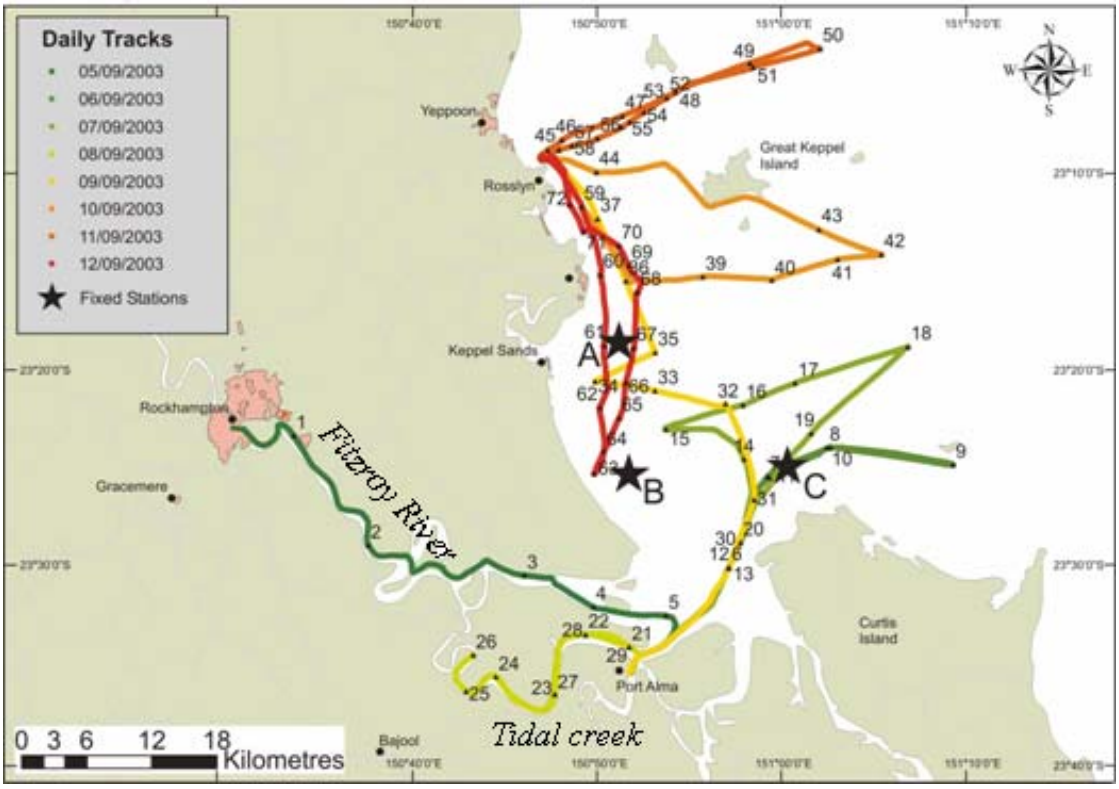

Figure 2-1. GIS map of the daily tracks and station locations during the first dry season survey of Fitzroy Estuary–Keppel Bay (5–12 September 2003), and of the three fixed sites (A, B and C) continuously sampled for more than 12 hours during the second dry season survey (15–18 August 2004).

2.2 Optical characterisation required for algorithm assessment

2.2.1 Spatial variability (September 2003)

Total suspended matter (TSM) concentrations varied in the near-surface layer over three orders of magnitude, ranging from 27.3 to 199.0 g m^{-3} in the estuary (at stations 1 and 3, respectively), 4.8 g m^{-3} in the transition zone (at station 15, between the turbid waters in the estuary and the blue waters offshore) and 0.3 g m^{-3} offshore (station 42) (Figure 2-1, Table 2-1; note that Table 2-1 presents the overall ranges measured).

Chlorophyll concentrations varied over nearly two orders of magnitude (Table 2-1) and ranged between 1.5 and 7.3 mg m^{-3} in the estuary (stations 5 and 1, respectively), and 0.15 and 1.7 mg m^{-3} in the bay (stations 18 and 50, respectively). These last values were low relative to chlorophyll concentrations (~ 15 mg m^{-3}) measured in the bay just after a large flood event in 1991 (Brodie & Mitchell, 1992).

The taxonomic composition of phytoplankton was highly variable from the estuary to the bay, as shown by the spatial distribution of the proportion of pico-, nano- and micro-phytoplankton estimated from pigment concentrations (Figure 2-2). Nano-phytoplankton represented the smallest proportion of the phytoplankton assemblage (~ 5–20%), while micro- and pico-phytoplankton exhibited reverse trends, with micro-phytoplankton dominating in the estuary.

Micro-phytoplankton corresponded mainly to diatoms at all stations in the estuary, except at station 1 where dinoflagellates were present in equal proportions to diatoms as derived from taxonomic pigments) (e.g. Jeffrey *et al.,* 1997). In the transition zone, a shift in phytoplankton composition was observed, with nearly equivalent proportions of micro- and pico-phytoplankton.

Table 2-1. Range of variability of biogeochemical and optical quantities over the Fitzroy Estuary–Keppel Bay system during the dry season extensive spatial sampling period (September 2003) (See Figure 2-3 for explanation of light absorption values; $b^p(555)$ is the particulate matter light scattering coefficient, $b^{bp}(555)$ is the particulate matter light backscattering coefficient and b^{bp}/b^p is the proportion of backscattered light to totally scattered light)

Parameter	Range of variability	Area, station number
TSM (g m^{-3})	0.3 – 326.2	Offshore, station 42; Casuarina Creek, station 25
TChl *a* (mg m^{-3})	0.15 – 7.28	Offshore, station 18; Estuary, station 1
$a_g(440)$ (m^{-1})	0.006 – 0.471	Offshore, station 42; Estuary, station 2
$a_\varphi(440)$ (m^{-1})	0.008 – 0.076	Western shore, station 60; Offshore, station 50
$a_{nap}(440)$ (m^{-1})	0.005 – 7.206	Offshore, station 18; Casuarina Creek, station 22
$b_p(555)$ (m^{-1})	0.298 – > 20	Offshore, station 42; some areas in the estuary and Casuarina Creek
$b_{bp}(555)$ (m^{-1})	0.002 – 2.806	Offshore, station 50; Estuary, station 5
$b_{bp}/b_p(555)$ (%)	0.006 – 0.034	Offshore, station 18; Transition zone, station 30

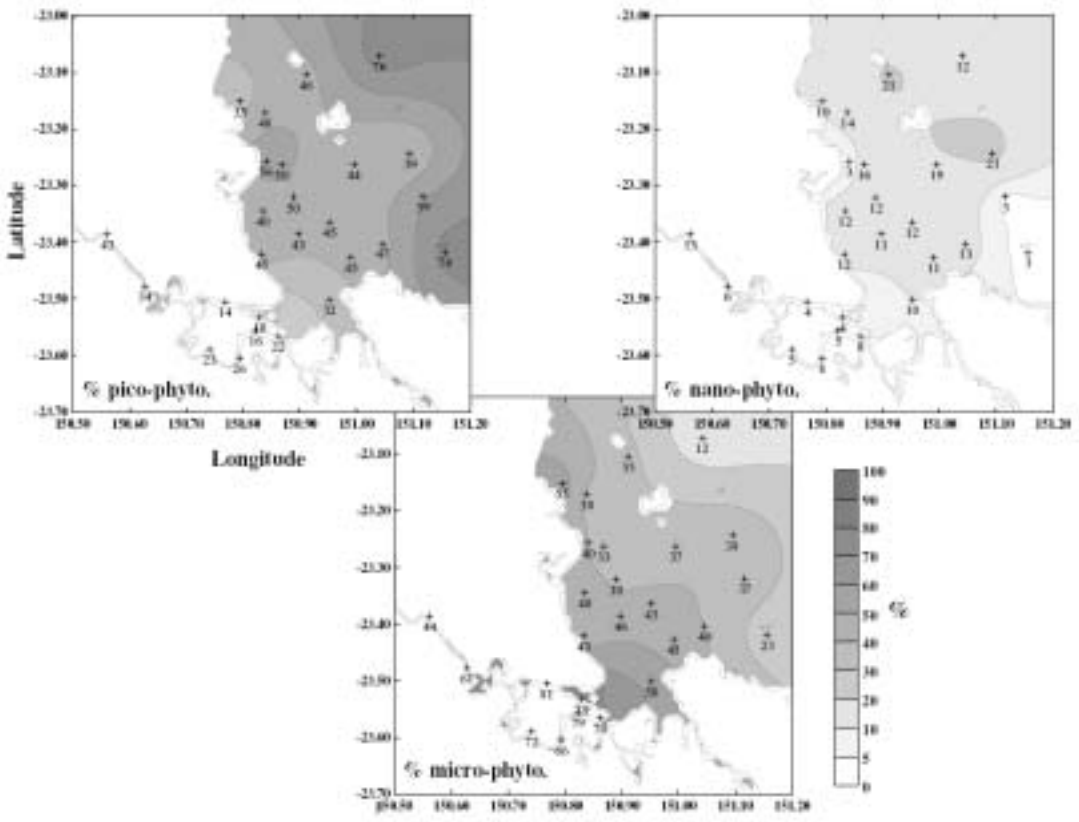

Figure 2-2. Spatial distribution of the relative contribution of pico-phytoplankton (< 2 µm), nano-phytoplankton (2–20 µm) and micro-phytoplankton (20–200 µm) to the algal population in the near-surface waters along Fitzroy Estuary–Keppel Bay in September 2003

A light absorption budget derived at 440 nm (the light wavelength at which chlorophyll *a* absorbs light in the blue region) showed that non-algal material dominated the total absorption, expressed as *a(440)* in the estuary and in Casuarina Creek. In contrast, phytoplankton was the main absorbing constituent further offshore in the bay (Figure 2-3). The non-algal contribution to particulate absorption was on average 25% at 440 nm in oceanic waters in the bay, which is in the range of values estimated by Bricaud *et al*. (1998) over a large range of trophic conditions and regions in the world's oceans. CDOM contribution was highest along the western shore. Note that the western shore is a shallow area (~8 m depth), where highest salinities were also observed, almost certainly due to local evaporation. In the transition zone, CDOM and non-algal particle contributions to total light absorption were similar.

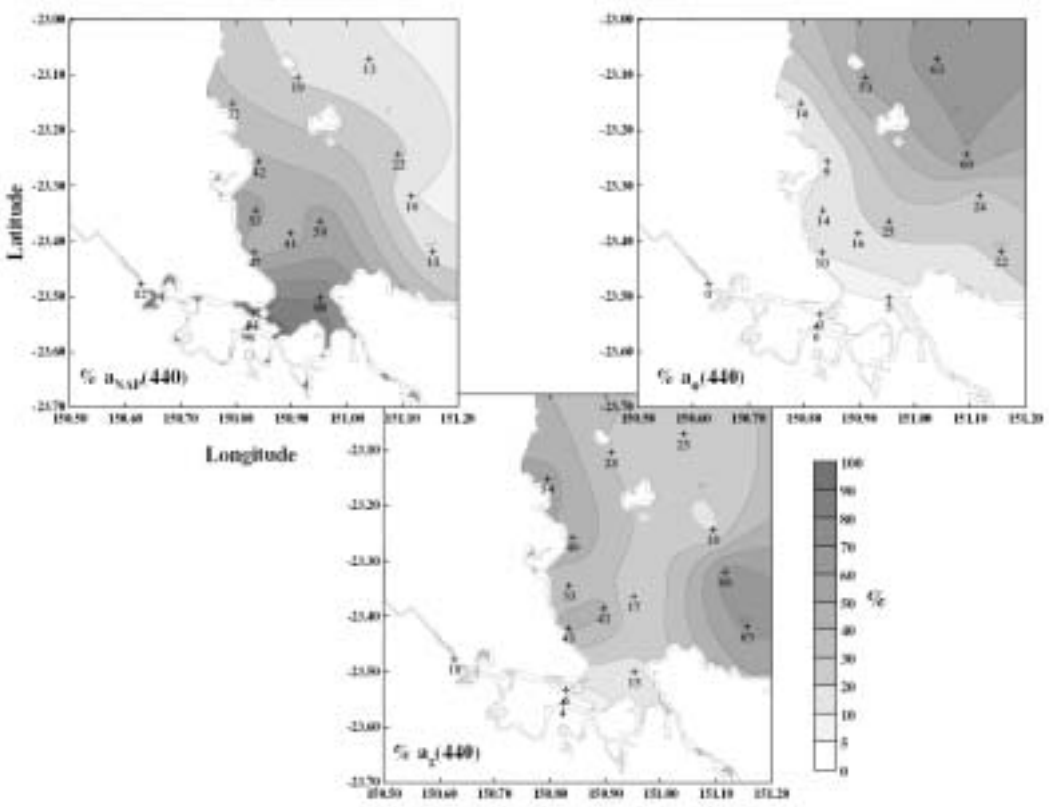

Figure 2-3. Spatial distribution of the relative contribution of non-algal particles [expressed as aNAP(440)], phytoplankton [expressed as aφ(44)] and CDOM [expressed as ag(440)] to the total light absorption coefficient at 440 nm in the near-surface waters along Fitzroy Estuary–Keppel Bay in September 2003 (note that the symbol notation is according to the publication guidelines of Oubelkheir *et al*. 2006, and different from the notation used throughout this report)

The spatial distribution of the light scattering at 555 nm [$b_p(555)$] in the near-surface layer is given in Figure 2-4A. $b_p(555)$ varied over two orders of magnitude from the estuary to the bay (16.46 to 0.30 m^{-1} at stations 1 and 42, respectively; Figure 2-4A). This range must be seen as a minimum range of variability, as $b_p(555)$ values higher than 20 m^{-1} in some areas of the estuary (e.g. station 3) could not be properly resolved with our *in situ* instrumentation. The particle backscattering ratio (b_{bp}/b_p) varied by a factor of six (Figure 2-5A): from 3.4% at 555 nm in the transition zone (station 30) to 0.6% in the eastern part of the bay (station 18). The ratios measured at stations 1 and 30 are exceptions (b_{bp}/b_p varied by up to 20% between 440 and 715 nm; Figure 2-5B), which might be due to significant errors associated with multiple scattering in ac-9 measurements (b_p was in the 15–20 m^{-1} range; Figure 2-4A).

The spectral dependency of the particle scattering (γ_b), an optical indicator of particle size, varied over FE–KB also (Figure 2-4B). As an example, for the 7 September 2003 transect (Figure 2-1), $b_p(555)$ and γ_b distributions differed between the estuary and offshore, and in the estuary between ebbing (morning) and flooding (afternoon) tides (Figure 2-4C). In the morning, γ_b decreased from the estuary to offshore, reflecting a probable increase in particle size. In the afternoon, γ_b decreased in the estuary, indicating slightly larger particles in the estuary mouth in the afternoon than in the morning. Note, however, that our *in situ* instrumentation could not accurately resolve the scattering values higher than 20 m^{-1} encountered in most of the estuary mouth (see Figure 2-4A), so that conclusions on the size of the particle assemblage in this area (e.g. relative to offshore) cannot be drawn. The 11 September 2003 transect also shows different spatial distributions in $b_p(555)$ and γ_b between morning and afternoon (Figure 2-4A and B), probably as a result of tidal effects.

The observed difference in the distribution of various properties at a given site between various times of the day demonstrates that our sampling of the spatial distribution of optical and biogeochemical properties over a large spatial domain such as FE–KB was partly confounded by tidal effects (see below for a more detailed study). The first dry season campaign (2003) was partly conducted during spring tides (7 September 2003 corresponded to the beginning of the spring tides, with a tidal amplitude of ~ 3 m). It is thus strongly recommended that for studies of large coastal areas, spatial sampling takes tidal conditions into account.

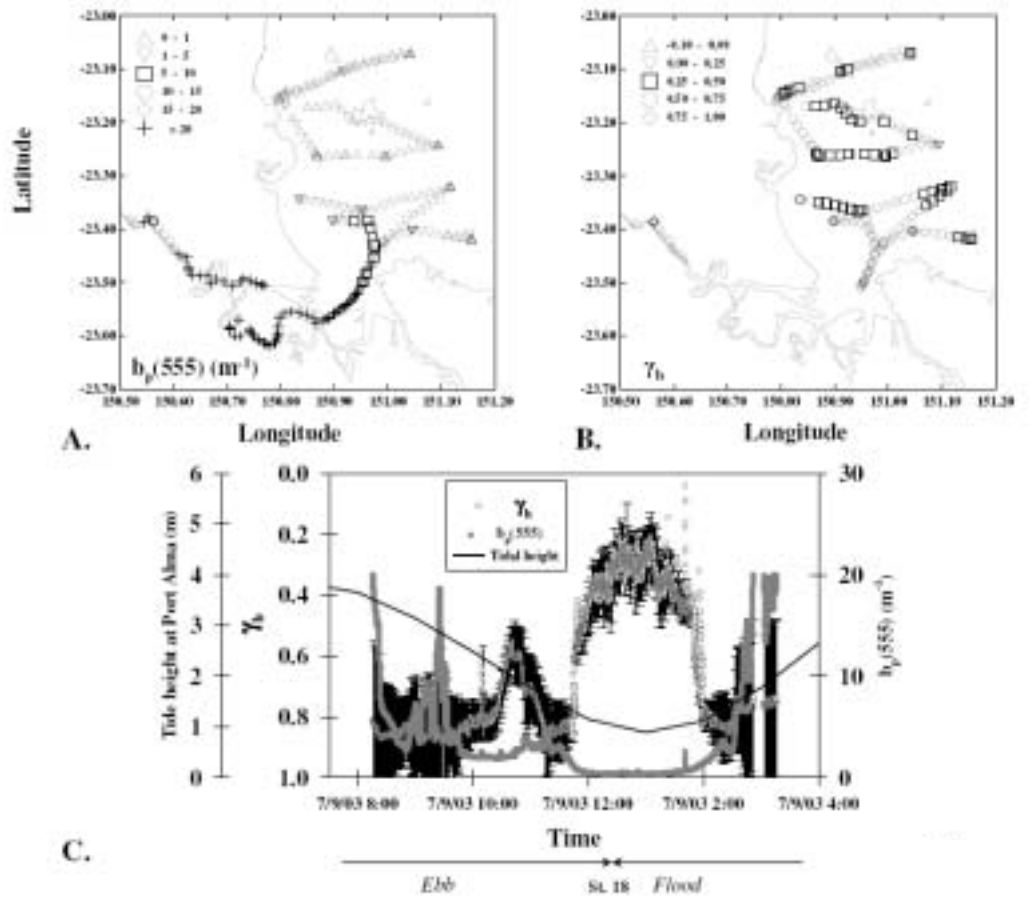

Figure 2-4. Spatial distribution of scattering properties in the near-surface waters along Fitzroy Estuary–Keppel Bay in September 2003 (see map of the daily tracks, Figure 2-1): A. Scattering coefficient at 555 nm [$b_p(555)$]; B. Spectral slope of the scattering coefficient [γ_b; values corresponding to $b_p(555)$ higher than 20 m^{-1} are not reported]; C. Temporal evolution (along track) of $b_p(555)$ and γ_b (and corresponding standard deviations of model adjustment in black vertical bars), during the 7 September 2003 transect [$b_p(555)$ higher than 20 m^{-1} and corresponding γ_b values are not reported]. The tide height at Port Alma is also indicated.

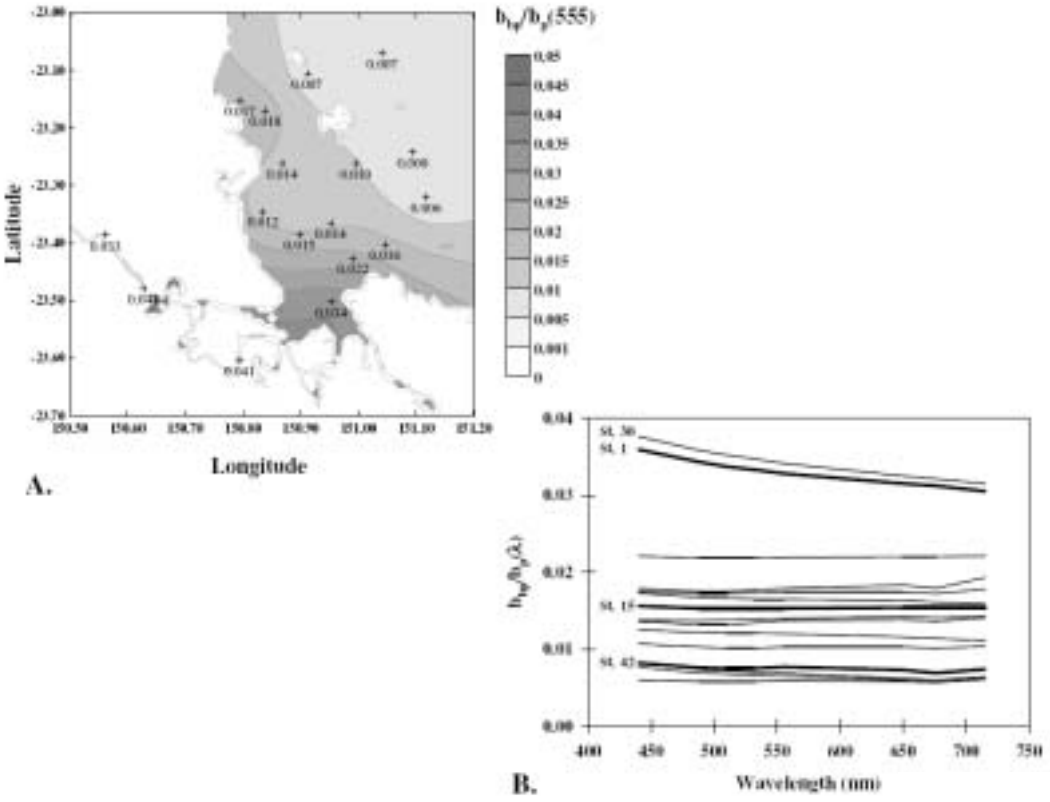

Figure 2-5. Spatial distribution of the backscattering ratio [$b_{bp}(\lambda)/b_p(\lambda)$] in the near-surface waters along Fitzroy Estuary–Keppel Bay in September 2003. A. At 555 nm (values corresponding to areas where b_p is higher than 20 m^{-1} must be discarded) B. Spectrally (spectra corresponding to stations 1, 15 and 42 are highlighted in bold; spectra derived from bp higher than 20 m^{-1} have been discarded from this graph).

2.2.2 Temporal variability (August 2004)

Total suspended matter (TSM) concentrations in the near-surface layer were highly variable over a tidal cycle at a fixed site, changing by a factor of five at sites B and C, and a factor of 20 at site A (Table 2-2). Corresponding chlorophyll concentrations varied only by a factor of 1.2 to 1.6. As in 2003, nano-phytoplankton contributed the smallest proportion at all sites (< 13%, Figure 7 in Oubelkheir *et al.,* 2006); while micro- and pico-phytoplankton were in equivalent proportions (except at site C). The phytoplankton assemblage composition varied at a given site along the tidal phase. The proportion of micro-phytoplankton tended to increase with the outflow of turbid waters from the estuary to the bay near the estuary mouth (site B) and the eastern part of the bay (site C), and to slightly decrease in the western part of the bay (site A).

The absorption coefficients measured at sites A, B and C in 2004 were comparable to the intermediate values measured over the FE–KB system in 2003 (Tables 2-1 and 2-2). CDOM and non-algal particle absorption at 440 nm varied by up to a factor five (at sites A and C, respectively) over the tidal phase, while phytoplankton absorption varied only by a factor of 1.4 (site A) to 2.3 (sites B and C) (Table 2-2).

Table 2-2. Range of variability of biogeochemical and optical quantities over the Fitzroy Estuary–Keppel Bay system during the dry season tidal phase sampling at three fixed sites A, B and C (August 2004)

Parameter	Site A	Site B	Site C
TSM (g m^{-3})	0.1–1.9	1.0–4.8	3.6–19
TChl *a*	0.17–0.20	0.17–0.28	0.50–0.74
$a_g(440)$ (m^{-1})	0.018–0.085	0.033–0.080	0.023–0.043
$a_\varphi(440)$ (m^{-1})	0.010–0.014	0.008–0.018	0.019–0.043
$a_{nap}(440)$ (m^{-1})	0.024–0.042	0.044–0.204	0.132–0.658
$b_p(555)$ (m^{-1})	0.13–0.53	0.63–1.51	1.62–10.97
$b_{bp}/b_p(555)$ (%)	1.7–3.9	1.6–2.3	1.6–4

2.3 Discussion of optical complexity

Remote sensing of coastal waters is a critical challenge in optical oceanography. Coastal waters are much more complex relative to oceanic waters, because of boundary conditions (bottom and land–ocean interfaces), which in turn affect the mixing of a variety of materials coming from various sources. Changes in the characteristics of the suspended particulate assemblages (composition and size) are often accompanied by changes in their IOPs and SIOPs. These changes can occur in the near-surface layer over a variety of scales: from a few metres (e.g. fronts between river plumes and oceanic waters) to kilometres, and from a few hours or tens of minutes (e.g. tidal phase or wind gust) to months. This leads to the following discussion of the spatial and temporal variability in this macrotidal system.

The properties of material in the water column of the FE–KB system show a continuum between what is characteristically land-derived material in the estuary to more typically oceanic material on the northern and eastern sides of Keppel Bay. The decrease in suspended matter concentration from the estuary to

offshore is not a simple dilution process. The particle size and chemical composition also change, leading to changes in the IOPs and specific IOPs of the particulate material.

The backscattering efficiency of particles varies by a factor of up to six over a single coastal system. The values measured here are in the range estimated by previous studies in oceanic and coastal waters (Oubelkheir *et al.,* 2006) and references therein). The large variability in backscattering efficiency observed in the FE–KB is a critical result for the application of remote sensing algorithms to similar complex coastal systems. Underwater light field modelling often assumes a constant backscattering ratio. The variation we observed here will prevent obtaining closure between the IOPs computed through radiative transfer modelling (based on i*n situ* or remote sensing apparent optical properties (AOPs) measurements) and the IOPs measured *in situ* (i.e. optical closure).

Oubelkheir *et al.* 2006 show that the effect of the tidal phase must be taken into account in the sampling strategies of macrotidal coastal systems. For example, the differences in the particle concentration (b_p) and size (γ_b) between the morning and afternoon in the estuary mouth on 7 September 2003 and in the north of the bay on 11 September 2003 can be explained by the effect of the tidal phase. The ‘morning‘ measurements in the estuary mouth started at high tide, while the ‘afternoon‘ measurements were performed during the incoming tide.

This observation strongly demonstrates the need to: (i) adapt *in situ* sampling strategies of macrotidal systems, and (ii) accurately characterise the effect of the tidal phase on the distribution of optical and biogeochemical properties in order to correctly interpret spatial data acquired in the near-shore coastal zone.

3 Assessment of the accuracy of MODIS global algorithms for the Fitzroy River Estuary

3.1 Algorithm validation: an introduction to methodology

Remote sensing algorithms that reliably translate the water colour measured from a sensor in space to a map of concentrations are required for managing and understanding coastal waters. The standard NASA algorithms for MODIS were developed for Atlantic and Pacific Ocean northern hemisphere waters. Increasingly our research is showing that these global algorithms lack validity in Australian coastal waters, specifically in complex estuarine areas where freshwater river–estuarine mixing and estuarine–ocean mixing take place.

NASA algorithms have changed quite markedly over the last two years, going from a pure science focus to a specific applications focus. This has led to a complex situation for Australian researchers, as prior to February 2004 we were dealing with NASA scientific algorithms with many variables and many permutations of algorithms, whereas since February 2004 the algorithms have been severely reduced in scope and broad applicability. Therefore, we are only comparing CHL and TSM global algorithms (instead of CHL, TSM, K490 and CDOM) for the following reasons:

- The three components that colour water are CHL, TSM and CDOM (see glossary for terms). However, CDOM is no longer a product delivered by the SEADAS algorithm, and
- K490 (the attenuation of light at 490 nm, ~inverse of turbidity) is a function of the reliability of TSM, CHL and CDOM.

At the initial stage of this project we did not anticipate that the results from our *in situ* measurement campaigns (Oubelkheir *et al.,* 2006) and our work in the Mossman–Daintree area would clearly demonstrate that the global algorithms are invalid and inaccurate (valid meaning where a map of CHL is shown it is actual chlorophyll concentrations you are looking at instead of a mixture of CDOM, chlorophyll and the organic-detrital component of TSM; accurate meaning where there is an acceptable level of correspondence between *in situ* measured and remotely sensed concentrations).

For many more turbid coastal waters the conventional blue-green band ratio algorithms developed for oceans are proven to fail.

The validation of remote sensing algorithms that produce maps of CHL and TSM may be carried out in several ways:

- Traditional: Comparing the *in situ* measured concentration with the MODIS algorithm estimated concentration from MODIS imagery data. This may include errors due to: (i) atmospheric correction, (ii) sensor calibration and (iii) the mismatch in size and time between the sampled water and the 1x1 km pixel;
- Applying the MODIS algorithms to an *in situ* measured colour spectrum [normalised water leaving radiance spectrum (nLw)], where *in situ* concentrations are also available. This only includes errors due to recalculation of an above-water or in-water measured spectrum to the nLw spectrum;
- Applying the MODIS algorithms to a simulated set of nLw which were created by using a radiative transfer model (Hydrolight 4.1) to calculate nLw from *in situ* measured spectral absorption and scattering measured by the AC-9 and the HydroScat-6. This method removes virtually all error sources (in processing real satellite data) and allows us to concentrate on the validity of the algorithm itself. This method focuses on understanding whether the algorithm adequately deals with the underlying light absorption and scattering conditions in the Fitzroy Estuary–Keppel Bay waters; and
- Applying the MODIS algorithms to a simulated set of nLw that were created by using a radiative transfer model (Hydrolight 4.1) to calculate nLw from *in situ* sampled, laboratory spectrophotometrically measured specific inherent optical properties (SIOPs) and the concentrations of chlorophyll, suspended matter and coloured dissolved organic matter. This method is another approach that removes virtually all error sources and allows us to concentrate on the validity of the algorithm itself. This method directly studies the assumptions about how light emanating from the water body (nLw) relates to actual chlorophyll and TSM concentrations without any influence of error-introducing effects of the atmosphere and air-water interface.

The above methodology is more thorough than any other research group in the world has published up till now. We had to develop this methodology because our initial remote sensing algorithm comparison results showed such large deviations that we needed to examine the sources of these deviations. Without knowledge of the sources of the deviations it is impossible to devise improved algorithm approaches that avoid the pitfalls of the standard global algorithms.

3.2 *In situ* measurement match-ups of GBRMPA long-term monitoring chlorophyll values and MODIS-derived chlorophyll using global algorithms

It is important to realise that when comparing *in situ* sampling results with MODIS pixel results we are comparing a point sample with an integrated 1x1 km pixel sample that by definition is an average of all that water body area. Also there is inevitably a time delay between the *in situ* sample and the MODIS overpass. Both the USA and the European space agencies (NASA and ESA) have validation protocols for *in situ* measurements and match-ups for pixels of coastal water. They require measurement within one hour of the overpass and the site should be 5–10 km away from any landmass.

This requirement is difficult to achieve as many groups involved in calibration and validation of remote sensing results over coastal waters have experienced.

Our solution for the current investigations was to access longer-term monitoring datasets. For the Keppel Bay area we used as *in situ* measurements the GBR long-term chlorophyll monitoring dataset measured by the Australian Institute of Marine Science (AIMS). The location of these sites (see Figure 3-1) was not suitable for remote sensing validation as several sites are located near islands.

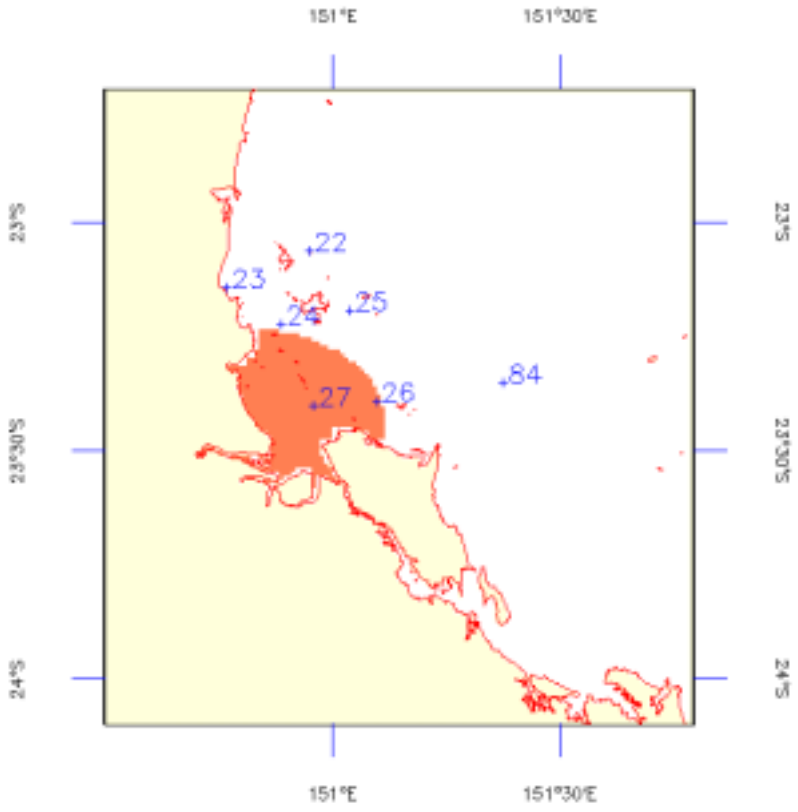

Figure 3-1. Locations of GBR long-term chlorophyll monitoring dataset measurement sites for Keppel Bay. The area in dark orange is the spatial domain of the biogeochemical model (BGCM)

Figures 3-2, 3-3, 3-4 and 3-5 compare the chlorophyll *a* measured on a monthly basis for the GBR long-term chlorophyll monitoring dataset with the chlorophyll *a* retrieved from the MODIS/Aqua data for that location.

Figure 3-2presents the comparison for station 'River Mouth' where the MODIS data significantly overestimates the *in situ* measurements; this is due to high CDOM and high TSM values confounding the standard CHL algorithm, likely augmented by a partly failing atmospheric correction for near coastal situations.

MODIS data overestimates the *in situ* chlorophyll measurements for Barren Island (Figure 3-3) and Hummocky Island (Figure 3-4) but less than at 'River Mouth'.

At station 'Mid Channel' (Figure 3-5), the MODIS data and *in situ* measurements appear to be in the same order of magnitude.

These results clearly indicate that the MODIS standard algorithms increasingly fail as we go from blue ocean water through green mixed ocean–estuarine waters to mixed green-to-brown estuarine–river waters (following the Figure 3-5 to Figure 3-2 sequence of sampling stations).

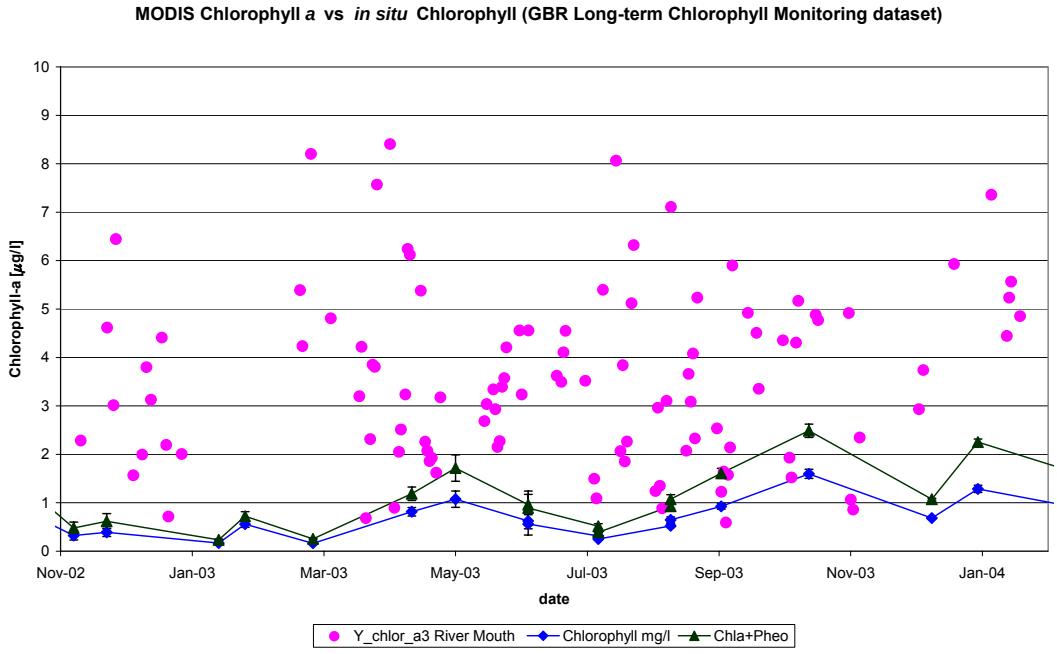

Figure[B1] **3-2. Chlorophyll validation: GBR long-term chlorophyll monitoring dataset station 'River Mouth'. Comparison of the chlorophyll *a* (as only chlorophyll or as sum of chlorophyll and phaeopigments) measured on a monthly basis with the chlorophyll retrieved from MODIS/Aqua (Y_chlora3 River Mouth) for this location**

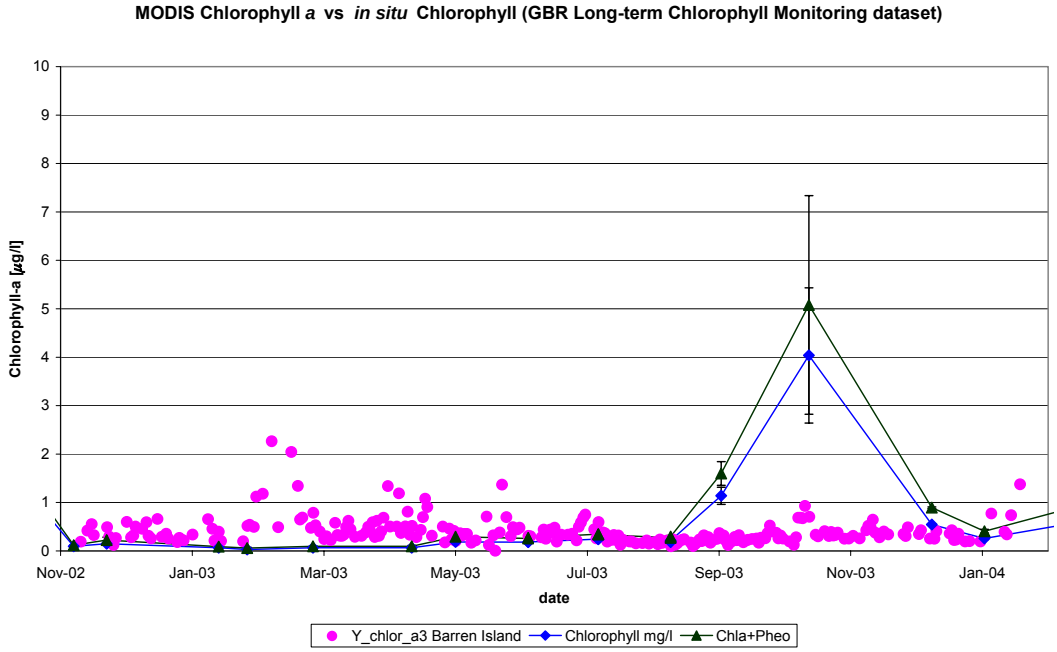

Figure 3-3. Chlorophyll validation: GBR long-term chlorophyll monitoring dataset station 'Barren Island'. Comparison of the chlorophyll *a* (as only chlorophyll or as sum of chlorophyll and phaeopigments) measured on a monthly basis with the chlorophyll retrieved from MODIS/Aqua (Y_chlor_Barren Island) for this location. The peak in MODIS derived concentrations in the Sep 03 to Nov 03 period is likely due to algal blooms affecting the chlorophyll concentrations—perhaps *Trichodesmium*

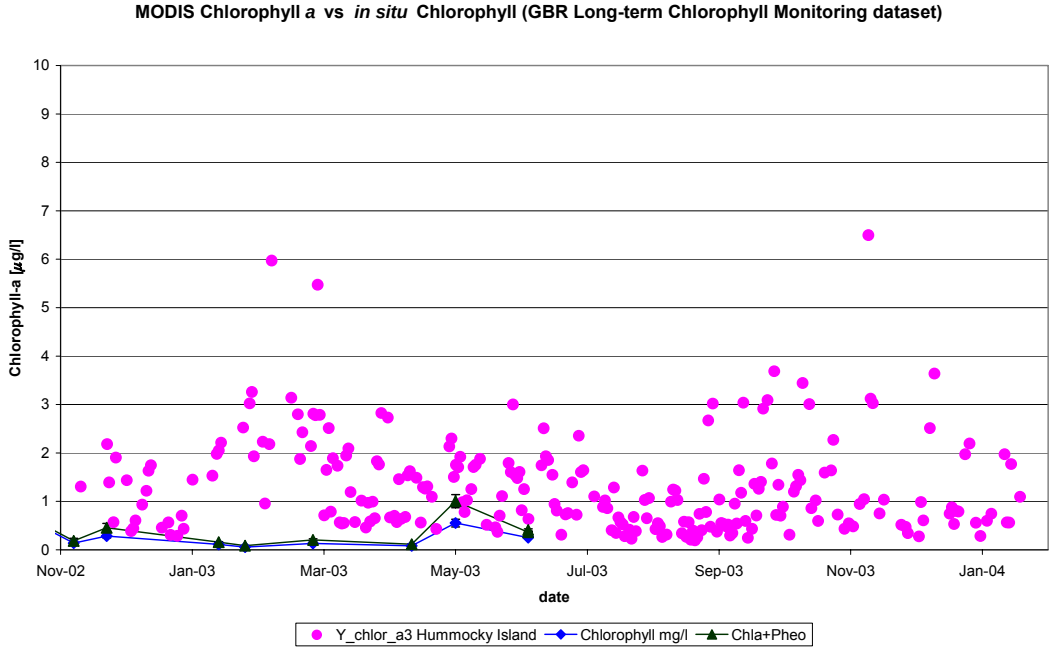

Figure 3-4. Chlorophyll validation: GBR long-term chlorophyll monitoring dataset station 'Hummocky Island'. Comparison of the chlorophyll *a* (as only chlorophyll or as sum of chlorophyll and phaeopigments) measured on a monthly basis with the chlorophyll retrieved from MODIS/Aqua (Y_chlor_Hummocky Island) for this location

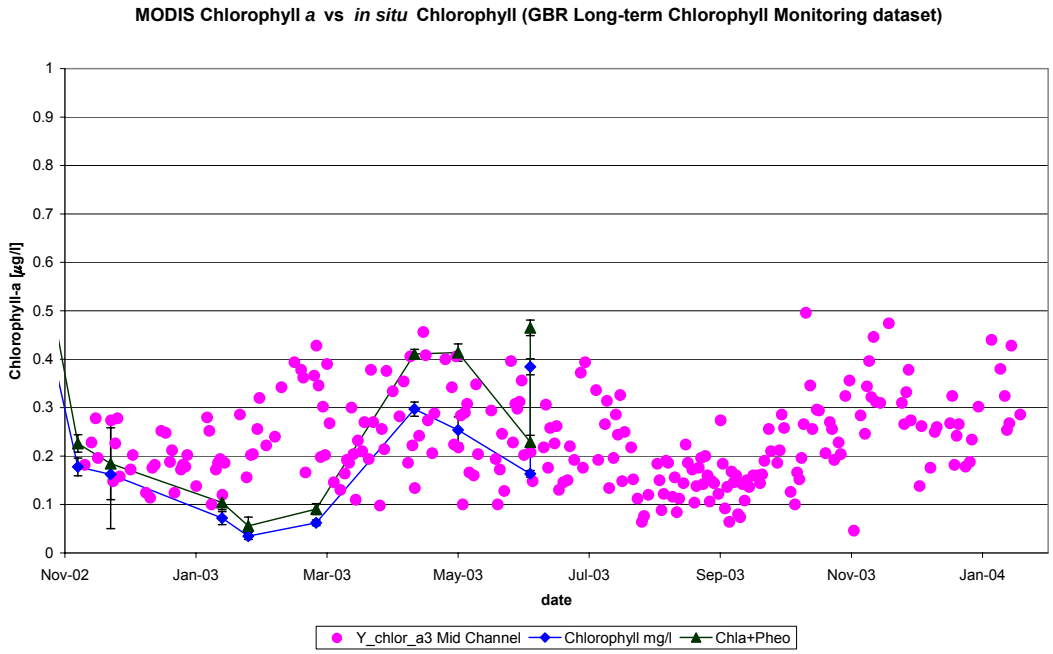

Figure 3-5. Chlorophyll validation: GBR long-term chlorophyll monitoring dataset station 'Mid Channel'. Comparison of the chlorophyll *a* (as only chlorophyll or as sum of chlorophyll and phaeopigments) measured on a monthly basis with the chlorophyll retrieved from MODIS Aqua (Y_chlor_Mid Channel) for this location

3.3 Comparison of chlorophyll and TSM measurements for the September 2003 Fitzroy sampling period

During the September 2003 Fitzroy Estuary–Keppel Bay fieldwork campaign, chlorophyll and TSM were measured twice for several sampling stations. One series was measured by GeoSciences Australia and CSIRO Land & Water (GA/CLW), collected as a series of four separate one-litre samples which were filtered in sequence. These samples were collected either with a bucket or from the underway system (pumping water from a depth of ~ 1 m).

The other series was measured by CSIRO Marine and Atmospheric Research (CMAR) collected as a single four-litre sample from the underway system (pumping water from a depth of ~ 1 m). HPLC estimates of chlorophyll were run for all the stations where optical characterisation was performed, while TSM was measured from only a few samples.

Since the samples were not collected at the same moment, the concentrations estimates do not refer to the same water parcel. The mismatch in retrieved concentrations between the two data sources (Figures 3-6 and 3-7) is higher than expected for duplicate and replicates (~ 10–20%). These varying results also pose a serious question: which data to use for validation purposes? To maintain continuity with other optical characterisations carried out by our group, we decided to use the CMAR data for this analysis and for our validation.

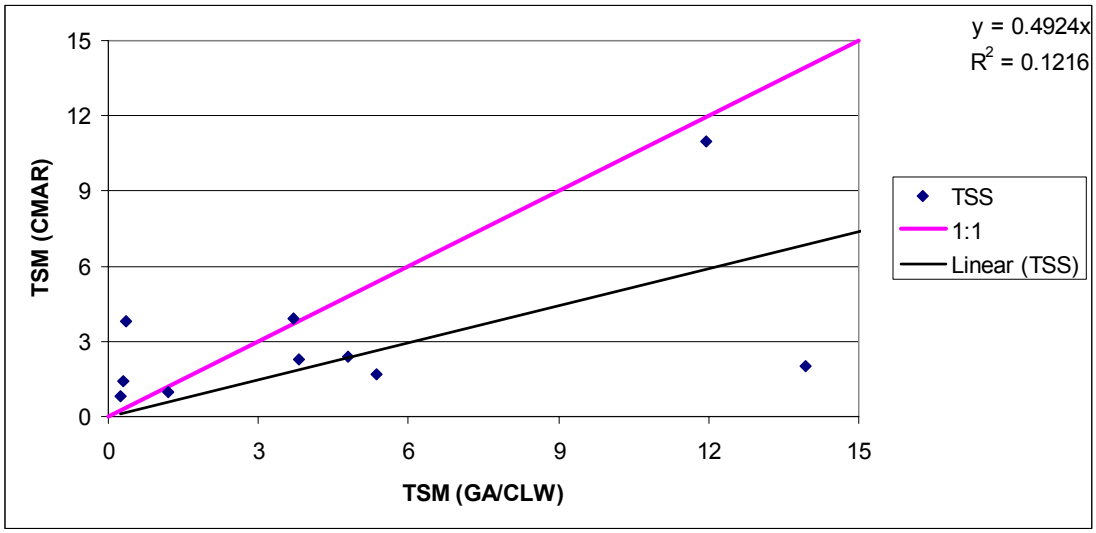

Figure 3-6. Comparison of *in situ* TSM concentrations measured by GA and by CMAR laboratories for the September 2003 field campaign. The relationship is poor (R^2 of 0.12) and a two-times underestimation of TSM

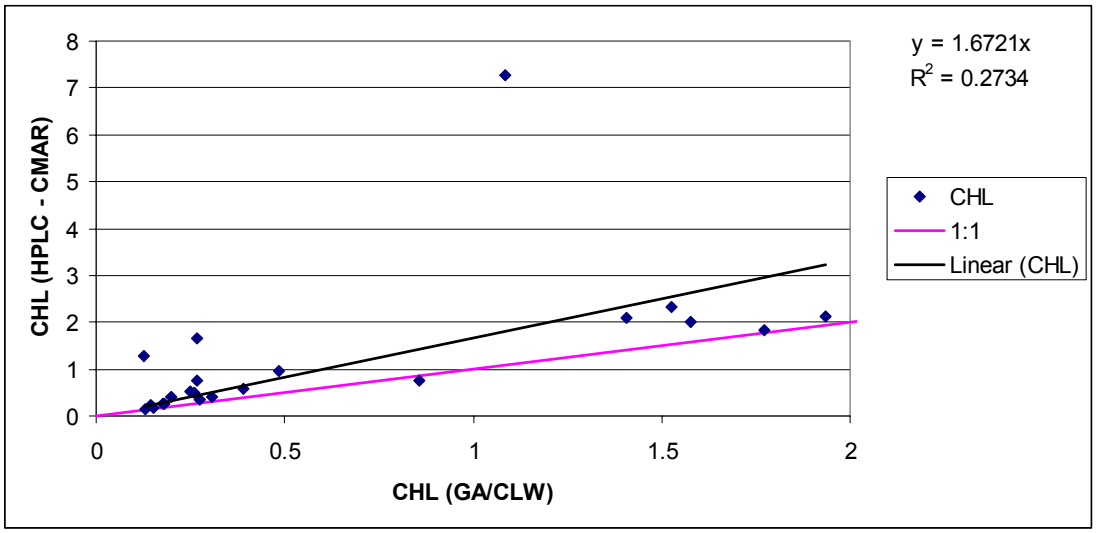

Figure 3-7. Comparison of *in situ* measured chlorophyll by the GA/CLW and the CMAR laboratories for the September 2003 field campaign. The relationship is poor (R^2 of 0.27)

3.4 Validation through modelled MODIS radiances

The advantage of using *in situ* measured normalised water leaving radiance spectra (nLw) (instead of MODIS satellite image-derived spectra) is that errors in MODIS processing such as (possible) incorrect atmospheric correction near turbid waters and the coastline are avoided. Moreover, all the *in situ* measured data can be used without being limited to the use of sites measured within one hour of the overpass. This is, therefore, a better way of checking the exact correctness of the MODIS algorithm.

The MODIS algorithms were applied to a simulated set of nLw which were created by using a radiative transfer model (Hydrolight 4.1) to calculate nLw from *in situ* measured spectral absorption and scattering measured by the AC-9 and the HydroScat-6 during the field campaigns. In simpler terms, we modelled the water colour using our *in situ* measurements that tell us how light is absorbed and scattered in the water column.

Figures 3-8 and 3-9 present the TSM concentration retrieved by the global MODIS algorithm vs. the TSM concentration measured *in situ*. Because of the previously mentioned mismatch in the *in situ* estimations, both the GA/CLW and CMAR data are presented. The MODIS global TSM algorithm underestimates the TSM values over a wide range of the GA measurements.

Figures 3-10 and 3-11 present the CHL concentration retrieved by the global MODIS algorithm vs. the chlorophyll concentration measured *in situ*. Again, because of the previously mentioned mismatch in the *in situ* estimations, both the GA and CMAR data are presented. The MODIS algorithm seems to be underestimating the chlorophyll values over the whole range.

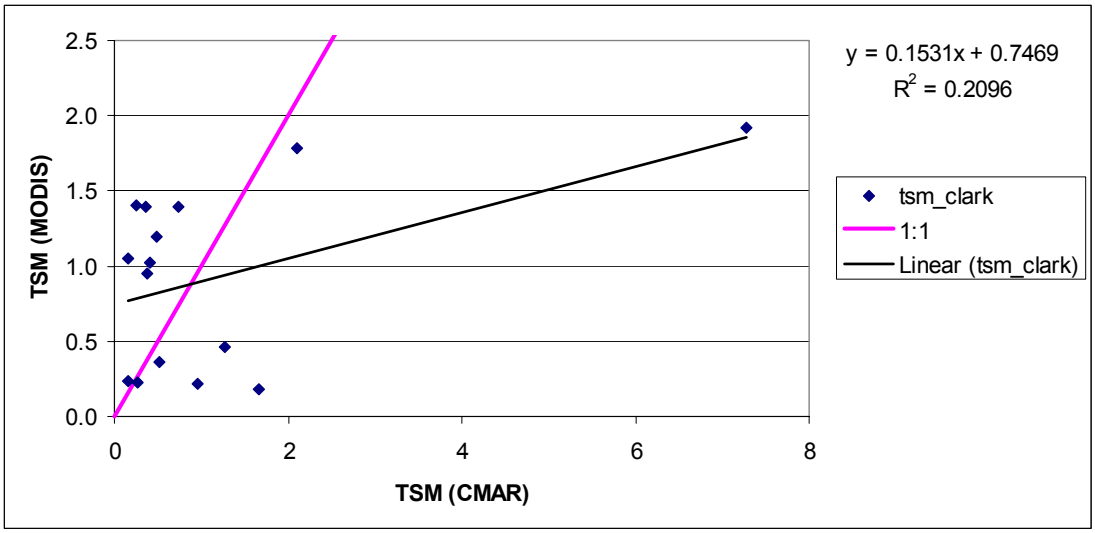

Figure 3-8. TSM concentration retrieved by the MODIS algorithm (tsm_clark) vs. the TSM concentration measured *in situ* by CMAR. The relationship is poor (R^2 of 0.09). Note the data distribution: many values randomly related in the 0–2 mg l^{-1} range; the one data point towards 8 mg l^{-1} strongly influences the result

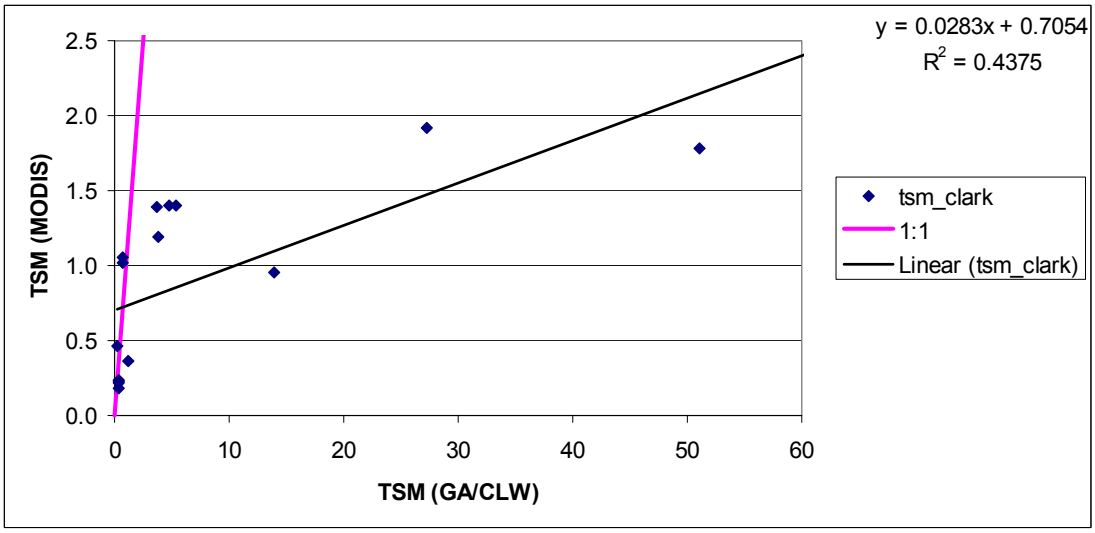

Figure 3-9. TSM concentration retrieved by the MODIS algorithm vs. the TSM concentration measured *in situ* by GA/CLW. The relationship is poor (R^2 of 0.44).

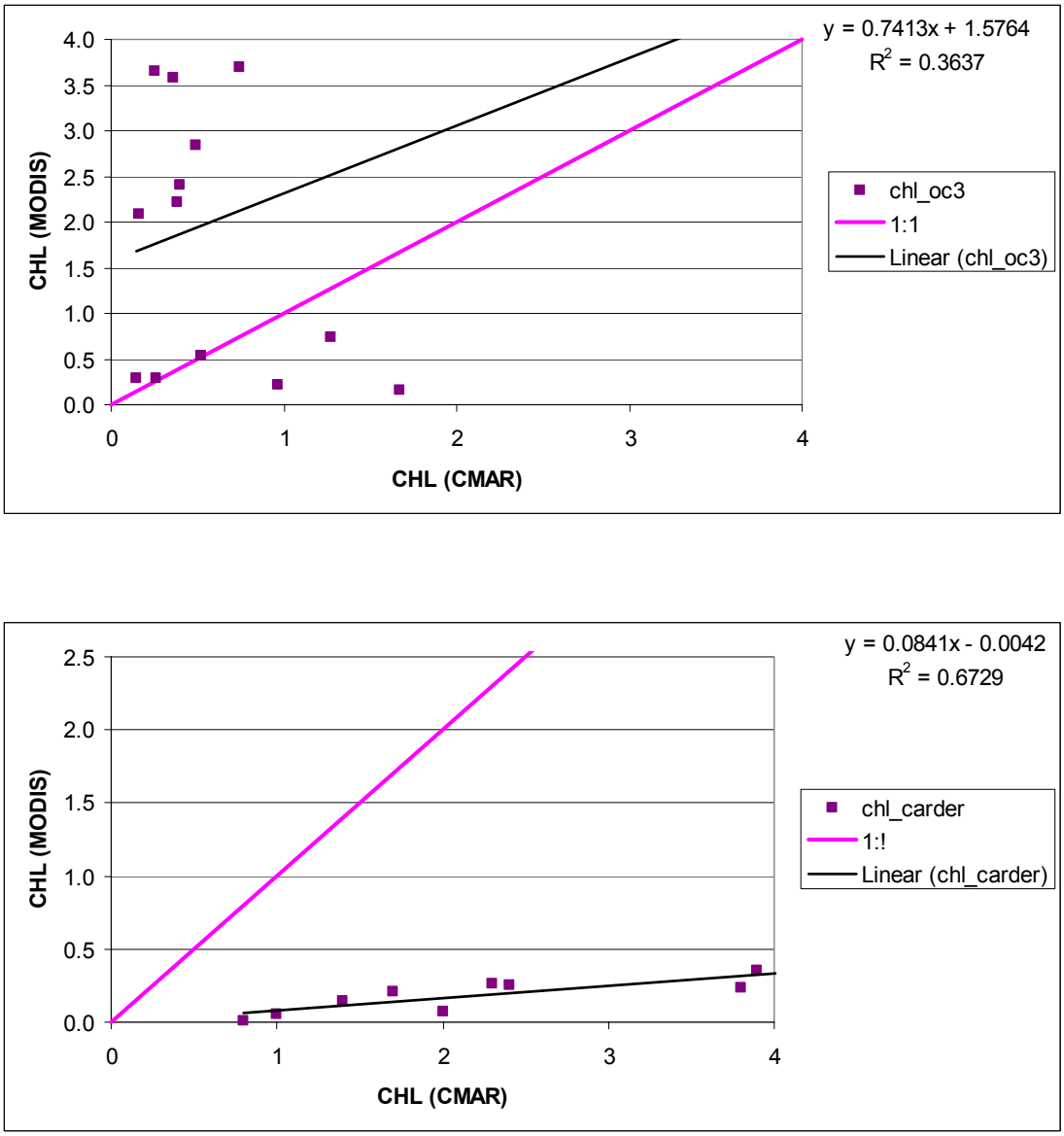

Figure 3-10. Chlorophyll concentration retrieved by the two most relevant CHL MODIS algorithms (chl oc3 and chl_carder) vs. the chlorophyll concentration measured in situ by CMAR. Note that the oc 3 algorithm has no clear relationship with the *in situ* chlorophyll concentrations whereas the chl_carder relationship is clear but seriously underestimates the chlorophyll *in situ* concentrations. (Figure 3-11 shows the same relationships for the GA/CLW measured concentrations.)

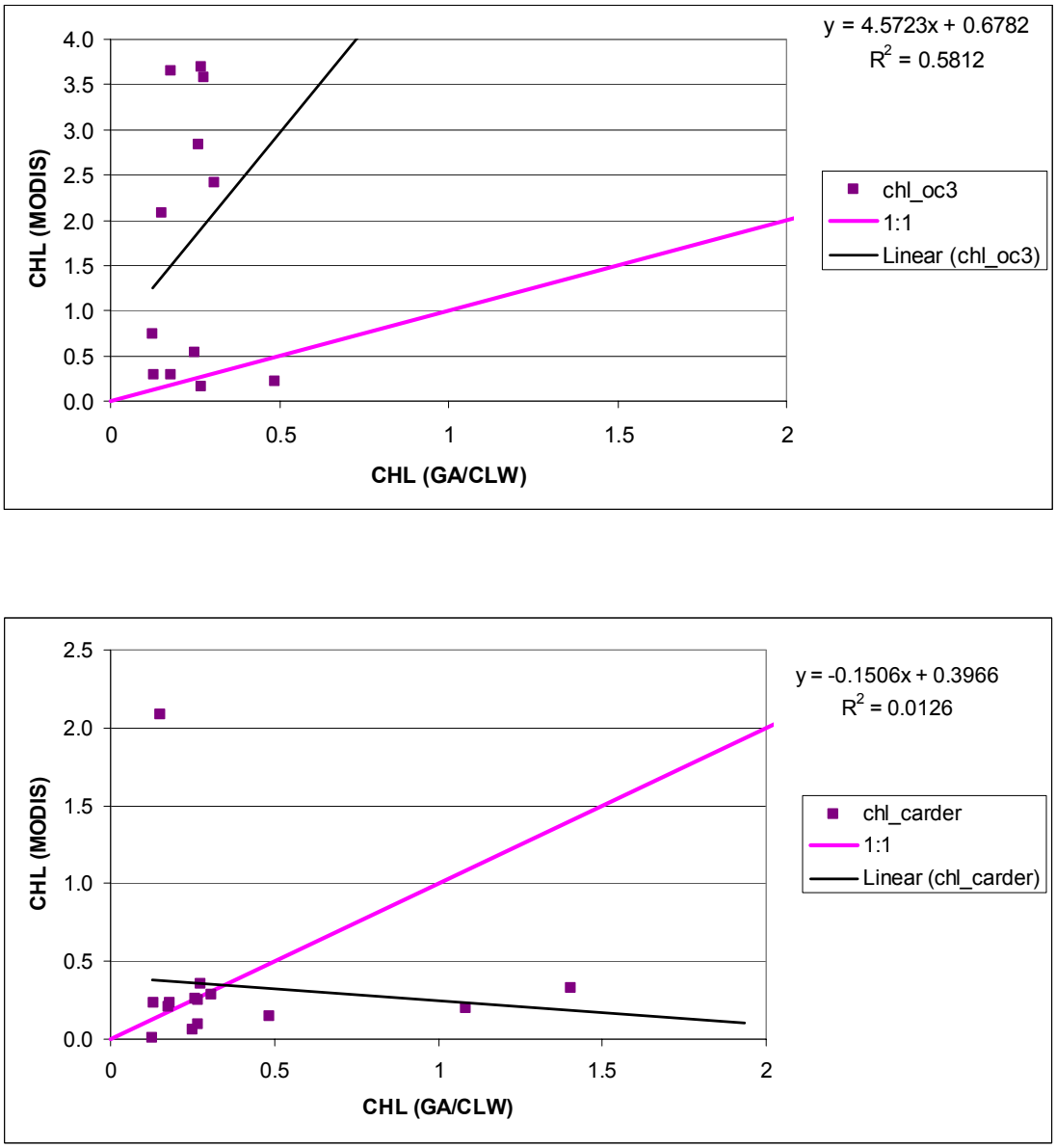

Figure 3-11. Chlorophyll concentration retrieved by the MODIS algorithm vs. the chlorophyll concentration measured *in situ* by GA/CLW. Note that the oc 3 algorithm has no clear relationship with the *in situ* chlorophyll concentrations whereas the chl_carder relationship is clear but seriously underestimates the chlorophyll *in situ* concentrations. (Figure 3-10 shows the same relationships for the CMAR measured concentrations.)

3.5 Sensitivity analysis of standard global algorithms (SEADAS) through modelled MODIS radiances

To further explore the behaviour of the MODIS standard SEADAS algorithms, a sensitivity analysis was performed using the SIOPs (specific inherent optical properties of light absorption and light scattering as a function of chlorophyll and TSM concentration) measured during the September 2003 fieldwork.

The MODIS SEADAS algorithms were applied to a simulated set of nLw (the water colour in radiance terms) created by the radiative transfer model (Hydrolight 4.1). The radiative transfer model was parameterised with the SIOPS of six stations measured *in situ* in September 2003 (as reported in Table 3-1). A series of 2240 permutations of spectra simulated varying CHL, CDOM and TSM concentrations over the actual *in situ* range during the September 2003 fieldwork: CHL = 0.1, 0.3,1.3 and 2 (in µg L^{-1}); CDOM = 0.01, 0.08, 0.25 and 0.50 (in m^{-1}); TSM = 0.25, 1, 5, 10 and 25 (in mg L^{-1}).

Table 3-1. SIOPs parameters estimated for six stations from data measured in situ in September 2003 used in the simulations of nLw to check the behaviour of standard MODIS algorithms. Station locations are shown in Figure 2-1.

Parameter	FK09	FK15	FK34	FK35	FK40	FK63
$b_b^*{}_{phy}$(542nm)	0.003	0.003	0.003	0.003	0.003	0.003
$b_b^*{}_{phy}$ slope	1.05	0.80	0.85	0.94	0.72	0.84
a^*_{cdom}	0.012	0.015	0.021	0.017	0.028	0.017
a_{tr}^* (440 nm)	0.028	0.038	0.020	0.029	0.015	0.040
a_{tr}^* slope	0.010	0.012	0.012	0.011	0.012	0.012
$b_b^*{}_{tr}$ (542nm)	0.006	0.018	0.010	0.010	0.003	0.016
$b_b^*{}_{tr}$ slope	1.05	0.80	0.85	0.94	0.72	0.84
b_b/b p (555 nm)	0.009	0.017	0.015	0.015	0.009	0.015
b_b/b phy (555 nm)	0.019	0.019	0.019	0.019	0.019	0.019

Figures 3-12 to 3-16 present the behaviour of MODIS standard SEADAS algorithms for the retrieval of CHL and TSM concentration as evaluated via this optical modelling.

Figures 3-12, 3-13 and 3-14 show that the MODIS standard SEADAS algorithm overestimates CHL substantially when CDOM and TSM are high. This result is in accordance with the initial comparison we did using the actual satellite-derived chlorophyll and the GBRMPA long-term monitoring data set (see Figures 3-2, 3-3 and 3-4). For the low concentrations of CDOM and TSM (Figures 3-13 and 3-14 and compare with Figure 3-5), the retrieval of chlorophyll performs better.

Figures 3-15 and 3-16 show that the MODIS standard SEADAS algorithm underestimates TSM for values higher than 5 mgL^{-1}. This result is also in accordance with the initial comparison we did using the actual satellite-derived TSM and the GBRMPA long-term monitoring data set (see Figures 3-2, 3-3 and 3-4). For the low concentrations of CDOM and chlorophyll (Figure 3-16), the retrieval of TSM performs better for low concentrations but still the MODIS standard SEADAS algorithm underestimates TSM for values higher than 5 mgL^{-1}.

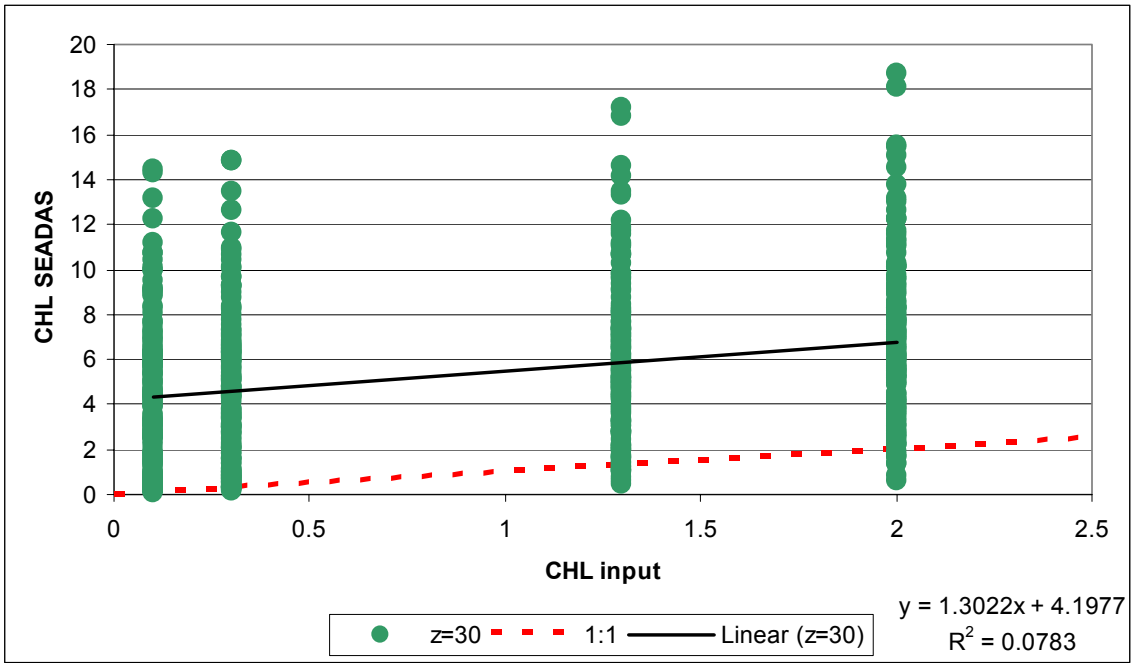

Figure 3-12. Sensitivity analysis for the SEADAS MODIS standard algorithm retrieval of chlorophyll concentration while varying the concentrations of CDOM and TSM (CDOM = 0.01, 0.08, 0.25, 0.50; TSM = 0.25, 1, 5, 10, 25) over their full range using the SIOPs (specific inherent optical properties of light absorption and light scattering as a function of chlorophyll and TSM concentration) measured during the September 2003 sampling. Chlorophyll is consistently overestimated (z = water column depth in m used in the simulations; Linear = the linear regression line; 1:1 is the correct relationship without errors)

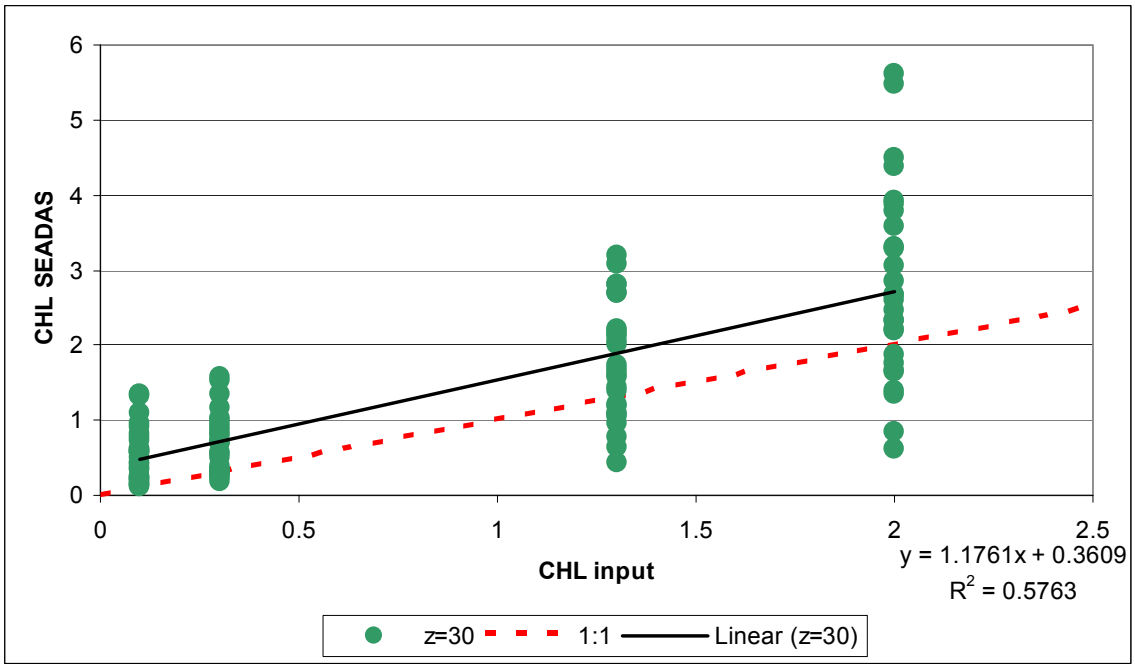

Figure 3-13. Sensitivity analysis for the retrieval of SEADAS chlorophyll concentration for low concentrations of CDOM and TSM (CDOM = 0.01, 0.08; TSM = 0.25, 1.). The relationship is much better than for the data presented in Figure 3-12.

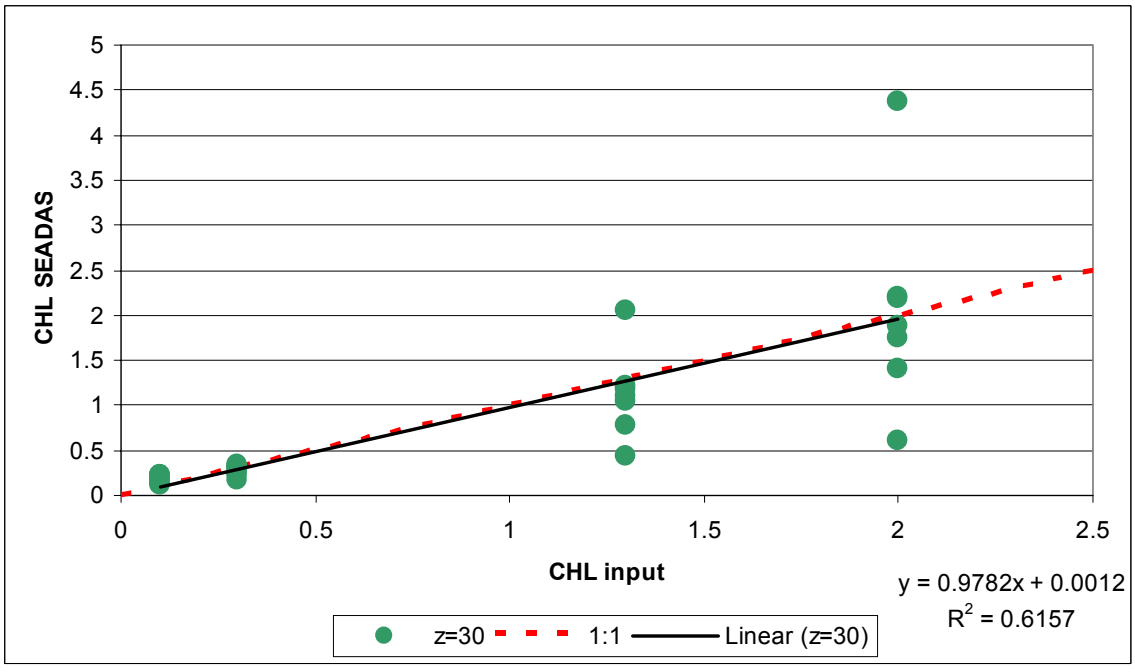

Figure 3-14. Sensitivity analysis for the retrieval of SEADAS chlorophyll concentration for lowest concentrations of CDOM and TSM (CDOM = 0.01; TSM = 0.25). Now the MODIS standard algorithm is performing well (but still with variations—see the spread of the green dots). (z = water column depth in m used in the simulations; Linear = the linear regression line; 1:1 is the correct relationship without errors.)

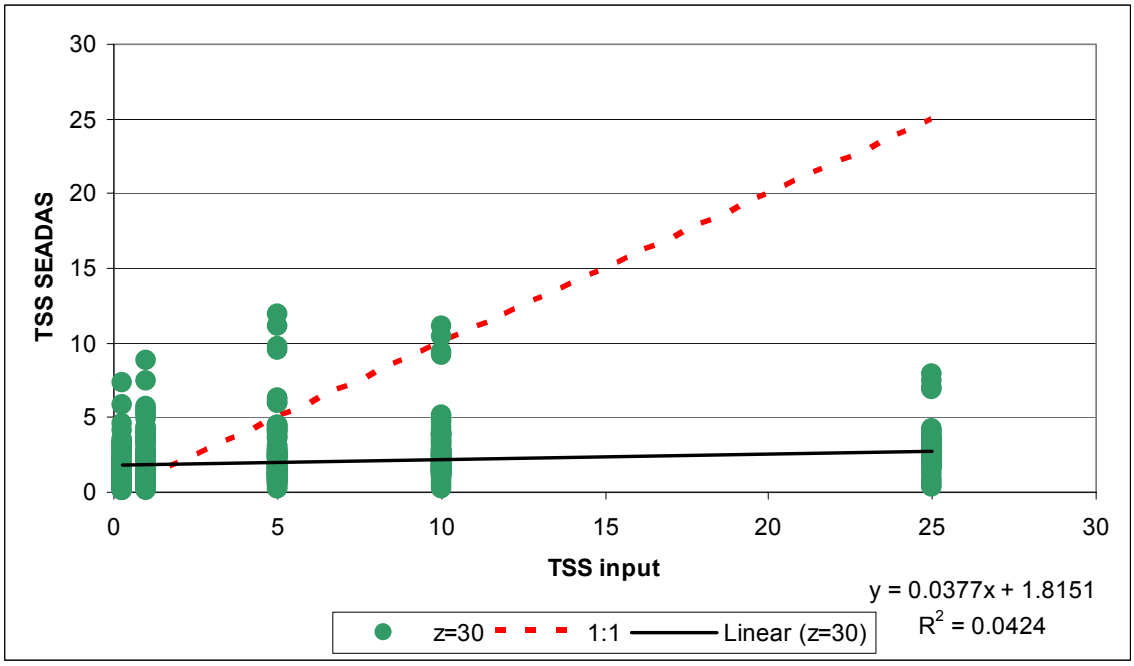

Figure[B2] **3-15. Sensitivity analysis for the SEADAS MODIS retrieval of TSM for all concentrations of CDOM and chlorophyll (CDOM = 0.01, 0.08, 0.25, 0.50; CHL = 0.1, 0.3, 1.3, 2). It is clear that there is a spurious relationship between the *in situ* measurements and the SEADAS MODIS algorithm results. (z= water column depth in m used in the simulations; Linear=the linear regression line; 1:1 is the correct relationship without errors).**

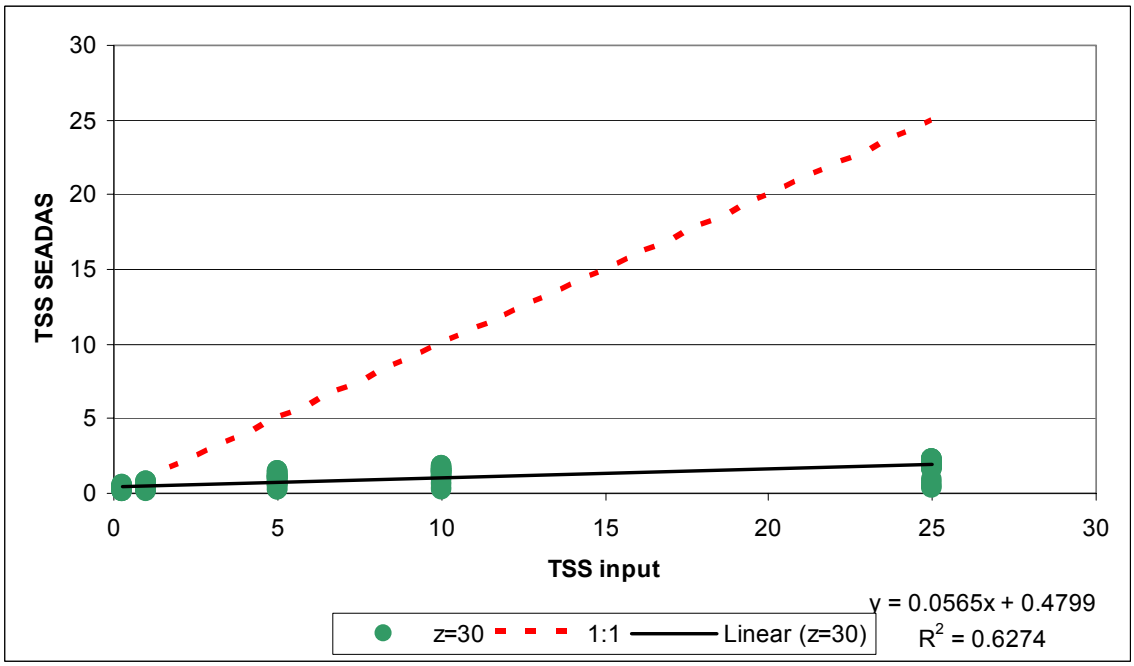

Figure 3-16. Sensitivity analysis for the retrieval of TSM for low concentrations of CDOM and chlorophyll (CDOM = 0.01, 0.08; CHL = 0.1, 0.3). It is clear that there is a spurious relationship between the *in situ* measurements and the SEADAS MODIS algorithm results. (z = water column depth in m used in the simulations; Linear = the linear regression line; 1:1 is the correct relationship without errors.)

4 A regional MODIS algorithm for the Fitzroy River Estuary

4.1 New proposed algorithms

The findings of the direct match-ups and the sensitivity analysis in previous milestone reports and summarised in Chapter 3 demonstrated that the MODIS global (standard or SEADAS) algorithms for TSM, CHL and CDOM fail in these optically complex waters. In general, for these global algorithm outputs, the CHL is overestimated and the TSM is underestimated, although for one algorithm (the CHL_Carder) we get an underestimation of CHL over the lower range of chlorophyll levels.

There is no systematic pattern in these relationships thus it is not possible to adjust any of the CHL or TSM algorithms by a simple gain and offset adjustment of the standard MODIS SEADAS algorithm outputs. If this latter option had been a possibility it would have greatly enhanced the speed of delivery of the final products. As this was not a possibility, a new approach needed to be developed and implemented. Therefore, the regional algorithm approach, based on concentration-specific inherent optical properties initially developed for Landsat image applications for the Moreton Bay and Fitzroy and Port Curtis Coastal CRC Phase I remote sensing projects, was further developed for the Fitzroy Estuary and Keppel Bay MODIS images and implemented.

4.2 Optical model

As mentioned in Chapter 1, there are two modelling approaches to determine the relationship between the inherent and apparent optical properties of the water column and the water constituents: analytical modelling and radiative transfer modelling. If an analytical approach is followed, there are two main categories of inverse methods for finding the concentrations of organic and inorganic materials (Mobley 1994). In the first category, implicit solutions are found whereas in the second category, direct or explicit estimates of the concentrations are obtained. With implicit methods the concentrations are varied to minimise the difference between calculated and measured reflectance. Implicit methods allow the use of both analytical and numerical radiative transfer models for calculating the reflectance. A more efficient method for retrieval of concentrations is a direct inversion of an analytical model using a linear matrix inversion method (MIM) as presented in Hoogenboom *et al.* (1998) and Brando and Dekker (2003).

Analytical model inversions have been applied to retrieve optical water quality variables from hyperspectral imagery (Brando & Dekker, 2003; Lee *et al.,* 2001; Hoogenboom *et al*., 1998). Hoogenboom *et al*. (1998) retrieved concentrations of chlorophyll and tripton of inland turbid waters using MIM with two spectral bands of an airborne hyperspectral R(0-) imagery. Brando and Dekker (2003) retrieved concentrations of chlorophyll, CDOM and tripton in Moreton Bay (Queensland) coastal waters using MIM with three spectral bands of a space-borne hyperspectral R(0-) imager. Lee *et al.* (2001) estimated five water column and bottom properties (chlorophyll, dissolved organic matter, suspended sediments, bottom depth and bottom albedo) by means of an optimisation scheme using all of the usable channels of a remote sensing reflectance airborne hyperspectral data set.

4.2.1 The analytical model and MIM

Here we describe the analytical model that simulates the remote sensing signal and the matrix inversion method that inverts this signal so we can estimate water quality concentrations from MODIS data. In order to retrieve TSM, CHL and CDOM from the reflectance values in a MODIS image, the analytical model that describes the colour of light emanating from the water column as a function of the light absorption and scattering by TSM, CHL and CDOM needs to be inverted. This required a rewriting of Equations 1-1 and 1-2.

Substitution of equation 1-2 in the reflectance model (Eqn 1-1) gives:

$$\frac{R}{f} = \frac{b_{b0} + \sum_{\mathrm{j}=1}^{N} b_{b\mathrm{j}}^{*} C_{\mathrm{j}}}{a_0 + \sum_{\mathrm{j}=1}^{N} a_{\mathrm{j}}^{*} C_{\mathrm{j}} + b_{b0} + \sum_{\mathrm{j}=1}^{N} b_{b\mathrm{j}}^{*} C_{\mathrm{j}}} \qquad \text{(Eqn 4-1)}$$

Since the inherent and apparent optical properties are dependent on wavelength, but the concentrations are not, this equation is rewritten to a set of M equations (for M wavelengths), where each equation has the form:

$$-a_0(\lambda_{\mathrm{i}})\frac{R(\lambda_{\mathrm{i}})}{f(\lambda_{\mathrm{i}})} + b_{b0}(\lambda_{\mathrm{i}})\left(1 - \frac{R(\lambda_{\mathrm{i}})}{f(\lambda_{\mathrm{i}})}\right) = \sum_{\mathrm{j}=1}^{\mathrm{N}}\left[a_{\mathrm{j}}^{*}(\lambda_{\mathrm{i}})\frac{R(\lambda_{\mathrm{i}})}{f(\lambda_{\mathrm{i}})} - b_{b\,\mathrm{j}}{}^{*}(\lambda_{\mathrm{i}})\left(1 - \frac{R(\lambda_{\mathrm{i}})}{f(\lambda_{\mathrm{i}})}\right)\right] C_{\mathrm{j}} \qquad \text{(Eqn 4-2)}$$

A more concise format of this equation is obtained by using matrix notation:

$$\mathbf{y} = \mathbf{A}\mathbf{x} \qquad \text{(Eqn 4-3)}$$

$$A_{ij} = a_j^*(\lambda_i)\frac{R(\lambda_i)}{f(\lambda_i)} - b_{bj}^*(\lambda_i)\left(1 - \frac{R(\lambda_i)}{f(\lambda_i)}\right), \qquad i = 1,\ldots,M \quad j = 1,\ldots,N$$
$$y_i = -a_0(\lambda_i)\frac{R(\lambda_i)}{f(\lambda_i)} + b_{b0}(\lambda_i)\left(1 - \frac{R(\lambda_i)}{f(\lambda_i)}\right), \qquad \text{(Eqn 4-4)}$$
$$x_j = C_j,$$

where **A** is an MxN matrix in which the M rows represent the number of wavelengths and the N columns represent the number of constituents. In order to distinguish vectors and matrices from other variables, they are shown in bold. The vector **x** contains the N unknown concentrations.

If the number of wavelengths equals the number of constituents the matrix A is an NxN square matrix and the concentration vector **x** can be directly calculated as the analytical solution of the linear system. If the system is overdetermined, that is, when the number of wavelengths is larger than the number of constituents to retrieve, the singular value decomposition (SVD) method can be used. This type of solution has the property of minimising the residual error in a least squares sense (for details of the method see Press *et al.,* 1992).

4.2.2 MIM implementation for the Fitzroy Estuary

To apply the MIM method to the MODIS reflectance [R(0-)] images, we need to parameterise the analytical model that describes the relationship between the R(0-) for optically deep waters as a function of the IOPs with a set of SIOPs. (We mention 'optically deep' here to distinguish the case where there is no measurable bottom influence to the remotely sensed signal).

Six sets of SIOPs were selected from the underwater light climate parameterisation of Fitzroy River Estuary fieldwork sites (see Oubelkheir *et al.,* 2006) to be used in the MODIS imagery inversion. These six SIOP sets represented the enormous diversity in the FE–KB waters with respect to their light absorption and scattering properties related to their composing materials, which vary from fine riverine suspended material to coarse resuspended estuarine material to more oceanic algae-dominated waters and all types of mixtures in between. It was this optical complexity that confounded the standard global MODIS algorithms.

The MIM inversion method was originally implemented for Australian coastal waters in Moreton Bay (Brando & Dekker, 2003) for the experimental

hyperspectral satellite Hyperion in 2003. An IDL/ENVI® routine was developed to produce chlorophyll (CHL), coloured dissolved organic matter (CDOM) and tripton (TR) maps by inverting three Hyperion R(0-) spectral bands (two centred at 490 nm and 670 nm and the bin of five of the Hyperion R(0-) bands in the 700–740 nm range). Cramer's rule was used for the analytical solution of the 3x3 linear system (Equation 4-4).

For the Phase I FE–KB Coastal CRC remote sensing project, Dekker and Phinn (2005) developed a method for processing four Landsat images over a period of 18 years (1985–2002). Unlike the Hyperion implementation where the three narrow bands are located in selected spectral ranges according to the R(0-) sensitivity model and to avoid substrate visibility, the implementation of MIM for Landsat TM 5 and ETM 7 involves the use of the three broad bands in the visible region of the spectrum. In these Landsat TM 5 and ETM 7 bands absorption features interfere and eliminate each other. Sensitivity analysis demonstrated that it was not possible to retrieve CHL at the concentration level present in Moreton Bay, Port Curtis or in the Fitzroy River Estuary with the level of noise associate with the Landsat 7 ETM imagery. Thus, for those studies CHL was fixed for all the inversions and we are left with a 3x2 linear system (three wavelengths and two constituents to retrieve, TR and CDOM for each pixel).

An outline of the steps used in the bio-optical model implementation used to estimate concentrations of water column constituents from the MODIS image data is presented in Figure 4-1. The eight spectral bands available with MODIS imagery (where Landsat only has three broad spectral bands in the visible wavelengths) enables chlorophyll estimation in addition to total suspended matter and coloured dissolved organic matter. Thus, for the current study we present the inversion of an 8x3 linear system (eight wavelengths and three constituents to retrieve, CHL, TR and CDOM for each pixel).The SVD method was used to solve this overdetermined system, as this type of solution has the property of minimising the residual error in a least squares sense.

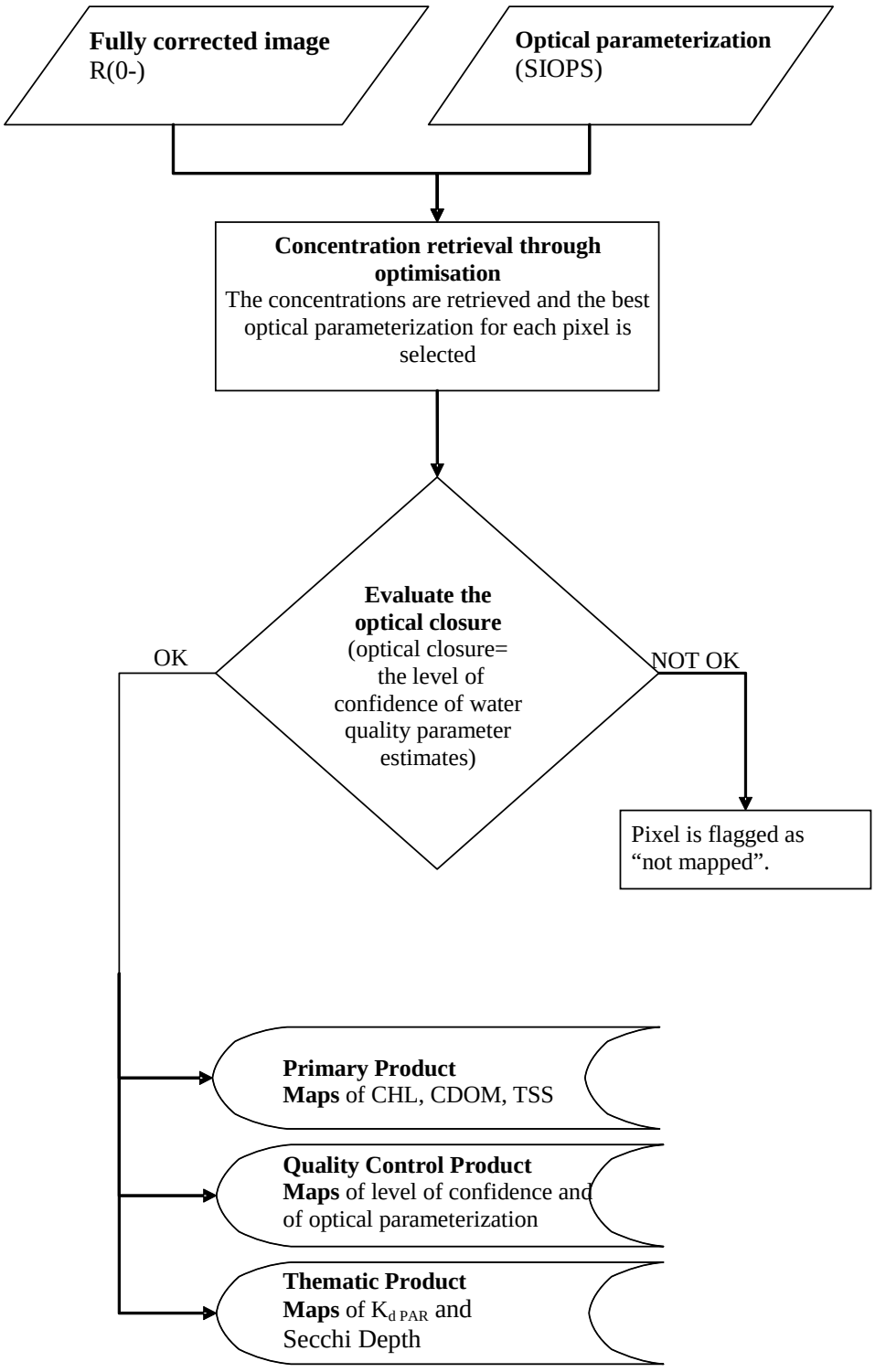

Figure[B3] **4-1. Outline of the steps used in the bio-optical model to estimate concentrations of water column constituents from the Landsat image data for the Fitzroy Phase I project (Dekker & Phinn, 2005); primary product maps were produced with MODIS**

The image inversion, that is, the water quality variable concentration retrieval in each pixel, was based on an optimisation technique that selected the best optical parameterisation for each pixel of the image. In fact, the SVD inversion (Equation 4-4), was applied iteratively to each pixel, varying the optical parameterisation within one of the six SIOP sets based on the September 2003 field campaigns for the Fitzroy River estuary. Thus we make no *a priori* assumptions about which water type is located where in the image. The inversion algorithm selects water type for each pixel, by estimating the best fit between the modelled and atmospherically corrected satellite sensor measured spectrum. Subsequently, for each selected SIOPs for that specific pixel, the correct analytical model R(0-) can be simulated allowing the use of the MIM to retrieve valid concentrations of TSM, CHL and CDOM for each pixel.

In order to calculate a measure of the optical closure in each pixel—that is, how close the reflectance spectrum from the model and satellite match each other: the closer the match the more likely the concentration estimate is valid and accurate)–d(R0-), which is the difference between the imagery reflectance [R(0-)] and the inverse-forward simulated reflectance [R(0-)], was used. The concentration values associated with the best optical closure are used for the maps and the value of d(R0-) calculated for each pixel can be presented as a map of the level of confidence of water quality parameter estimates. If the value of d(R0-) exceeds a threshold, if the retrieved concentrations are negative, or if one or more of the spectral bands of the image gives anomalous values (perhaps due to sun glint or some atmospheric haze etc.), the pixel is flagged as not mapped.

4.3 Sensitivity analysis of new regional MODIS algorithms through modelled MODIS radiances

To explore the behaviour of the proposed MODIS regional algorithms, a sensitivity analysis was performed using the SIOPs measured during the September 2003 fieldwork.

The proposed MODIS regional algorithm was applied to the same simulated set of nLw used for the sensitivity analysis of standard global algorithms (Section 1.5). The radiative transfer model (Hydrolight 4.1) was parameterised with the SIOPs of six stations measured *in situ* in September 2003 (as reported in Table 3-1).

A series of 2240 permutations of spectra were simulated varying CHL, CDOM and TSM concentrations over the actual *in situ* range during the September 2003 fieldwork (CHL = 0.1, 0.3,1.3 and 2; CDOM = 0.01, 0.08, 0.25 and 050; TSM = 0.25, 1, 5, 10 and 25).

Figures 4-2, 4-3, 4-4 and 4-5 present the behaviour of proposed regional MODIS algorithms for the retrieval of CHL, CDOM and TSM concentration as evaluated via this optical modelling, inverting R/f as estimated directly by Hydrolight.

Figures 4-6, 4-7, 4-8 and 4-9 present the behaviour of proposed regional MODIS algorithms for the retrieval of CHL, CDOM and TSM concentration as evaluated via this optical modelling, inverting R/f using the average f for each SIOP set as estimated by Hydrolight.

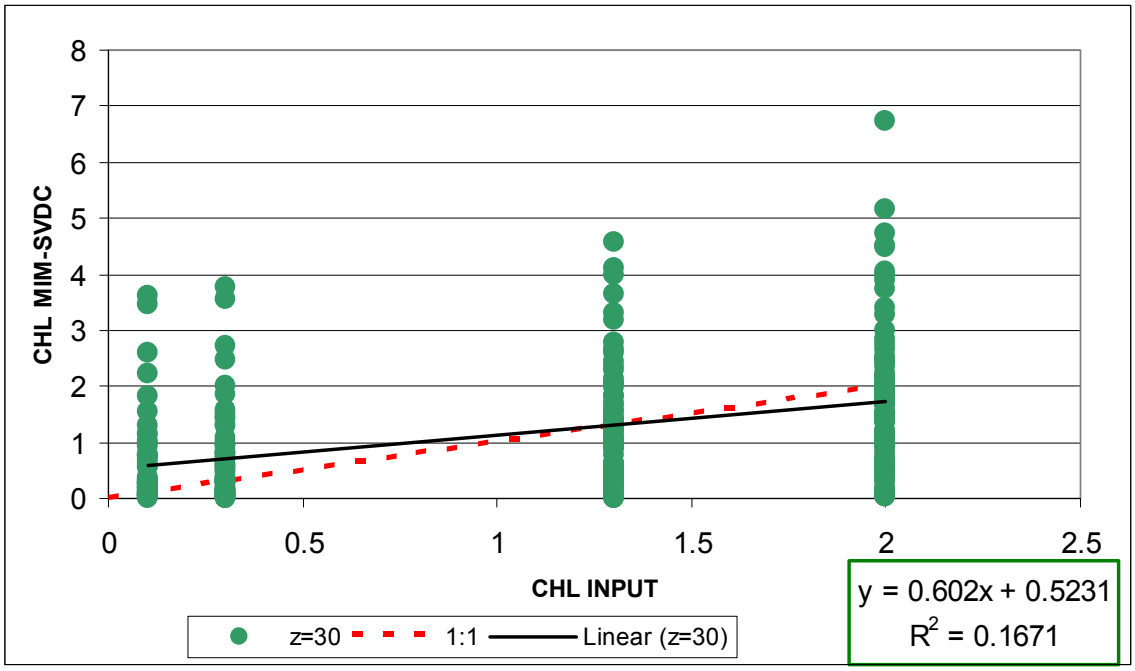

Figure 4-2. Sensitivity analysis for the proposed regional MODIS algorithm for retrieval of chlorophyll concentration while varying the concentrations of CDOM and TSM (CDOM = 0.01, 0.08, 0.25, 0,50; TSM = 0.25, 1, 5, 10, 25) over their full range using the specific inherent optical properties of light absorption and light scattering as a function of chlorophyll and TSM concentration) measured during the September 2003 fieldwork. Chlorophyll is consistently slightly overestimated but the performance of the regional algorithm is better than the SEADAS algorithm (Figure 3-12). (z = water column depth in m used in the simulations; Linear = the linear regression line; 1:1 is the correct relationship without errors)

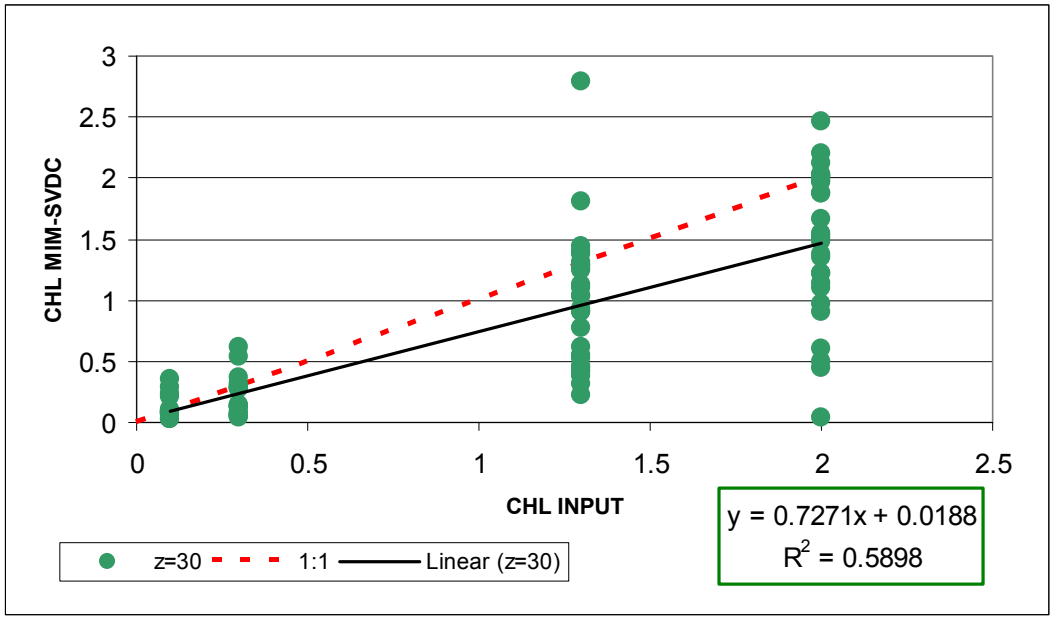

Figure 4-3. Sensitivity analysis for the proposed regional MODIS algorithm for retrieval of chlorophyll concentration for low concentrations of CDOM and TSM (CDOM = 0.01, 0.08; TSM = 0.25, 1)

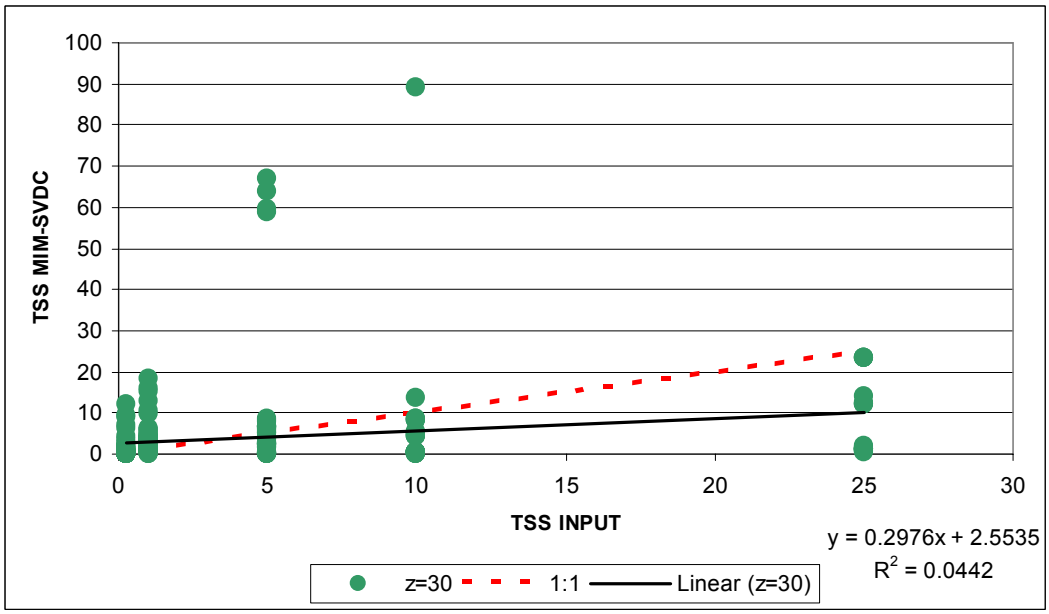

Figure 4-4. Sensitivity analysis for the proposed regional MODIS algorithm for the retrieval of TSM: All concentrations of CDOM and chlorophyll (CDOM = 0.01, 0.08, 0.25, 0.50; CHL = 0.1, 0.3,1.3, 2) (z = water column depth in m used in the simulations; Linear = the linear regression line; 1:1 is the correct relationship without errors)

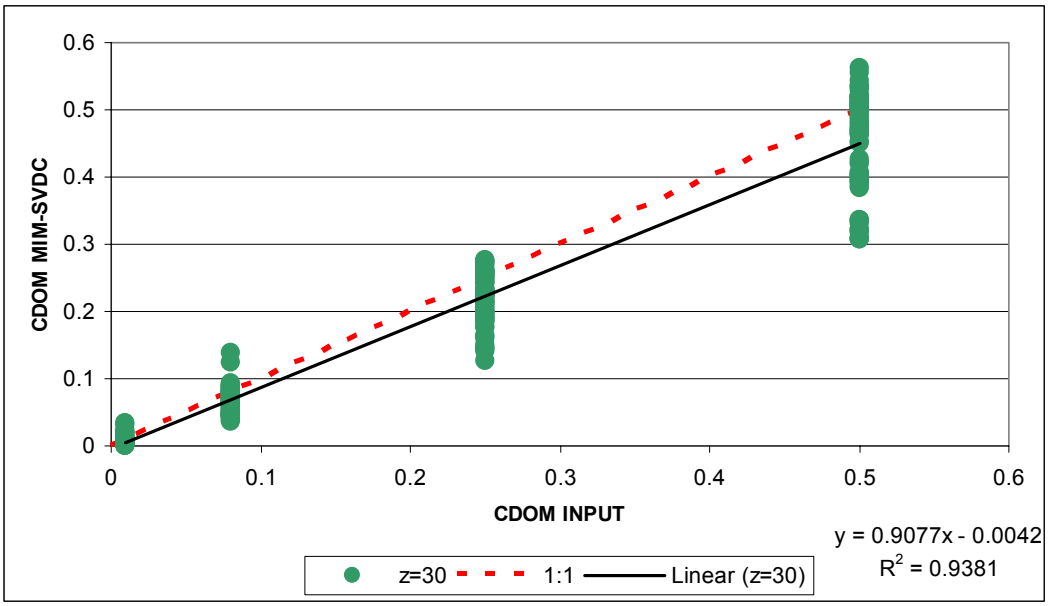

Figure 4-5. Sensitivity analysis for the proposed regional MODIS algorithm for the retrieval of CDOM: All concentrations of chlorophyll and TSM (CHL = 0.1, 0.3,1.3, 2; TSM = 0.25, 1, 5, 10, 25) (z = water column depth in m used in the simulations; Linear = the linear regression line; 1:1 is the correct relationship without errors)

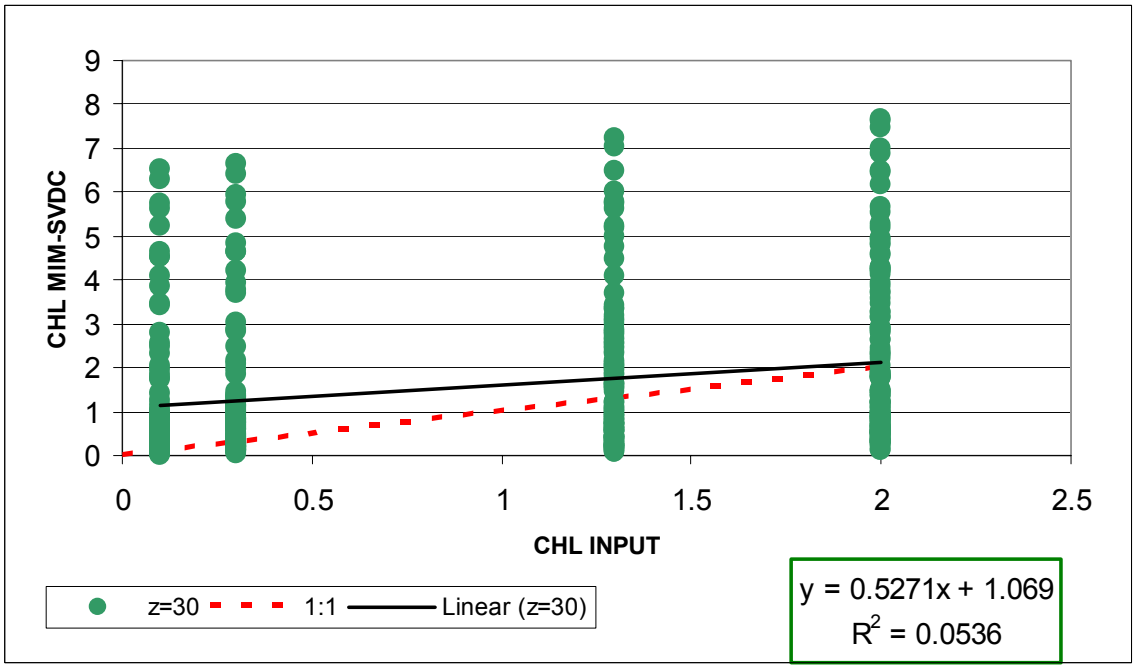

Figure 4-6. Sensitivity analysis for the proposed regional MODIS algorithm for retrieval of chlorophyll concentration while varying the concentrations of CDOM and TSM (CDOM = 0.01, 0.08, 0.25, 0.50; TSM = 0.25, 1, 5, 10, 25) over their full range using the specific inherent optical properties of light absorption and light scattering as a function of chlorophyll and TSM concentration measured during the September 2003 fieldwork. Chlorophyll is consistently overestimated but the performance of the regional algorithm is better than the SEADAS algorithm. (z = water column depth in m used in the simulations; Linear = the linear regression line; 1:1 is the correct relationship without errors)

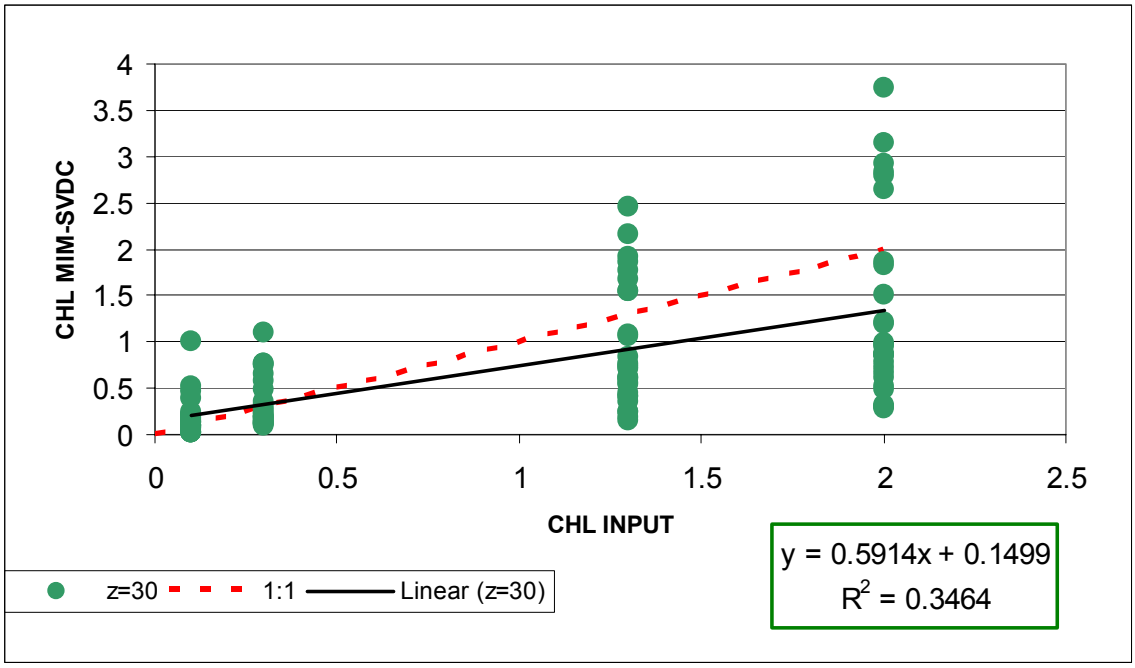

Figure 4-7. Sensitivity analysis for the proposed regional MODIS algorithm for retrieval of chlorophyll concentration for low concentrations of CDOM and TSM (CDOM = 0.01, 0.08; TSM = 0.25, 1) (z = water column depth in m used in the simulations; Linear = the linear regression line; 1:1 is the correct relationship without errors)

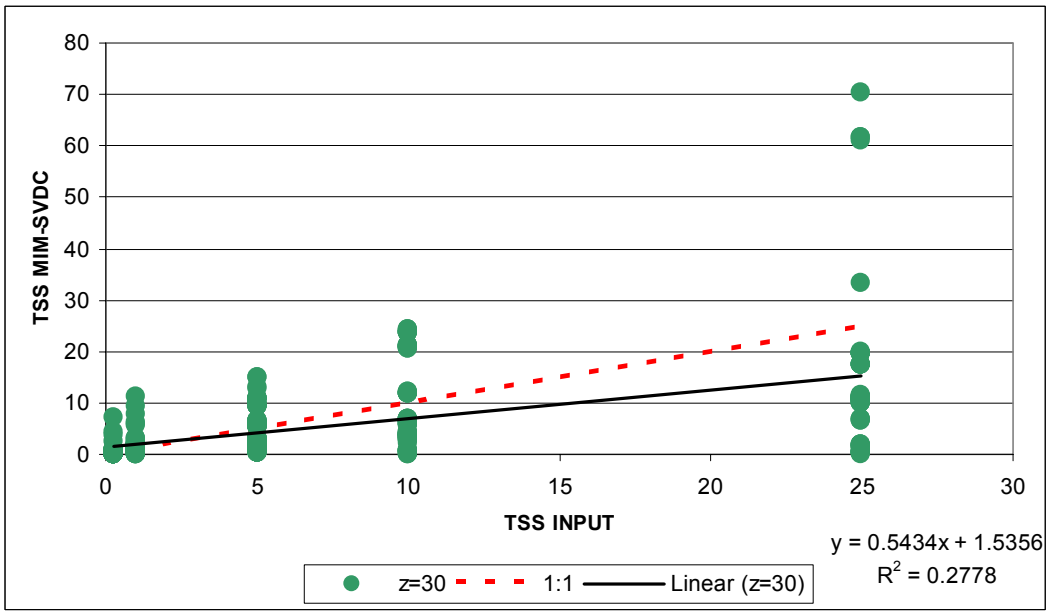

Figure 4-8. Sensitivity analysis for the proposed regional MODIS algorithm for the retrieval of TSM: All concentrations of CDOM and chlorophyll (CDOM = 0.01, 0.08, 0.25, 0.50; CHL = 0.1, 0.3, 1.3, 2). (z = water column depth in m used in the simulations; Linear = the linear regression line; 1:1 is the correct relationship without errors)

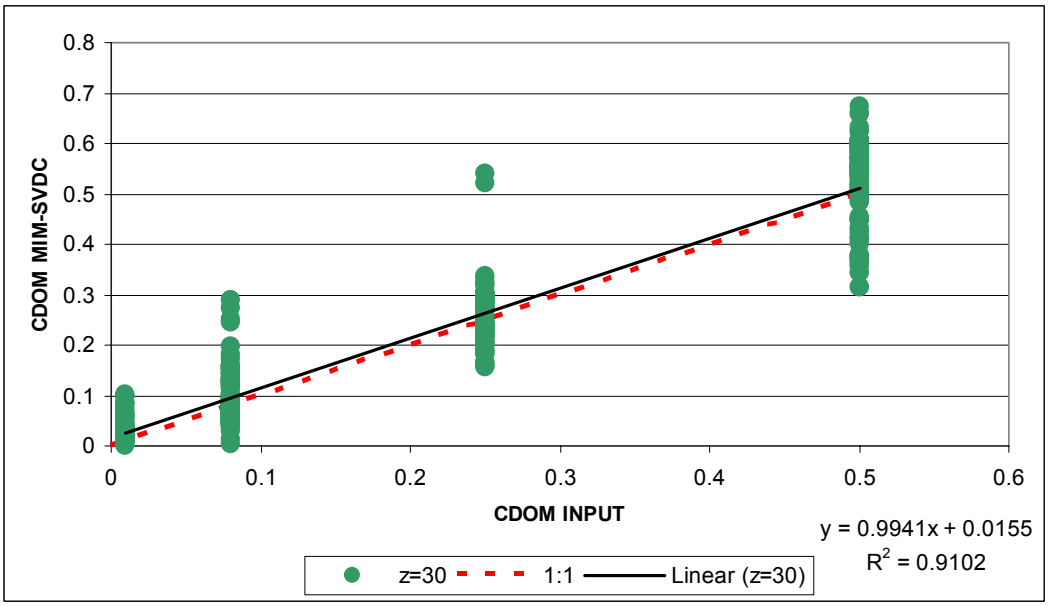

Figure 4-9. Sensitivity analysis for the proposed regional MODIS algorithm for the retrieval of CDOM: All concentrations of chlorophyll and TSM (CHL = 0.1, 0.3, 1.3, 2; TSM = 0.25, 1, 5, 10, 25). (z = water column depth in m used in the simulations; Linear = the linear regression line; 1:1 is the correct relationship without errors)

4.3.1 Implementation to MODIS imagery

To apply the MIM method to the MODIS imagery, we need to adjust the formulation of Equations 4.1–4.3 to use spectral quantities adopted as output by SEADAS: nLw (normalised water leaving radiance) or R_{rs} (the remote sensing reflectance). Note that we do not use the standard algorithms for the water quality estimation from SEADAS as they were shown to be erroneous. Thus we are using as much as possible of the standard processing for MODIS, as the correction of MODIS satellite imagery for atmospheric or air–water interface effects is very complex. R_{rs} is a quantity measured above the surface and r_{rs} is its counterpart measured below the surface. According to Lee *et al.* (1999) R_{rs} and r_{rs} are interchangeable using the following relationship:

$$r_{rs} = \frac{R_{rs}}{0.52 + 1.7R_{rs}} \qquad \text{(Eqn 4-5)}$$

The subsurface remote sensing reflectance r_{rs} is directly derived for the MODIS data with SEADAS. Our MIM inversion algorithm is, however, based on the subsurface irradiance reflectance. In order to convert r_{rs} to R(0-) we need to introduce the Q factor that transforms r_{rs} to R(0-). However, this Q factor is very

hard to measure or to model adequately. Therefore, the MIM equation has been rewritten for r_{rs} . Equation 1-1 can be re-written as:

$$r_{rs} = \frac{f}{Q}\frac{b_b}{a+b_b} \qquad \text{(Eqn 4-6)}$$

Or as

$$\frac{r_{rs}}{f/Q} = \frac{b_b}{a+b_b} \qquad \text{(Eqn 4-7)}$$

Hence Equation 4-1 becomes:

$$\frac{r_{rs}}{f/Q} = \frac{b_{b0} + \sum_{j=1}^{N} b_{bj}^{*} C_j}{a_0 + \sum_{j=1}^{N} a_j^{*} C_j + b_{b0} + \sum_{j=1}^{N} b_{bj}^{*} C_j} \qquad \text{(Eqn 4-8)}$$

Then Equation 4-8 becomes

$$A_{ij} = a_j^{*}(\lambda_i)\frac{r_{rs}(\lambda_i)}{f(\lambda_i)/Q(\lambda_i)} - b_{bj}^{*}(\lambda_i)\left(1 - \frac{r_{rs}(\lambda_i)}{f(\lambda_i)/Q(\lambda_i)}\right), \qquad i = 1,...,M \quad j = 1,...,N$$

$$y_i = -a_0(\lambda_i)\frac{r_{rs}(\lambda_i)}{f(\lambda_i)/Q(\lambda_i)} + b_{b0}(\lambda_i)\left(1 - \frac{r_{rs}(\lambda_i)}{f(\lambda_i)/Q(\lambda_i)}\right),$$

$$x_j = C_j, \qquad \text{(Eqn 4-9)}$$

Based on an extensive series of Hydrolight simulations, Lee *et al.* (1999) suggest including the second order of the Taylor series to describe the relationship:

$$r_{rs} = (0.084 + 0.17 * \frac{b_b}{a+b_b})\frac{b_b}{a+b_b} \qquad \text{(Eqn 4-10)}$$

This quadratic equation can be solved for $\frac{b_b}{a+b_b}$ and written as:

$$\frac{b_b}{a+b_b} = -0.84 \pm \frac{\sqrt{0.84^2 - 4*0.17*r_{rs}}}{2*0.17} \qquad \text{(Eqn 4-11)}$$

This was used as input in the left-hand side of Equation 4.7.

4.4 Distributed processing of the large MODIS dataset

For this project we processed the MODIS/Aqua time series covering the period from November 2002 to the end of 2004 as this covers the biogeochemical model data runs and the *in situ* measurement campaigns of this project. MODIS/Aqua (with a general overpass time of 13:30 in the afternoon) was chosen over MODIS/Terra (with a general overpass time of 10:30 in the morning) as MODIS/Aqua is a better calibrated instrument (NASA is currently in the process of reprocessing the MODIS/Terra datasets to improve the calibration errors).

The processing method was to first run the MODIS data through the SEADAS 4.8.4 version installed at the CSIRO Marine and Atmospheric Research data processing cluster in Canberra. This produced MODIS images of 'at surface' reflectance data (thus corrected for all earth's curvature, sensor to earth distance, atmospheric haze, sky and sun glint at the water surface, etc.). This processing was done via distributed processing scripts set up and run by Dr Edward King and Dr Matt Paget. The roughly 1000 images were processed in 12–24 hours using ~20 Linux machines. The SEADAS flag 'Hi radiance' was turned off to increase the near-shore data availability of pixels (The Fitzroy waters are too light and too brown for the standard flags to understand correctly).

After the whole set of MODIS image data was SEADAS-processed, the second processing (for the matrix inversion) was carried out to estimate TSM, CHL and CDOM from the at-surface reflectance data. This processing took about 8–10 hours using five Linux machines. For this final processing to concentrations we discarded the deep blue MODIS spectral band at 412 nm because research within another CSIRO project (Wealth from Oceans) has demonstrated that atmospheric correction of this blue band is often too erroneous to accept.

The final MIM processing was carried out with the spectral bands located between 441 nm and 678 nm.

An ancillary program 'HDFLook MODIS' was adopted to extract the parameters of interest for the geographical region of interest (the Fitzroy River estuary and Keppel Bay area) from the on-line data storage. 'HDFLook MODIS' is a comprehensive Unix-based application developed by NASA for MODIS data users to access, visualise, re-map and subs*et* all the parameters contained in the SEADAS HDF files. A series of Linux scripts were implemented to extract and calibrate to SI units the SEADAS plus MIM-derived parameters and to build the ENVI-IDL headers, to ensure compatibility with our image processing package

ENVI. Finally an in-house tool for visualisation of the results was implemented: the ‘MODIS time series visualisation tool‘.

4.5 Validation of the new MIM algorithm with available field data and comparison with standard ‘global’ MODIS products

For validation purposes the only data set that was independently available from the remote sensing algorithm development is the GBRMPA ‘long-term *in situ* chlorophyll data set‘, which includes measurements going back as far as 1992 (thus including the start of the first contemporary ocean colour sensor SeaWiFS, launched in 1997).

The GBRMPA measurements were not designed for remote sensing validation purposes and thus the sampling protocols do not follow remote sensing validation guidelines {i.e. minimum distance of 10 km from land or islands (see Figure 3-1), HPLC estimate of chlorophyll *a* etc.}. For this reason, in this work this data set will be used to assess the ‘suitability‘ more than the absolute ‘validity‘ of the remote sensing data.

The long-term *in situ* chlorophyll data were used to evaluate the CHL_MIM product as well as the most suitable standard MODIS coastal water (as opposed to ocean water) algorithm called CHL_Carder. For this comparison, we extracted from the remote sensing data the average value of the nine pixels (a square of 3x3 pixels) centred at the GPS location of the *in situ* measurements, for each available date. The reason for this was that the long-term *in situ* chlorophyll data is presented as being measured at exactly the same location since 1992 whereas in reality wind and wave conditions cause the boat to be placed at different locations in the lee of the islands for safety. In addition, the time of the measurement was not coincidental with the satellite overpass and thus the water sampled by the *in situ* program may not have been in the same location as when the satellite passed over.

Another reason for selecting a 3x3 pixel area is that it avoids comparing a single, less valid or accurate pixel with an *in situ* measurement. Unfortunately it should also be realised that the AIMS *in situ* sample is of a few litres of water only, whereas the MODIS pixels are 1 km x 1 km (and then averaged over 3x3 pixels) to 9 km^2. The variability across this area is much better captured by the MODIS imagery. All the above qualifications of the validation method should be taken into consideration when interpreting these results.

Table 4-1 presents the summary of the comparison of chlorophyll retrieval from MODIS/Aqua data with the CHL_Carder and MIM algorithm for 2003–2004 with

the AIMS data. The number of pixels that are available for the comparison with *in situ* data is lower for the CHL_MIM (20 pixels) than for CHL_Carder retrieval (70 pixels). As is evident from the comparison of CHL_MIM and CHL_Carder in Figures 3-2 to 3-8, the MIM implementation suffers from an 'over-cautious' flagging that limits the number of processed pixels. This is probably due to the necessity of CHL_MIM to use all the available MODIS bands for the inversion. Thus, although the MIM method is better and uses more spectral bands it is also more susceptible to error flagging as it relies on more spectral bands data.

Table 4-1. Root mean square error of chlorophyll (in µg l^{-1}) retrieval from MODIS/Aqua data using the CHL_Carder and MIM algorithm for MODIS validation 2003–2004 and AIMS biogeochemical modelling data

Comparison	No. of points	RMSE
CHL_MIM	20	1.55
CHL_Carder all points	70	2.22
CHL_Carder same points as MIM	20	2.00
CHL_BGCM same as MIM	20	2.87

The root mean square error (RMSE) of the CHL_Carder retrieval vs. the AIMS data did not vary significantly when we use only those pixels that were also inverted by our CHL_MIM algorithm for comparison with *in situ* data (a RMSE of 2.22 µg l^{-1} for 70 points and a RMSE of 2.00 µg l^{-1} for 20 points).

Figure 4-10 presents the comparison of chlorophyll retrieval from MODIS/Aqua data with the CHL_Carder and MIM algorithm with the AIMS data for the points common to the two sets. The difference in the RMSE between the two retrieval algorithms (1.55 µg l^{-1} for CHL_MIM and 2.00 µg l^{-1} for CHL_Carder) can be explained by a higher occurrence of gross overestimations of chlorophyll by the CHL_Carder algorithm (see values over 100% error in Figure 4-11).

The CHL_Carder algorithm is a switch-algorithm, which means that it uses a semi-analytical inversion for concentrations ranging from 0 to 1.5 to 2 µg l^{-1} whereas above this threshold it uses an empirical two-wavelength bands algorithm based on the MODIS bands $R_{rs}(488)/R_{rs}(551)$ ratio. These ratio-based empirical algorithms have a tendency to grossly overestimate chlorophyll in the presence of moderate or high TSM and CDOM as occurs frequently in the FE–KB system.

In this study, focus was on the chlorophyll estimations as that is the only suitable data available for validation. The MIM inversion method also simultaneously retrieves TSM and CDOM. Thus, these estimates are based on an internally consistent, physics-based description of light in water as a function of light absorption and light scattering by the three water quality variables. This is unlike the standard algorithms that use individual (but sometimes the same) spectral bands in an empirical band ratio to estimate different components (thus, often these standard algorithm assessments are not independent of each other and may cause erroneous cross-correlation such as a confusion of high CDOM with high chlorophyll). Therefore, although the RMSE values are not far apart for the CHL_Carder and MIM methods, the validity of the MIM algorithm product is higher (i.e. the chlorophyll map is really depicting chlorophyll and not perhaps something spectral that co-varies with chlorophyll).

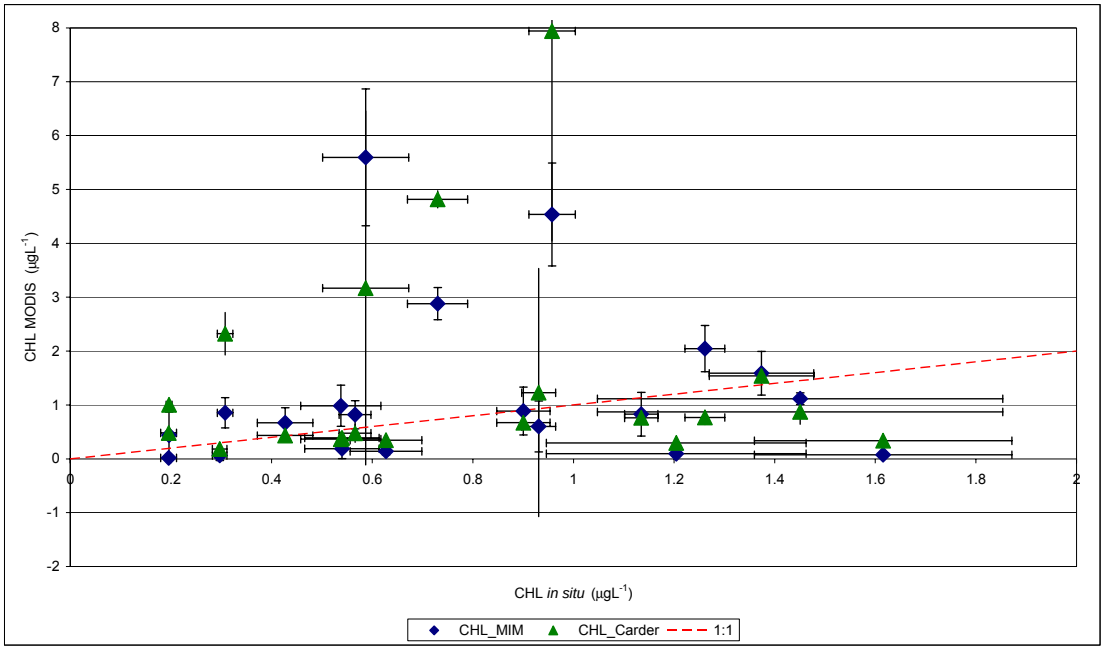

Figure 4-10. Comparison of chlorophyll estimates from MODIS/Aqua data using the CHL_Carder and MIM algorithms with the AIMS data. Only the points common to the two sets are plotted. See Table 4-1.

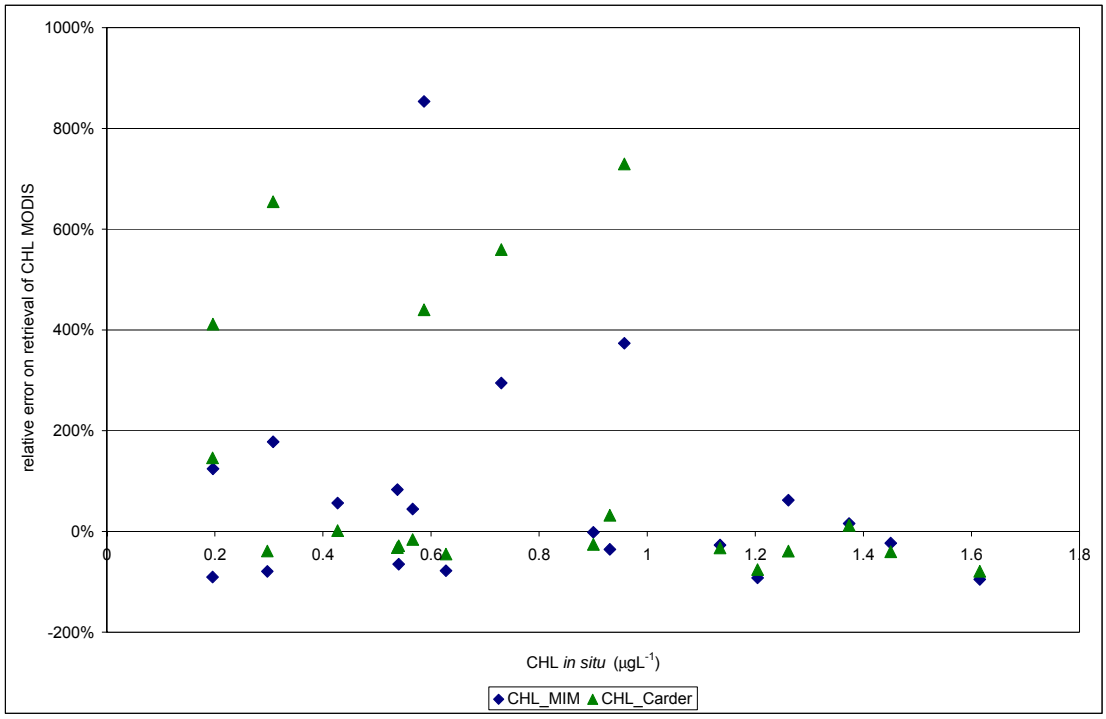

Figure 4-11. Relative error of chlorophyll estimates from MODIS/Aqua data using the CHL_Carder and MIM algorithms with the AIMS data. Only the points common to the two sets are plotted.

5 Description of spatial and temporal variability in the MODIS data

5.1 Introduction

In this chapter a qualitative analysis of the spatial and temporal patterns contained in one year of MODIS/Aqua chlorophyll and total suspended solids data was undertaken to describe patterns of regional and temporal variability as well as considering the implications for long-term monitoring.

5.2 General methods

This qualitative analysis was primarily concerned with characterising natural variation and how this may affect the comparison of the MIM outputs with the Fitzroy Estuary biogeochemical model products. This analysis builds on the characterisation of the biases in the data, described in the section on validation (Section 4.5).

We also assess whether some of the assumptions on the boundary conditions of the biogeochemical model that were made earlier in the project do hold true. In fact the concentration of chlorophyll and total suspended matter were fixed to one value over the year across the boundary.

For this analysis all data were log (Ln) transformed and mean values over the year of data were computed for each pixel, as a log distribution of concentrations is most likely.

Temporal analysis of the dataset needs to elucidate the major temporal patterns (e.g. months, seasons and inter-annual patterns) of variation that might need to be accounted for in the design of a monitoring program.

However, at finer scales of days to weeks, analysis must determine the implications of any significant short-term variation (e.g. short-term blooms or resuspension events) that might be missed by aggregation to larger temporal domains. Alternatively, where a correlation structure is present over these scales, the implications for meeting assumptions of independent samples need to be addressed.

5.3 Description of variability

Figure 5-1 presents the map of the log-transformed values for all suitable images over 2003 of the CHL retrieval by the MIM algorithm. The CHL log_mean value is higher than 2 µg l^{-1} in most of the inner Keppel Bay, and a band of CHL concentration ranging from 0.8 to 1.4 µg l^{-1} is evident all along the coastline from Yeppoon to the North of Curtis Island.

Figures 5-2 and 5-3 present the map of the log-transformed values for the wet and dry season of 2003 of the CHL retrieval by the MIM algorithm. The CHL log_mean value for the wet season (January to April 2003, Figure 5-2) has generally higher values than the CHL log_mean value for the dry season (May to December, Figure 5-3). This probably responds to the occurrence of a minor flood event in February 2003, or may only be a result of the higher summer temperatures in the water body.

Figure 5-4 presents the map of the log-transformed values for 2003 of the TSM (as tripton) retrieval by the MIM algorithm. The TSM log_mean is higher than 15–20 g l^{-1} in the inner Keppel Bay, with the concentration rapidly decreasing towards concentrations lower than 1 g l^{-1} in the outer Keppel Bay.

Figures 5-5 and 5-6 present the map of the log-transformed values for the wet and dry season of 2003 of the TSM retrieval by the MIM algorithm. The TSM log_mean value for the wet season (January to April, Figure 5-5) has generally similar values to the TSM log_mean value for the dry season (May to December, Figure 5-6). The occurrence of the minor flood event in February 2003 is not visible at this scale in the TSM data. However, as mentioned previously, the tidal resuspension is strongly dependent on the occurrence of king tides in this area. The MODIS image data may also be influenced by a relatively high number of king tide situations.

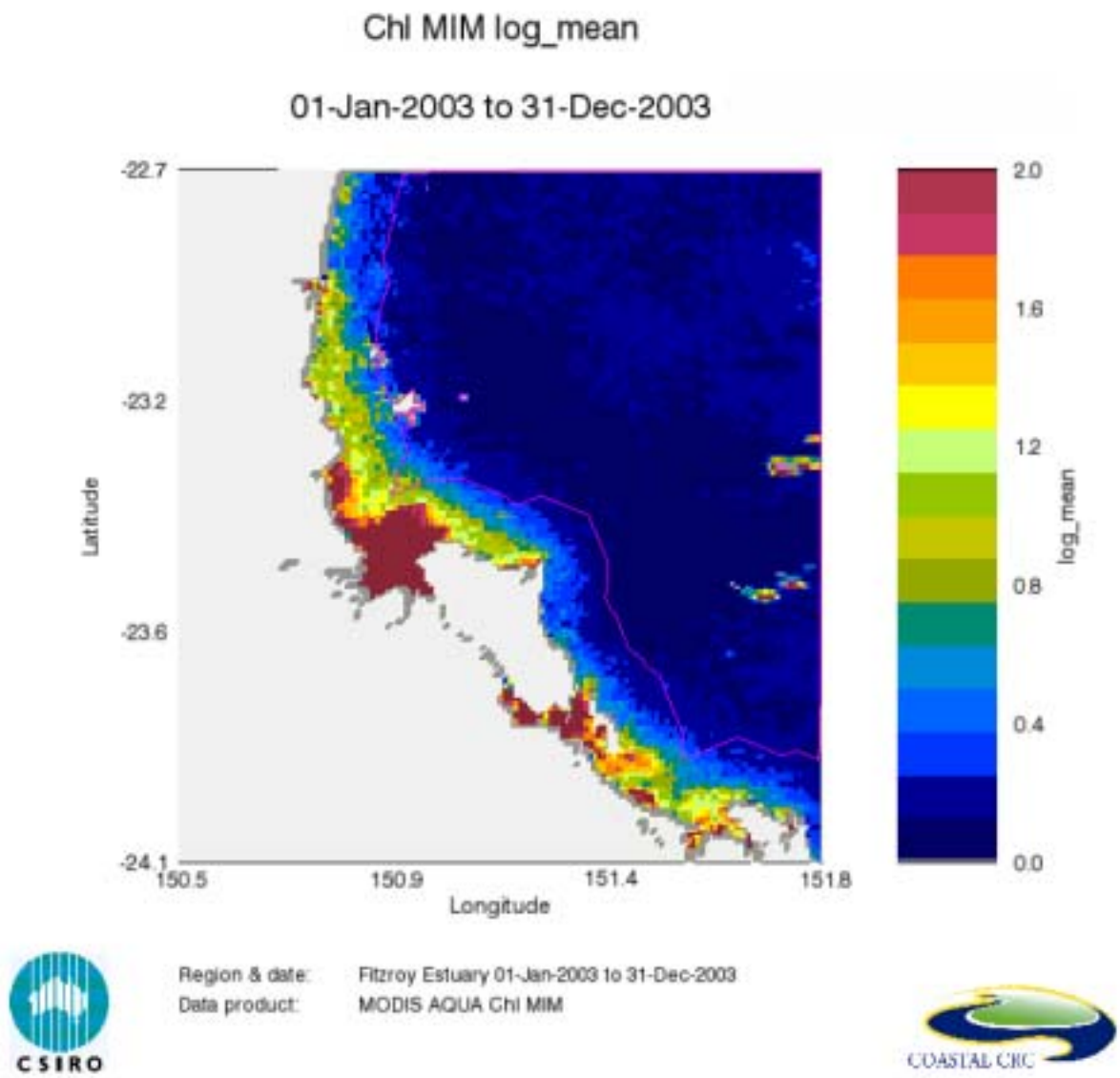

Figure 5-1. Map of the log-transformed values (log_mean) for 2003 of the CHL retrieval by the MIM algorithm

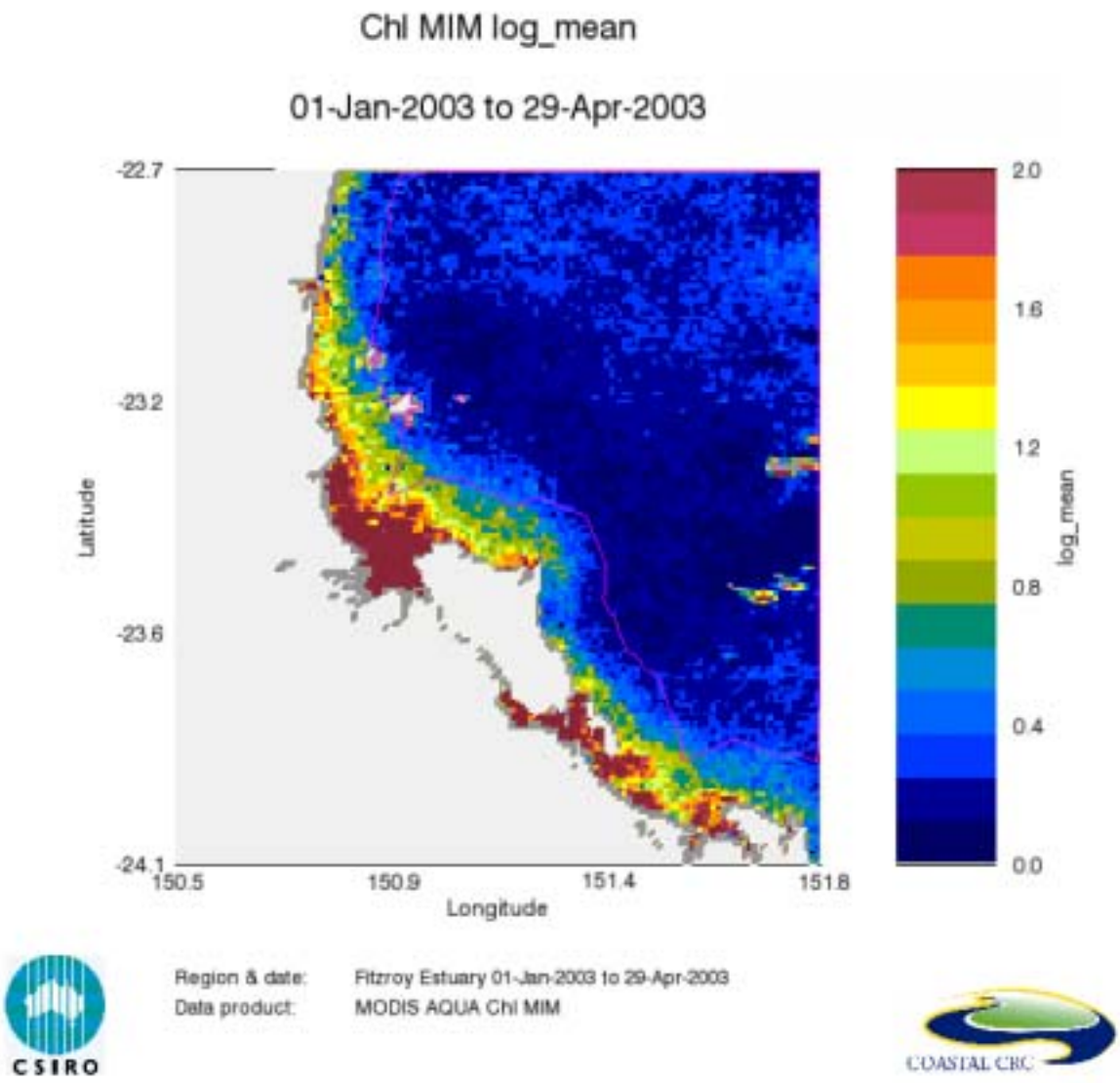

Figure 5-2. Map of the log-transformed values (log_mean) for the wet season covering January–April 2003 of the CHL retrieval by the MIM algorithm

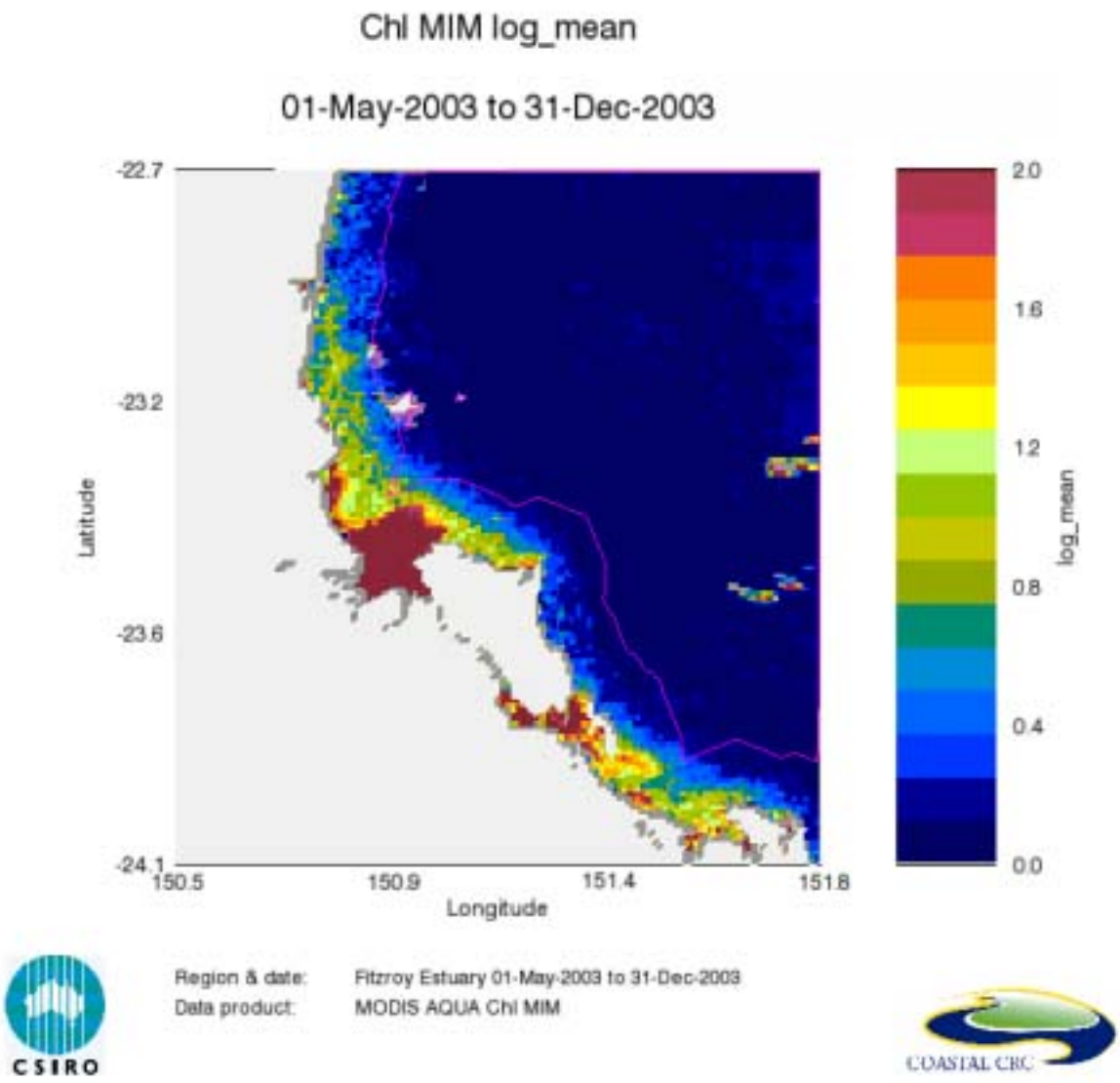

Figure 5-3. Map of the log-transformed values (log_mean) for the dry season covering May–December 2003 of the CHL retrieval by the MIM algorithm

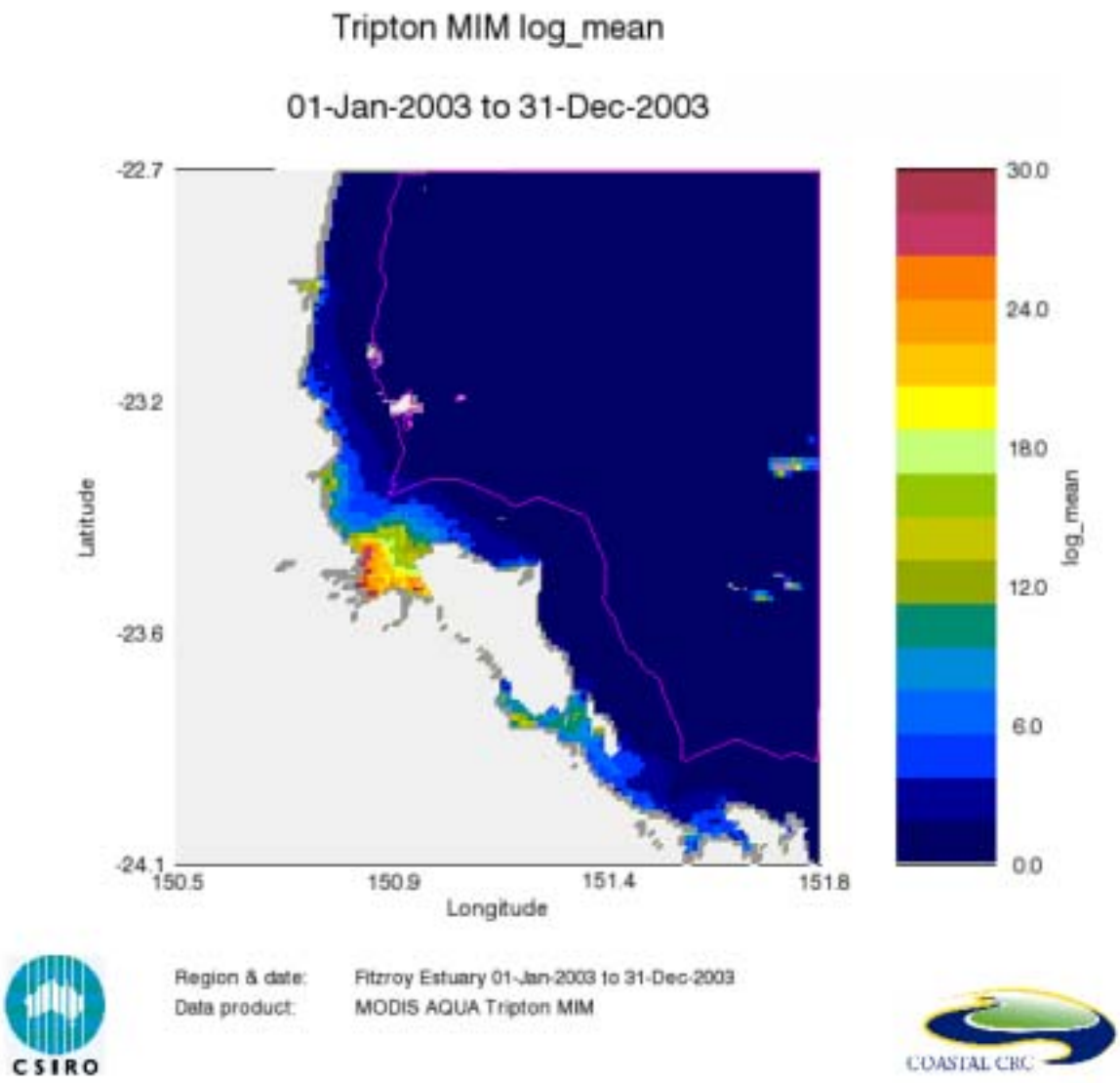

Figure 5-4. Map of the log-transformed values (log_mean) for all 2003 of the TSM (as tripton) retrieval by the MIM algorithm

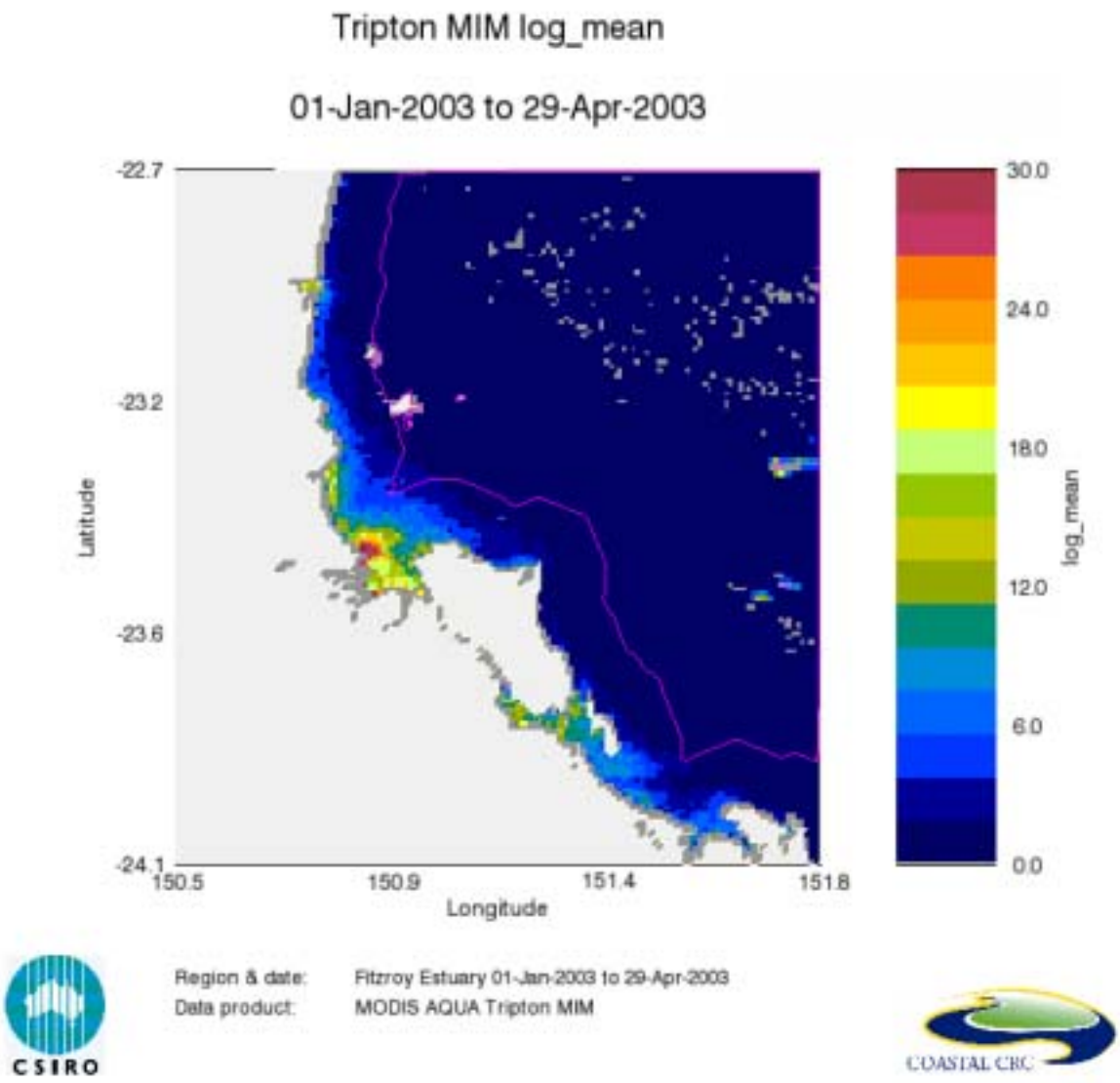

Figure 5-5. Map of the log-transformed values (log_mean) for January–April 2003 of the TSM (as tripton) retrieval by the MIM algorithm

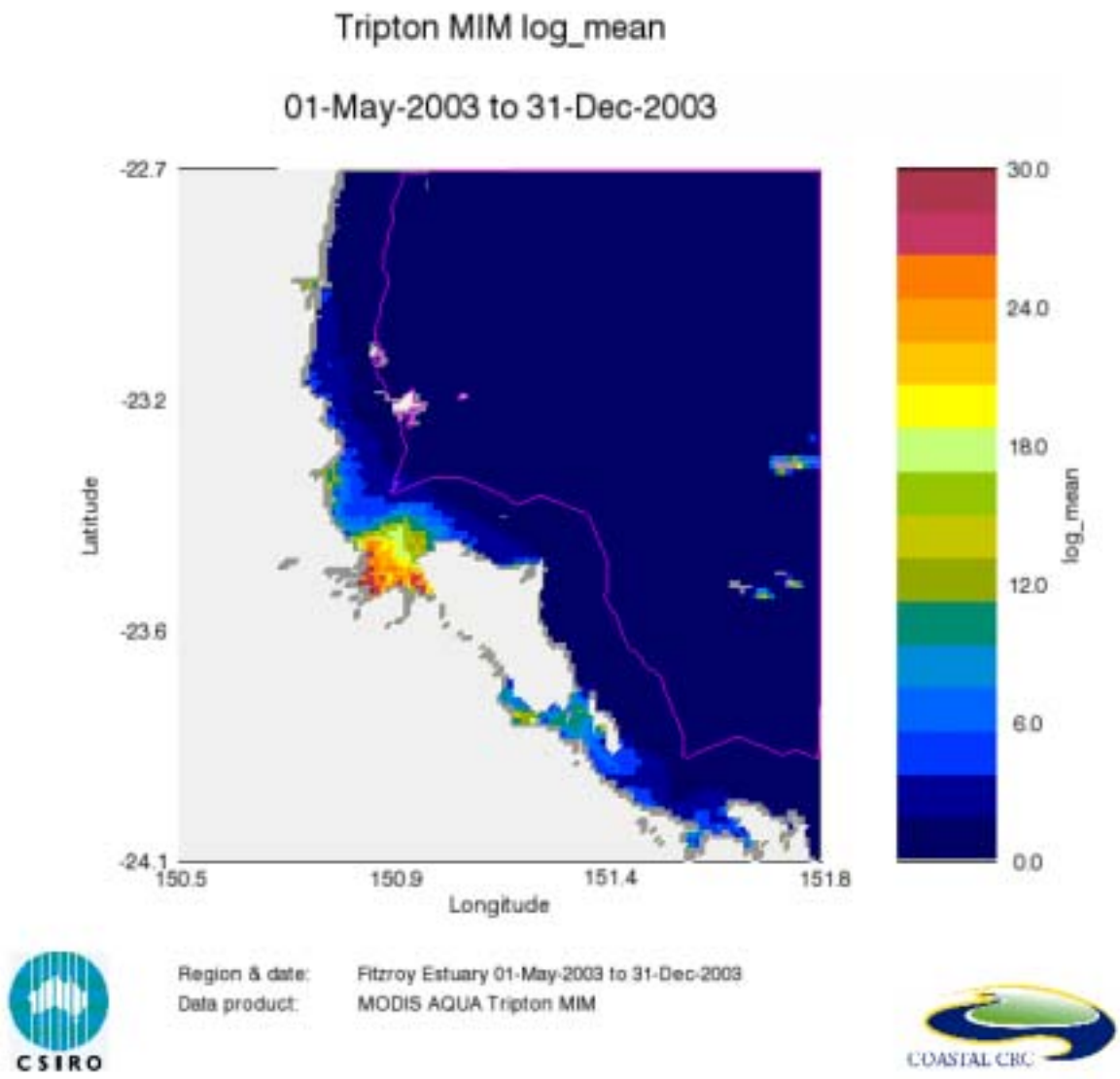

Figure 5-6. Map of the log-transformed values (log_mean) for May–December 2003 of the TSM (as tripton) retrieval by the MIM algorithm

6 Comparison of chlorophyll and TSM fields from MODIS with Fitzroy Estuary model products

6.1 Introduction to estuary model products

The details in this section were extracted from Robson *et al.* (2006).

6.1.1 Purpose of the model

The purpose of the biogeochemical model study was, in combination with field and laboratory studies, to:

1. Understand how nutrients are transported through and transformed within the Fitzroy estuary and Keppel Bay; and
2. Predict how this will change in response to changes in flows and nutrient loads resulting from changes in catchment land use.

In general terms, the aim of the biogeochemical model was to provide information to facilitate management of the estuary and its catchment in the context of ameliorating the impact of catchment-derived materials on the Great Barrier Reef lagoon. The Fitzroy model was based on the model of Murray and Parslow (1999) for Port Phillip Bay.

For the Coastal CRC Fitzroy contaminants project, the aim was to develop a model that would allow us to improve our understanding of the system dynamics and predict the effects of changes in loads and flows on primary production, water column concentrations of sediments and nutrients, and exports to the Great Barrier Reef lagoon over a time scale of a year or more. It follows that the model could be assessed as performing well if it could reproduce observed variations in salinity, sediment concentrations, nutrients (especially total nitrogen and dissolved inorganic nitrogen) and chlorophyll *a* along the length of the estuary over a 12-month period that includes a wet season and a dry season, using process-based algorithms, a consistent set of parameter values and realistic inputs.

6.1.2 Processes and parameters

Processes included in the biogeochemical model for the Fitzroy contaminants project included remineralisation of organic material, growth and mortality of benthic micro-algae, growth and mortality of three phytoplankton groups (small and large phytoplankton and *Trichodesmium*), growth and mortality of two zooplankton size classes (including grazing of phytoplankton), nitrogen fixation by benthic micro-algae and *Trichodesmium*, nitrification, denitrification, phosphorus adsorption and desorption, exchanges between sediment layers and between sediments and the water column, growth and mortality of seagrasses and macro-algae, and physical processes affecting hydrodynamics and sediment dynamics. The algorithms used to define each of these processes are described by Robson *et al*. (2006) and Murray and Parslow (1999).

Water column and sediment-bed nutrient and sediment concentrations in the FE–KB system were initialised with observations from the first intensive field campaign in the Fitzroy contaminants project in September 2003. This survey occurred during the long dry season, when concentrations were not changing rapidly. The model was then run from September 2003 through to the end of February 2005. This allowed a run-up of almost a year between the start of the simulation and the time of the next major field campaign (August 2004), and allowed comparison of model results with observations during the two major seasons (a second dry-season field campaign was conducted during August 2004 and a wet-season campaign was conducted in February 2005).

6.1.3 Scales (time and space)

For this model the emphasis was on prediction of seasonal patterns and trends, ideally with a sufficient resolution to simulate the effects of events such as storms that may have immediate influences on a daily to weekly scale. At the same time, we wanted to be able to conduct scenarios to predict responses on a scale of one to three years.

The area selected for modelling included the Fitzroy estuary below the barrage at Rockhampton and much of Keppel Bay. A curvilinear grid was applied Figure 6-1), with grid resolution varying from 200 m in Fitzroy estuary to 2 km at the seaward boundary of Keppel Bay and vertical layers varying from 0.5 m at the surface to 2 m at the bottom near the maximum depth of 18 m (Herzfeld *et al*., 2005). For numerical stability, hydrodynamic models on these scales require integration with time steps on the order of 20 seconds.

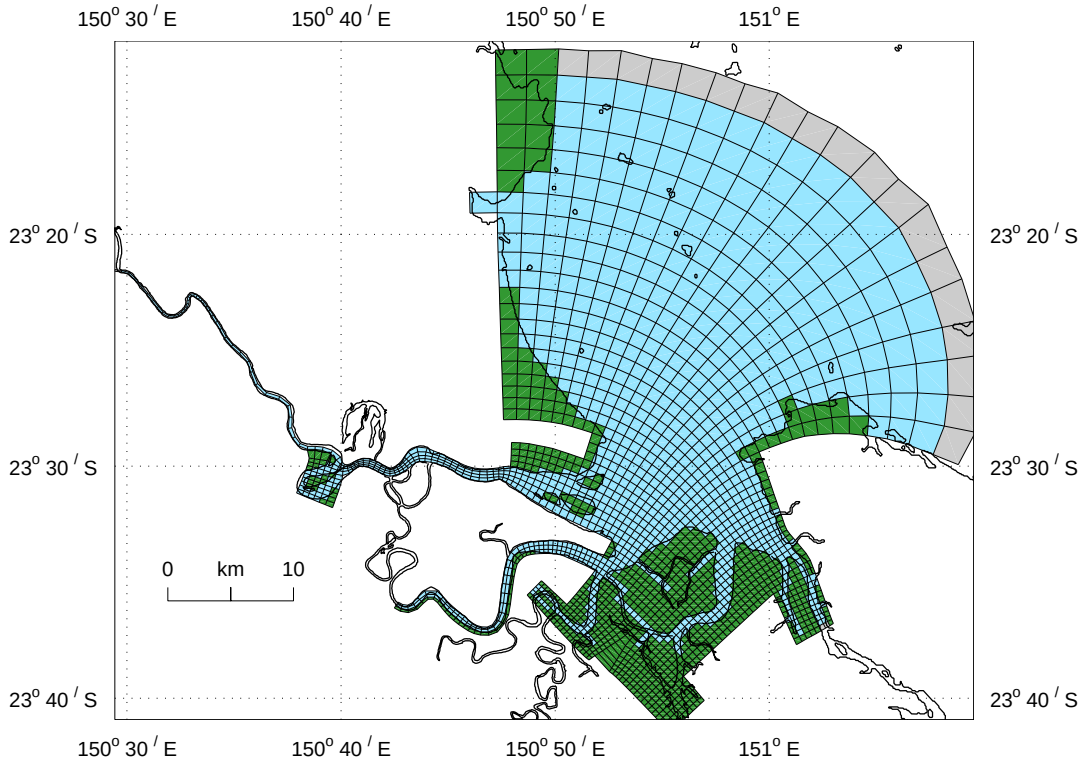

Figure 6-1. A two-dimensional view (looking down from above) of the three-dimensional model grid used for the Fitzroy Estuary–Keppel Bay model (from Herzfeld *et al.,* 2005). Green cells represent land and grey cells represent the ocean boundary, where Keppel Bay meets the Great Barrier Reef lagoon

The real-time to run-time ratio for the coupled Fitzroy model on 12 processors of a high-performance scientific computer in 2005 was about 70:1 (allowing a one-year simulation to be completed within one week).

6.1.4 Model output

For the FE–KB biogeochemical model, required outputs included (a) predicted concentrations of nitrogen in the water column and (b) an estimate of how much nitrogen is exported to the Great Barrier Reef lagoon. Also important, but secondary to these factors, were concentrations and exports of phosphorus, an estimate of primary production, and an understanding of the relative of importance of processes such as settling and resuspension, nitrification and denitrification, nitrogen fixation, remineralisation, benthic and pelagic primary production.

6.1.5 Model calibration

In the case of the Fitzroy contaminants project, model calibration was conducted primarily against observational data from the August 2004 (dry-season) field campaign, leaving only the February 2005 (wet-season) field campaign for independent verification. Unfortunately, the calibration period did not include a significant inflow event and thus parameters relating to freshwater nutrient loads were not adequately calibrated in the first instance. Comparison of model results with field observations for February 2005 indicated a need to increase the value of the parameter defining the breakdown rate of detrital material in incoming freshwater to reflect that this material was more readily bio-available than 'old' detrital material in the estuary. Hence, there was no completely independent verification dataset for the FE–KB model. As is often the case, resource constraints did not allow additional field campaigns.

Spatial comparisons of wet- and dry-season observational data and simulated concentrations of total nitrogen, total phosphorus, dissolved organic nitrogen, dissolved inorganic nitrogen, dissolved organic phosphorus, dissolved inorganic phosphorus, chlorophyll *a* and dissolved oxygen are given by Robson *et al.* (2006).

In general, Robson *et al.* (2006) concluded that the FE–KB model simulates dry-season concentrations of nitrogen and phosphorus (as dissolved organic nitrogen – DON, dissolved organic phosphorus – DOP, dissolved inorganic nitrogen – DIN, dissolved inorganic phosphorus – DIP, particulate nitrogen – PN and particulate phosphorus – PP) well.

Simulation of wet-season conditions is reasonable, with some reservations: wet-season particulate nitrogen and dissolved organic nitrogen and phosphorus are underestimated by the model. This may be due to the difficulty of estimating inflow nutrient concentrations under high flow conditions or to overestimation of the rate of deposition of fresh particulate material in the Fitzroy Estuary. Analysis of sediment modelling results (Margvelashvili *et al*., 2005) found that suspended solids were underestimated during high flow events. Possible reasons discussed by Margvelashvili *et al.* (2005) include insufficient data to prescribe the inflow boundary condition and gaps in our understanding of sediment processes.

6.2 Temporal and spatial comparison of the MODIS/Aqua image results and the biogeochemical model results: making the data sets comparable

In order to compare the model output of chlorophyll and total suspended matter with the equivalent remote sensing product outputs, we adopted a common spatial and temporal resolution: the model state was output at 10.30 am and 1.30 pm to match the nominal overpass time of the MODIS/Terra and MODIS/Aqua sensors to minimise any difference due to tidal dynamic and resuspension.

The model output was regridded from the curvilinear grid to the 1 km remote sensing data raster grid and imported to ENVI format to be handled by the 'MODIS time series visualisation tool'.

Both the remote sensing products and biogeochemical products of chlorophyll and suspended matter only became available towards the end of this research in a format that allowed direct comparison. Here we report on the initial comparison carried out by a visual analysis of a series of maps for some representative dates chosen from the available set (28 January 2004 to 5 December 2004).

A more quantitative analysis is required in the future. However, as this is such an innovative research result, no off-the-shelf methodology is available for immediate application. Investment will be required in tools that can deal with the differing nature of these two chlorophyll and suspended matter data products (e.g. remote sensing data that covers a larger area, has significant random pixel dropouts—caused by clouds and quality flags in the MODIS data—versus a biogeochemical model output).

The initial comparison was performed as follows: each figure will present six maps: the CHL and TSM retrieval by the MIM algorithm are in the first row, the CHL and TSM as simulated by the biogeochemical model in the second row and the CHL and TSM retrieval by the NASA standard algorithm in the third row. To improve readability, the three CHL and TSM maps all have the same scale and colour bar.

Examples of agreement and disagreement between the two sets are described, and the possible reasons for the agreement and disagreement identified and discussed. Figures 4-2 to 4-8 show comparisons on six selected dates. An analysis of the more than 50 of these MODIS regional product images (representing a 13:30 overpass on any specific date with good MODIS imagery over 2004) with the simultaneous output of the biogeochemical model showed overall agreement in the range of concentrations for chlorophyll and TSM

(CDOM is not an output of the model). The six displayed daily images are selected to adequately represent the information in all the suitable MODIS/Aqua images over 2004. As the MODIS images tend to be clustered (around clear sky conditions) there is little difference from one MODIS image to the next day's image at 13:30, as the only major systematic change is the tidal cycle shift at 13:30 which progresses by half an hour to an hour each day.

6.3 Chlorophyll and TSM products comparison

A first comparison of the results for the new MIM algorithm-based maps, the biogeochemical (BGCM) maps and the standard global SEADAS CHL_Carder and TSM_Clark algorithm maps shows that the standard global SEADAS algorithm maps are the least similar to the two other products.

For the CHL_Carder maps the CHL is confused with CDOM and/or with the organic (or yellow-to-brown-coloured) component in the suspended matter.

For TSM the TSM_Clark algorithm underestimates TSM concentrations as the algorithm divides two blue-to-green spectral MODIS bands (a spectral band ratio) and thereby removes a lot of scattering information (as the spectral scattering in a short spectral range is highly correlated, whereas spectral absorption may not be correlated) which is the prime source for estimating TSM concentrations. Therefore, we will not discuss the standard global SEADAS CHL_Carder and TSM_Clark algorithm maps any further. These maps of standard global SEADAS CHL_Carder and TSM_Clark algorithm outputs are presented for the sake of illustration of the invalid nature of the information. Qin *et al.* (submitted) discuss the lack of validity in the standard global SEADAS CHL_Carder and TSM_Clark algorithm outputs thoroughly.

As already mentioned in Section 4.5, the MIM implementation to MODIS/Aqua images suffers from an 'over-cautious' flagging that limits the number of processed pixels, especially in the estuarine part of the bay. This is probably due to the necessity of CHL_MIM to use all the available MODIS bands for the inversion. Any error in any of these spectral bands causes a pixel to be flagged as 'error' and is coloured grey in Figures 6-2 to 6-8.

Before we discuss the initial comparison of the output results from the MODIS MIM processed images and the biogeochemical model outputs, it is useful to summarise some of the *a priori* issues that need to be understood to arrive at a correct interpretation of these comparison issues:

- Spatial boundaries set for the model were based on best information at that time (among others using the standard global SEADAS CHL_Carder and TSM_Clark algorithm outputs—which are now shown to be wrong).
- Neither the BGCM or the MIM outputs were able to be fully validated due to a lack of suitable *in situ* data covering all seasons and circumstances or due to most data being required to parameterise the model or the remote sensing MIM method.
- The BGCM outputs are purely mathematically calculated products based on processes and input data and parameterisation data. As such they contain no direct or indirectly measured information from the FE–KB physical system at each image overpass. The remote sensing images are based on an actual physics-based signal for the FE–KB system: the reflectance values of the water body at each satellite overpass time. The MIM-calculated chlorophyll and suspended matter concentrations are inferred water quality products, but are still directly linked with the reflectance measurement.
- In this comparison we assume that the BGCM and the MIM remote sensing output maps are two indirect estimates (hence not direct *in situ* measurements) of the variables in the FE–KB system. In this case it is not clear which is the dependent and which is the independent data source.

In the following comparison we presume that:

- The remote sensing images show the correct distribution of chlorophyll and suspended matter at the surface.
- The BGCM can estimate the vertical water column composition.
- The remote sensing images are not initially constrained by any presetting of spatial boundary conditions, whereas the BGCM is constrained by initial assumptions about boundary conditions.
- For rigorous validation we have insufficient *in situ* data covering all the environmental circumstances of the 50 images where we have both BGCM and MODIS output.

- The validation methods for both the BGCM and the MODIS MIM outputs are different, non-traditional (in the statistical validation sense) and probably require the development of a novel validation methodology.

For all the dates, both the biogeochemical model and the remote sensing MIM CHL image show a sharp transition between the zones of high and low chlorophyll concentration. Inherent to the nature of remote sensing satellite images, the spatial patterns of concentrations cover a much larger area and thus show the FE–KB system in context of the larger picture of the surrounding waters with, for example, interactions with the East Australia Current or longshore transport of chlorophyll and TSM.

Chlorophyll concentrations and distribution from the MODIS/Aqua MIM outputs ranged in general from similar to the biogeochemical model to twice as high as the biogeochemical model output (see summary of comparisons in Table 6-2). A comparison of the distribution (the patterns) of the chlorophyll concentrations in the FE–KB system vary from the same to completely different between the MODIS/Aqua MIM chlorophyll image and the BGCM chlorophyll output.

The CHL boundary conditions as assessed from the MODIS/Aqua MIM images vary from similar to quite different for the model. In most cases where the boundary conditions differ, the model has presumed lower boundary conditions than occur in reality.

Two distinct features are clear: there is a higher concentration of CHL in most MODIS/Aqua MIM images towards the north-west of Keppel Bay. These images indicate that there is a considerable chance of high near-coastal chlorophyll values that (perhaps) flow down the coast into Keppel Bay from further north. In some cases there is a significant lobe of CHL-rich water visible in the satellite images, that passes across the top (north) of Curtis Island, travels to the east and then after Curtis Island tends to turn south-east. The model does not show this pattern, although this may be a significant conduit of nutrient-rich waters not returning into Keppel Bay after each tidal cycle. If this is the case, then the nitrogen and phosphorous budget of the FE–KB system to the GBR lagoon as calculated by the model will be underestimated.

TSM from MODIS/Aqua MIM was in general similar to the biogeochemical model or up to 40% less at high concentrations (see summary of comparisons in Table 6-2).

A comparison of the spatial distribution of the TSM concentrations in the FE–KB system vary from similar to completely different between the MODIS/Aqua MIM

image and the BGCM output. Specifically the BGCM often predicts higher TSM concentrations towards the north-west of Keppel Bay while the MODIS/Aqua MIM TSM images do not show these high TSM values.

If we presume the MODIS MIM TSM images to be valid, comparison suggests that the boundary conditions set for the model are either correct or too low. In general the distribution varies from agreement to partial agreement to total disagreement between the MODIS/Aqua MIM TSM images and the biogeochemical model output.

In particular, remote sensing image products show some limitations of the biogeochemical model. The remote sensing image shows how the assumption of low chlorophyll concentration along the coast misrepresents the likely true situation. In other images it is clear that the initial boundary conditions were too low (they were among others derived from averaged global remote sensing products provided earlier on in the study that were not correct in retrospect).

The seven MODIS MIM image-to-biogeochemical model comparison dates (see Tables 6-1 to 6-3 and Figures 6-2 to 6-8) are well distributed across tidal phases. There is no apparent pattern in agreement/disagreement between the biogeochemical model and the MODIS/Aqua MIM outputs as related to tidal phase. This indicates other drivers are responsible for the mismatch between the spatial information in these two different information products (Webster and Robson (pers. comm.). Possible drivers that need to be reassessed are the wind forcing (for the BGCM input a 30-year climatological average was used) or improved East Australia Current forcing values.

Table 6-1. Date and time of overpass of the MODIS/Aqua satellite with respect to the tidal phase information during the relevant tidal cycle

Date	Low/high tide preceding MODIS/Aqua overpass	Tide @ MODIS/Aqua overpass (13:30)	Low/high tide after MODIS/Aqua overpass	Tidal excursion (in m) and rising or falling tide at overpass of MODIS/Aqua
7 March 2004 Halfway through falling tide	High of 5.30 m at 10:30	3.08 m	Low of 0.73 at 16:45	4.57 m (spring tide)
14 March 2004 Halfway through rising tide	Low of 1.99 m at 11:30	2.47 m	High of 3.36 at 17:15	1.37 m (Neap tide)
27 June 2004 Halfway through rising tide	Low of 1.22 m at 10:30	2.41 m	High of 4.03 at 17:15	2.81 m
24 July 2004 At high tide	Low of 1.18 m at 07:30	3.79 m	High of 3.81 at 16:00	2.63 m
8 October 2004 Halfway through rising tide	Low of 1.87 m at 11:30	2.46 m	High of 4.00 at 17:35	2.13 m
11 October 2004 At low tide	High of 4.08 m at 07:15	1.04 m (= low tide)	High of 4.68 m at 19:30	3.04 m (preceding overpass)
24 October 2004 Just after low tide	Low of 0.84 m at 12:45	1.00 m	High of 4.87 at 19:00	4.03 m (towards spring tide)

Table 6-2. Visual comparison of results for the MODIS/Aqua MIM CHL algorithm maps and the biogeochemical model (BGCM) output maps. See Table 6-1 for the relevant tidal cycle and Figures 6-2 to 6-8 for related images

Date	CHL concentration range similarity MODIS MIM and BGCM	CHL distribution similarity/deviation MODIS MIM and BGCM	Relative accuracy of model's boundary conditions	Additional comments
7 March 2004 Halfway through falling tide	MIM CHL twice as high as BGCM	No similarity	Too low	Along coast from N to S and across Curtis Island ,much higher levels of CHL in MIM image
14 March 2004 Halfway through rising tide	MIM CHL 20–30% higher than BGCM	Some similarity	Incorrect in north and across Curtis Island	Along coast from N to S and across Curtis Island, much higher levels of CHL in MIM image
27 June 2004 Halfway through rising tide	High similarity	High similarity	Correct	
24 July 2004 At high tide	Good similarity	Higher CHL in MIM to NW Keppel Bay	Correct	
8 October 2004 Halfway through rising tide	High similarity	MIM image shows higher CHL towards part of NW Keppel Bay and across Curtis Island to the east	Incorrect to NW Keppel Bay and to east across Curtis Island	The BGCM model tries to send a lobe of high CHL across Curtis Island to east but boundary conditions prevent lobe from continuing far enough
11 October 2004 At low tide	High similarity	Correct	Correct	
24 October 2004 Just after low tide	Similar	MIM image shows higher CHL towards part of NW Keppel Bay and across Curtis Island to the east	Incorrect to NW Keppel Bay and to east across Curtis Island	Similar to 8 October image and BGCM results

Table 6-3. Comparison of results for the MODIS/Aqua MIM TSM maps and the biogeochemical model output maps. See Table 6-1 for the relevant tidal cycle and Figures 6-2 to 6-8 for related images

Date	TSM concentration range similarity MODIS MIM and BGCM	Distribution similarity/deviation MODIS MIM and BGCM	Relative accuracy of model's boundary conditions	Additional comments
7 March 2004 Halfway through falling tide	MIM about 60% of levels by BGCM	Poor	Slightly too low	The MIM image shows much lower levels in NW Keppel Bay
14 March 2004 Halfway through rising tide	MIM about 60% of levels by BGCM	High similarity	Reasonable	
27 June 2004 Halfway through rising tide	High similarity	High similarity except for NW coastal area of KB where TSM BGCM levels are higher	Correct	
24 July 2004 At high tide	High similarity	MIM concentrations lower to NW in Keppel Bay	Correct	
8 October 2004 Halfway through rising tide	High similarity	MIM concentrations in NW Keppel Bay much lower	Correct	
11 October 2004 At low tide	High similarity in low concentration areas; few pixels in high concentration areas of BGCM	Correct	Correct	MODIS image at high angles (elongated pixels); few pixels in Keppel Bay
24 October 2004 Just after low tide	Below 12 mg L^{-1} similar; above 12 mg L^{-1} unknown as no MIM data in Keppel Bay	Low	Correct, except too low towards east of Curtis Island	Similar to 8 October image and BGCM results

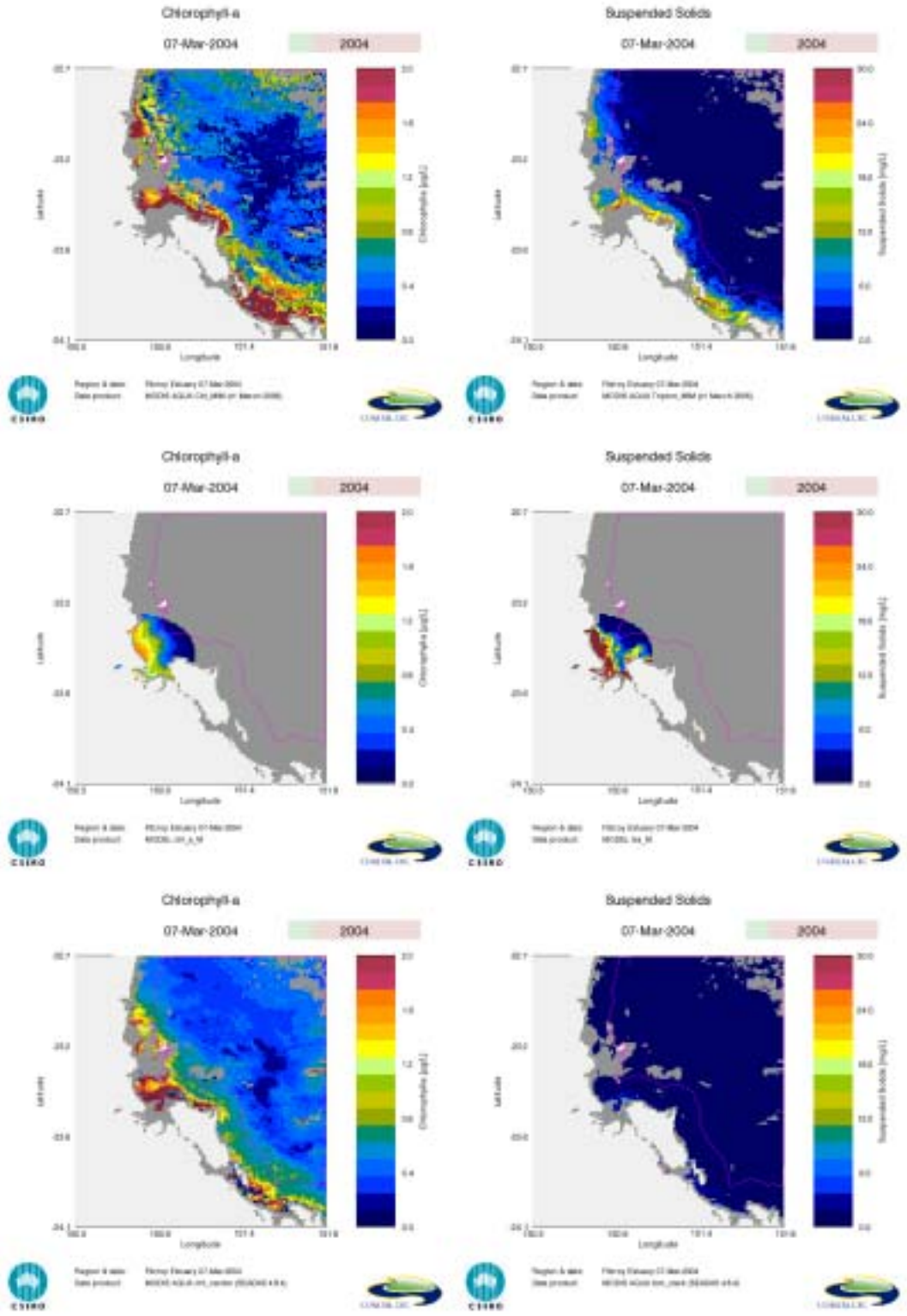

Figure 6-2. Comparison of the remote sensing products and model outputs for 7 March 2004 CHL and TSM retrieval by the MIM algorithm in first row; CHL and TSM as simulated by the biogeochemical model in second row; CHL and TSM retrieval by NASA global SEADAS algorithms in third row

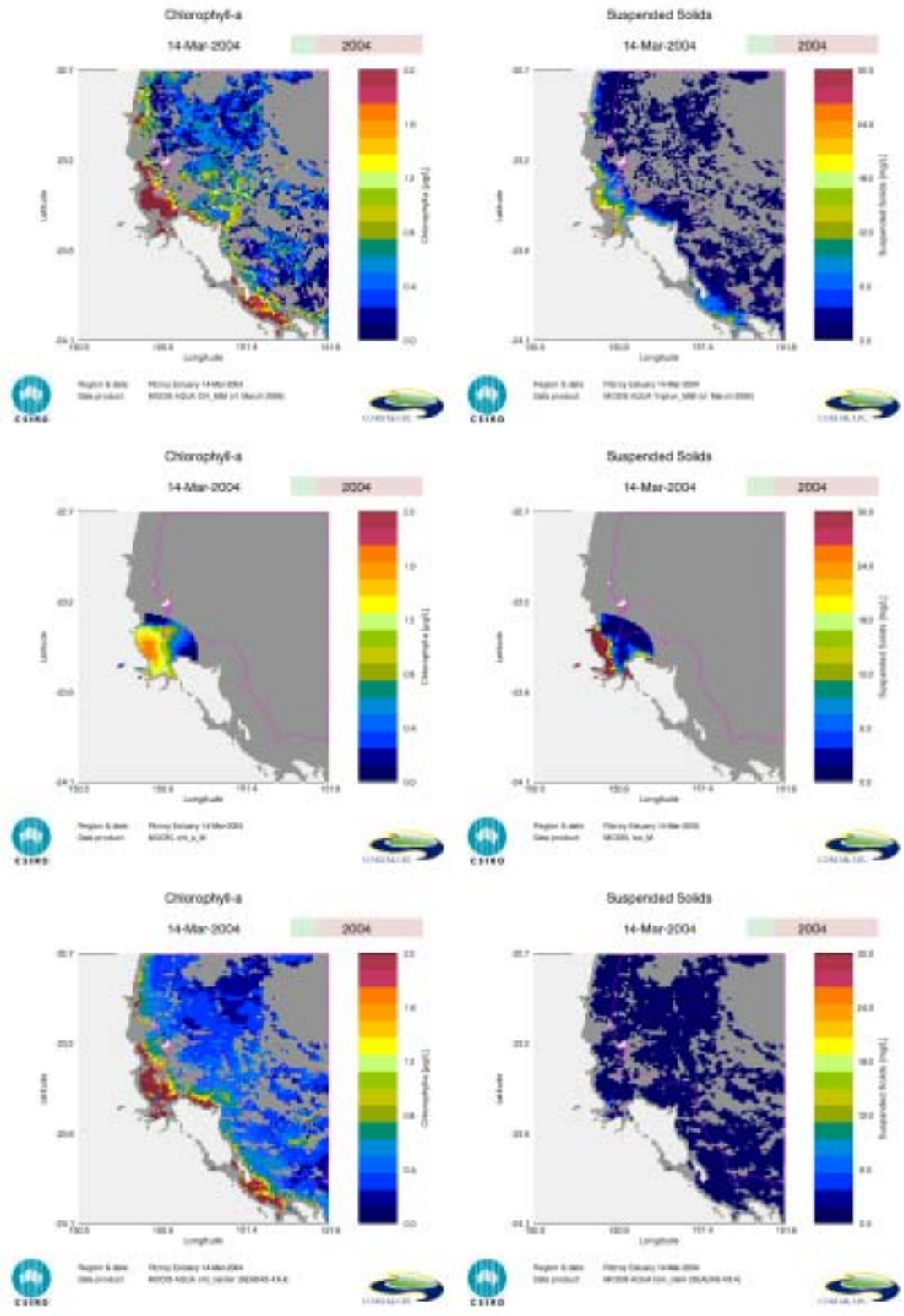

Figure 6-3. Comparison of the remote sensing products and model outputs for 14 March 2004 CHL and TSM retrieval by the MIM algorithm in first row; CHL and TSM as simulated by the biogeochemical model in second row; CHL and TSM retrieval by NASA global SEADAS algorithms in third row

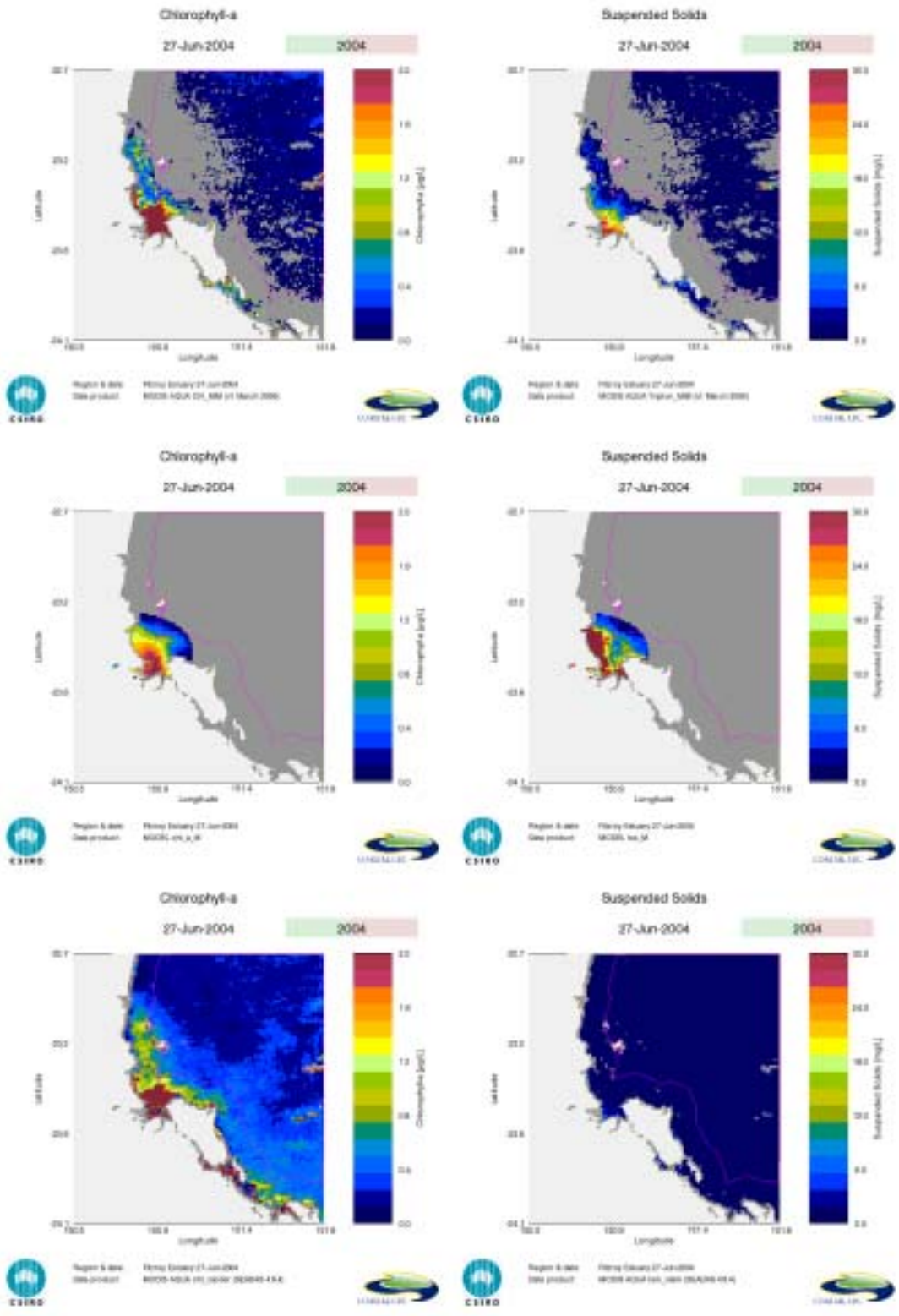

Figure 6-4. Comparison of the remote sensing products and model outputs for 27 June 2004 CHL and TSM retrieval by the MIM algorithm in first row; CHL and TSM as simulated by the biogeochemical model in second row; CHL and TSM retrieval by NASA global SEADAS algorithms in third row

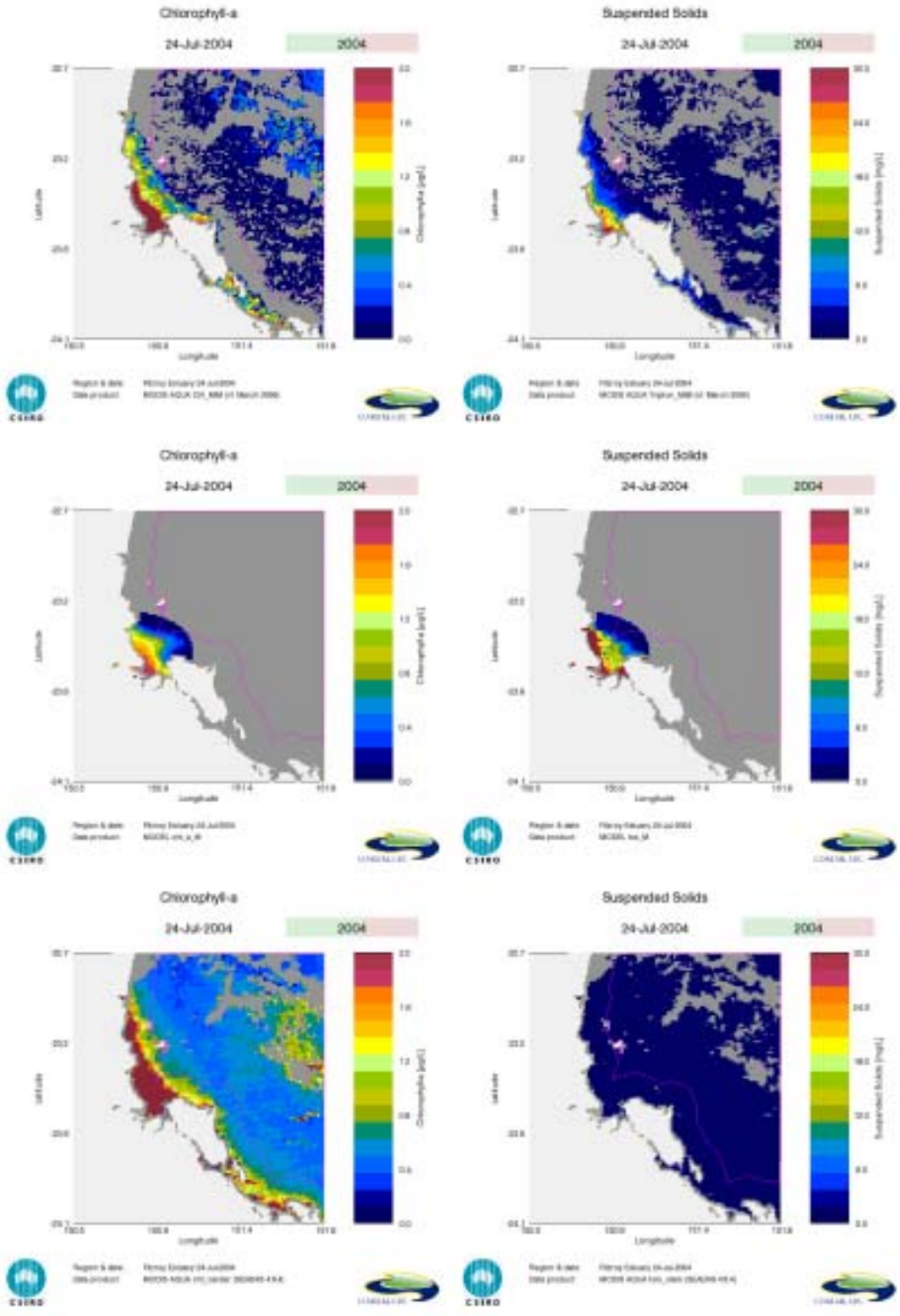

Figure 6-5. Comparison of the remote sensing products and model outputs for 24 July 2004 CHL and TSM retrieval by the MIM algorithm in first row; CHL and TSM as simulated by the biogeochemical model in second row; CHL and TSM retrieval by NASA global SEADAS algorithms in third row

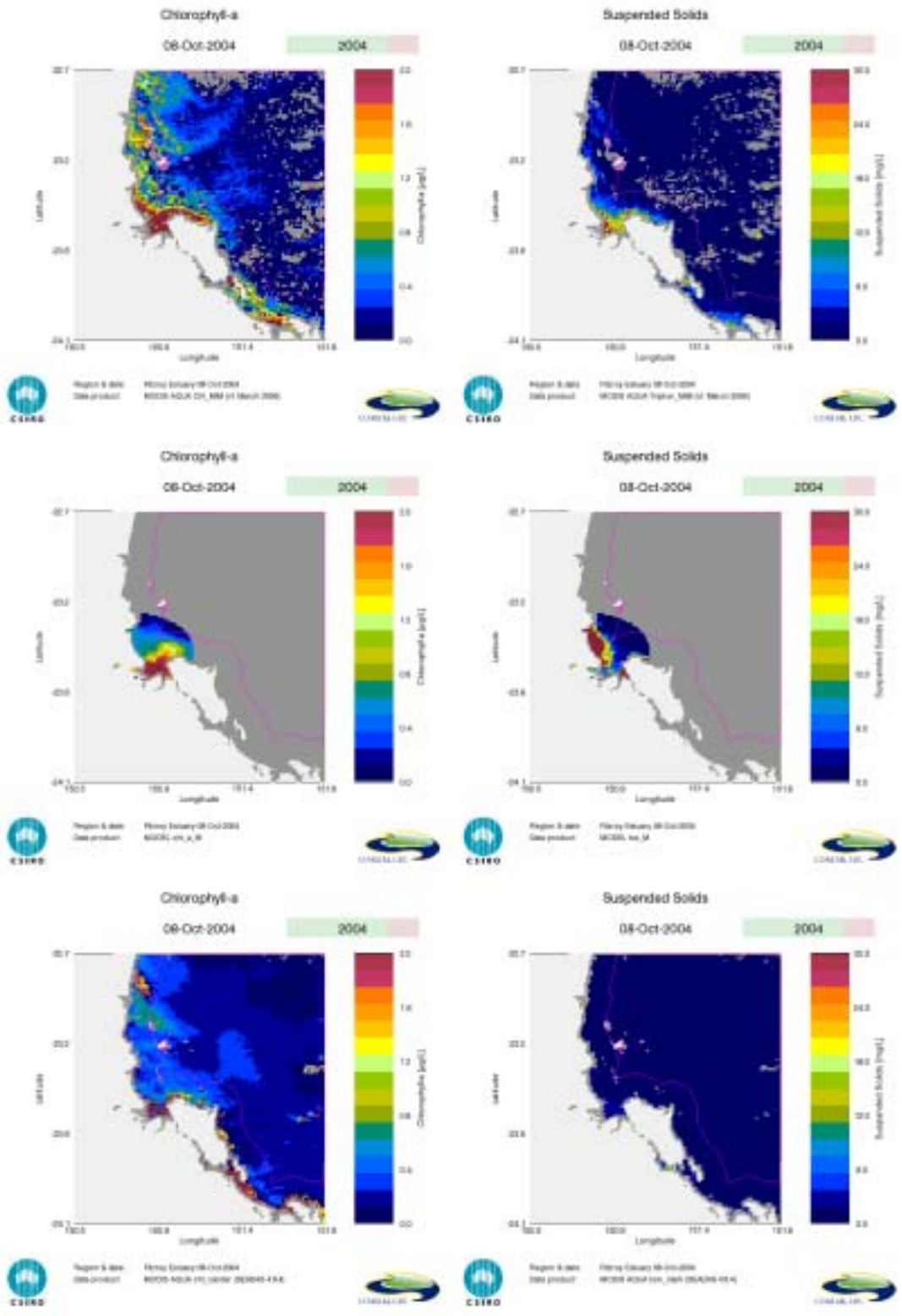

Figure 6-6. Comparison of the remote sensing products and model outputs for 8 October 2004 CHL and TSM retrieval by the MIM algorithm in first row; CHL and TSM as simulated by the biogeochemical model in second row; CHL and TSM retrieval by NASA global SEADAS algorithms in third row

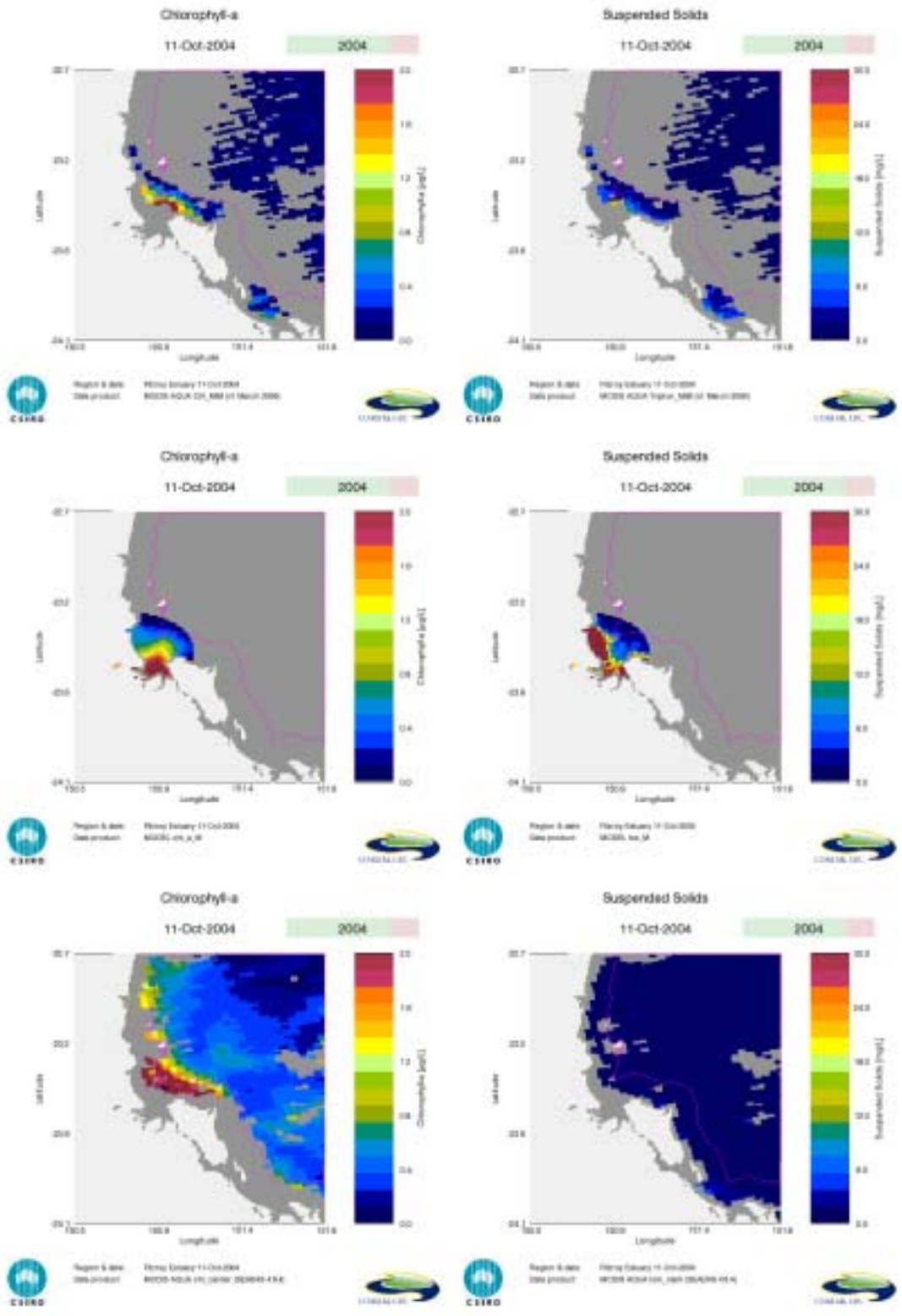

Figure 6-7. Comparison of the remote sensing products and model outputs for 11 October 2004 CHL and TSM retrieval by the MIM algorithm in first row; CHL and TSM as simulated by the biogeochemical model in second row; CHL and TSM retrieval by NASA global SEADAS algorithms in third row

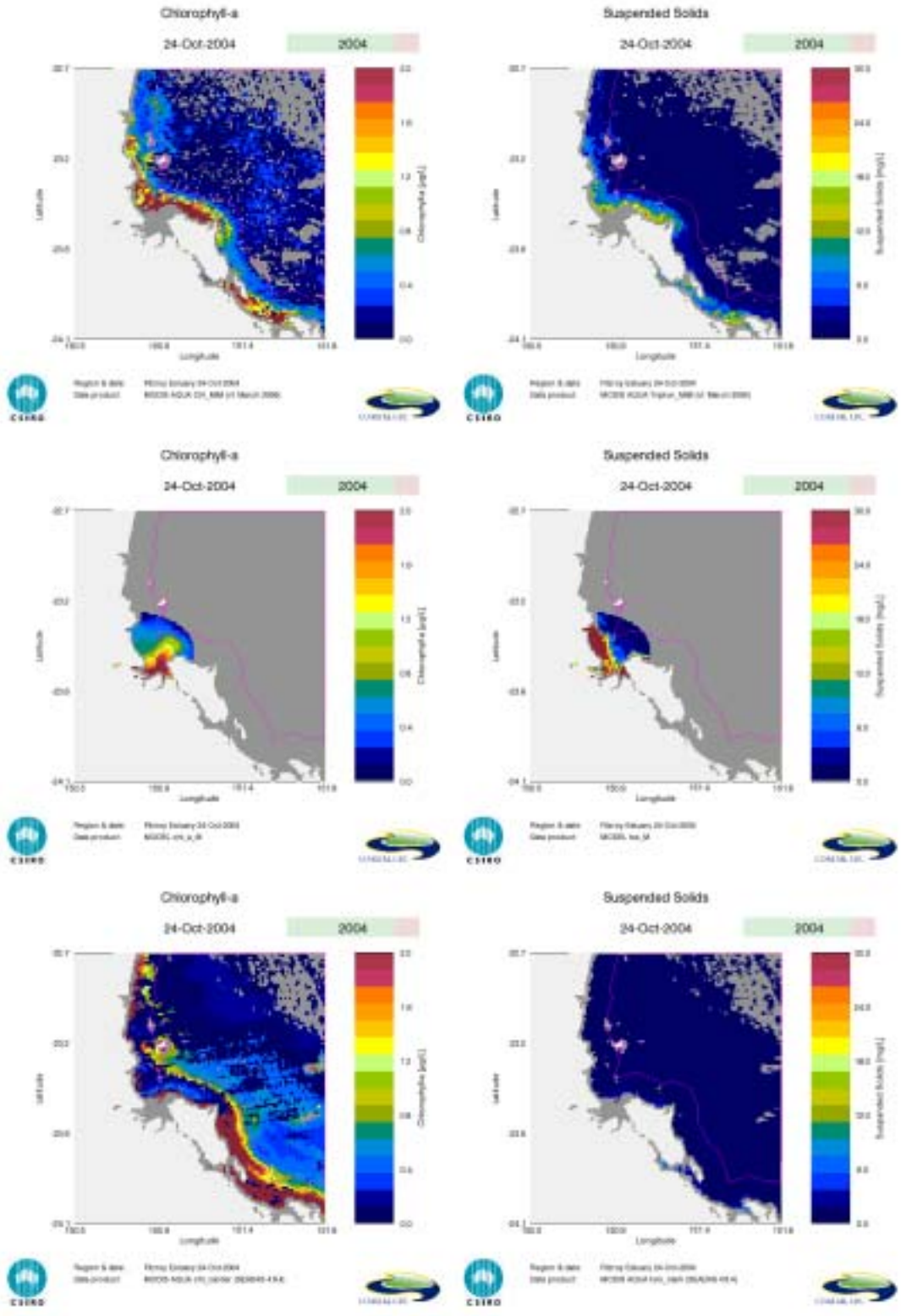

Figure 6-8. Comparison of the remote sensing products and model outputs for 24 October 2004 CHL and TSM retrieval by the MIM algorithm in first row; CHL and TSM as simulated by the biogeochemical model in second row; CHL and TSM retrieval by NASA global SEADAS algorithms in third row

7 Conclusion and recommendations

7.1 A new regional algorithm for processing MODIS data for chlorophyll and suspended matter using the matrix inversion method

The standard global algorithms provided by NASA for chlorophyll and total suspended matter (and coloured dissolved organic matter) produced through the standard SEADAS processing system are unreliable in complex coastal waters such as the Fitzroy Estuary–Keppel Bay system.

The newly developed matrix inversion method (MIM) for processing MODIS/Aqua images for chlorophyll, total suspended matter and coloured dissolved organic matter is robust and suitable for processing large amounts (hundreds or thousands) of images.

MODIS images processed through MIM inversion as was applied in this project have more data misses (MODIS image pixels excluded) compared to MODIS images processed with the standard algorithms. This is perhaps due to too stringent quality criteria for acceptance of pixels by the MIM inversion algorithms. We recommend a more thorough study into the criteria for flagging pixels as not suitable in the entire SEADAS processing package.

Remote sensing data from satellites such as MODIS is often from the same time of day, susceptible to prevailing cloudiness conditions and is therefore non-uniformly distributed throughout the year. Satellite images also may have part cloud cover and part visibility, or indeed may have some other errors throughout the scene causing ‘failed‘ pixels. Nevertheless satellite images are by far the cheapest and most spatially and temporally complete datasets available, when compared against any other measurement method.

Archives of MODIS-like satellite images are available from 1997 onwards (from SeaWiFS), from 1999 onwards from MODIS/Terra, from 2002 onwards for both MODIS/Aqua and MERIS. The MIM algorithm can easily be adapted and applied to all these satellite data sets thus giving a climatology of the FE–KB system from 1997 to present. The applicability to multiple sensors is another reason why it was well worth investing so much effort into developing regionally correct algorithms. As the same approach is applied to sensors with different ‘standard‘ algorithms (e.g. the MODIS and MERIS algorithms are based on entirely different inversion approaches: empirical versus neural networks) we can now access their comparable information with relative ease.

7.2 Comparing MIM estimates of chlorophyll and suspended matter values and distribution with the biogeochemical model output

The concentration ranges determined from the MODIS/Aqua MIM images and the output of the biogeochemical model are in a high level of agreement. As these two data products are produced independently of each other this is an indication that the two information sources are correct for concentration assessments, especially as the ranges in the FE–KB system are similar to those measured *in situ*. This could mean a significant shift in the requirements for a monitoring program in the FE–KB system: remote sensing using MODIS (or similar sensor data such as SeaWiFS and MERIS) for TSM and CHL (and other products such as Secchi disk transparency, turbidity, vertical attenuation of light and coloured dissolved organic matter concentrations) can provide the monitoring data at an unsurpassed temporal and spatial scale.

When the CHL and TSM dynamic in Keppel Bay is dominated by processes occurring at a larger scale, the model is unable to appropriately recreate the spatial distribution of those processes and the measured remote sensing–derived values versus the biogeochemical model calculated values show divergence.

The remote sensing image shows how the assumption by the model of low chlorophyll concentration along the coast misrepresents the likely true situation. In some cases there was a significant lobe of chlorophyll-rich water visible in the satellite images, that passes across the top (north) of Curtis Island, travels to the east and then after Curtis Island tends to turn south-east. The model does not show this pattern, although this may be a significant conduit of nutrient-rich waters not returning to Keppel Bay after each tidal cycle. If this is the case, then the nitrogen and phosphorous budget of the FE–KB system to the GBR lagoon as calculated by the model will be underestimated.

The biogeochemical model output can be improved (forced/nudged) by the remote sensing–derived information to become more representative of the FE–KB system, in the first instance by improving the boundary conditions or expanding the boundary.

An improved biogeochemical model (with all its output variables) and the 40 (minimum amount) to 100 (maximum current amount) of satellite images per year (with its more limited set of output variables), can in combination give a management-relevant set of water quality indicators for the FE–KB system at a relatively low cost now that both the regional algorithms and the biogeochemical model have been developed.

The satellite images can cover a much larger area than shown here (typically up to 1000 km^2); the biogeochemical model can also become as large as required (although necessarily at a coarser scale). A nested approach of larger scale to finer scale remote sensing and biogeochemical modelling would be appropriate to model and manage much larger parts of the Queensland coast. It would also put the FE–KB system into a much larger context as is likely to be required to understand broader-scale issues affecting the FE–KB system. Specifically this research showed that significant amounts of chlorophyll may enter the FE–KB system from the north, and there could be larger amounts of export across Curtis Island to the south-east.

The comparison between biogeochemical model outputs and regionally valid satellite images of TSM and chlorophyll is a first step towards data integration of these two sources of information. The next step should be to confirm this preliminary analysis with a more rigorous statistical comparison of the datasets. This will involve the use of advanced geostatistical and temporal statistical methods that can deal with these two very different data sets in their time and space domains. A next step is to incorporate any *in situ* measurements into these two innovative methods. Alternatively the results of these two independent assessment methods can be used to devise an optimum *in situ* sampling program that has a maximum cost–benefit ratio.

The biogeochemical model (together with the underlying hydrodynamic model) has a 24 hour/7days a week/52 weeks a year capacity at almost any desired interval and for many more variables than remote sensing can deliver. However, the concentrations and patterns may not be real or correct. The biogeochemical model has a three-dimensional depth component whereas the remote sensing information is from the top layer of water only, varying from the top 20 cm in the Fitzroy River to the top one or two metres in the estuary to more than five or seven metres deep into the Keppel Bay and GBR waters.

The biogeochemical model can extrapolate the top layer, remote sensing–based information to the deeper parts of the water column. Therefore, it is recommended to expand the comparison of the biogeochemical model output and the satellite image–derived information to all the variables that both methods can determine—not only chlorophyll and TSM but also the optically active CDOM (an inverse tracer of salinity as well as a conservative carbon content component), measurement of cyanobacteria such as *Trichodesmium* and the physically based light variables of turbidity, Secchi disk transparency, vertical attenuation coefficient of diffuse light.

It is recommended to begin the process of data assimilation, which is another step of sophistication above data integration. Data assimilation is the process in which the information from remote sensing interacts with the biogeochemical model and vice versa to obtain improved information from both. One example is that the model is forced/nudged/improved to adopt the patterns that remote sensing images demonstrate repeatedly under certain standard conditions. This will lead to better predictions. Another example is to apply boundary conditions from remote sensing to improve the biogeochemical model parameterisation.

The improved biogeochemical model can also improve the remote sensing by understanding what happens under sub-optimal remote sensing conditions when large parts of the image are influenced by factors such as bushfire smoke, jet contrails, wind blown dust, etc. Also the improved biogeochemical model can aid in establishing where bottom visibility may occur in a remote sensing image (which can then be corrected for this effect). Another example is using the vertical attenuation of light from the satellite images to give a more realistic approximation of the photosynthetically available light in the biogeochemical model.

In the long term, linking quantitative remote sensing and hydrological, biogeochemical and hydrodynamic models for the Fitzroy catchment to estuary through to Keppel Bay would provide the most powerful tool for understanding and managing the entire Fitzroy catchment to Keppel Bay and GBR receiving waters.

References

Aas, E. (1997) Two-stream irradiance model for deep waters, *Applied Optics*, 26: 2095-2101.

Blondeau-Patissier, D., Tilstone, G.H., Martinez-Vicente, V. & Mooreet, G.F. (2004) Comparison of biophysical marine products from SeaWiFS, MODIS and a bio-optical model with *in situ* measurements from Northern European waters. *Applied Optics,* 6: 875–889.

Brando, V.E. & Dekker, A.G. (2003) Satellite hyperspectral remote sensing for estimating estuarine and coastal water quality. *IEEE Transactions on Geoscience and Remote Sensing,* 41(6): 1378–1387.

Bricaud, A., Morel, A., Babin, M., Allali, K. & Claustre, H. (1998) Variations of light absorption by suspended particles with chlorophyll *a* concentration in oceanic (case 1) waters: Analysis and implications for bio-optical models. *Journal of Geophysical Research, 103:* 31033–31044.

Brodie, J. & Mitchell, A.W. (1992) Nutrient composition of the January 1991 Fitzroy River flood plume. *Workshop on the impacts of flooding,* ed. G.T. Byron. Workshop Series No. 17, Great Barrier Reef Marine Park Authority, pp. 56–74.

Dekker, A.G., Brando, V.E., Anstee, J.M., Fyfe, S., Malthus, T.J.M. & Karpouzli, E. (2006) Remote sensing of seagrass ecosystems: Use of spaceborne and airborne sensors. Chapter 15 in: *Seagrass biology, ecology and conservation*, A. Larkum, B. Orth & C. Duarte (eds), Springer Verlag, Germany, pp. 630.

Dekker, A.G. & Phinn, S. (eds) (2005) *Final report – Fitzroy Estuary and Port Curtis remote sensing tasks* (FE2 and PC2). Cooperative Research Centre for Coastal Zone, Estuary and Waterway Management, Brisbane.

Dekker, A.G., Brando, V.E., Anstee, J.M., Pinnel, N., Kutser, T., Hoogenboom, H.J., Pasterkamp, R., Peters, S.W.M., Vos, R.J., Olbert, C. & Malthus, T.J. (2001) Imaging spectrometry of water. Chapter 11 in: *Imaging spectrometry: Basic principles and prospective applications – Remote sensing and digital image processing*, v. IV. Dordrecht, Kluwer Academic Publishers, pp. 307–359.

Furnas, M. (2003) *Catchments and corals: Terrestrial runoff to the Great Barrier Reef*. CRC/AIMS, Townsville, Australia.

Herzfeld, M., Andrewartha, J.R., Sakov, P. & Webster, I. (2005) *Numerical hydrodynamic modelling of the Fitzroy Estuary*. Cooperative Research Centre for the Coastal Zone, Estuary and Waterway Management, Brisbane.

Hoogenboom, B.W., Hesper, R., Tjeng, L.H. & Sawatzky G.A. (1998) *Charge transfer and doping-dependent hybridization of C_{60} on noble metals.* Solid State Physics Laboratory, Materials Science Centre, University of Groningen, Nijenborgh 4, 9747 AG Groningen, The Netherlands

Jeffrey, S.W., Mantoura, R.F.C. & Wright, S.W. (1997) *Phytoplankton pigments in oceanography*. UNESCO, Paris.

Lee, Z.., Carder, K.L.., Mobley, C.D., Steward, R.G. & Patch, J.F. (1999) Hyperspectral remote sensing for shallow waters: 2. deriving bottom depths and water properties by optimization. *Applied Optics*, 38(18): 3831–3843.

Lee, Z., Kendall, L.C., Chen, R.F. & Peacock, T.G. (2001) Properties of the water column and bottom derived from airborne visible imaging spectrometer (aviris) data. *Journal of Geophysical Research*, 106(C6): 11639–1165.

Margvelashvili, N., Herzfeld, M. & Webster, I. (2005) *Modelling of fine sediment transport in Fitzroy Estuary and Keppel Bay*. Technical Report No. 39, Cooperative Research Centre for Coastal Zone, Estuary and Waterway Management, Brisbane.

Mobley, C.D. (1994) *Light and water: Radiative transfer in natural waters*. Academic Press, London, 592 pp.

Murray, A.G. & Parslow, J.S. (1999) Modelling of nutrient impacts in Port Phillip Bay – A semi-enclosed marine Australian ecosystem. *Marine and Freshwater Research*, (50): p 597–611.

Oubelkheir, K., Dekker, A.G., Clementson, L., Webster, I., Ford, P., Radke, L. and Daniel, P. (2006) Using inherent optical properties to investigate biogeochemical dynamics in a tropical macrotidal coastal system; *Journal of Geophysical Research*, 111, C07021,15 pp.

Phinn, S., Roelfsema, C., Scarth, P., Dekker, A., Brando, V., Anstee, J. & Marks, A. (2004) *An integrated remote sensing approach for adaptive management of complex coastal waters: The Moreton Bay Case Study.* Technical Report No. 23. 142 pp. Cooperative Research Centre for Coastal Zone, Estuary and Waterway Management, Brisbane.

Press, W.H. Teukolsky, S.A., Vetterling, W.T. & Flannery B.P. (1992) *Numerical recipes in C: The art of scientific computing,* Second edition, Cambridge University Press.

Qin, Y., Brando, V., Dekker, A., Oubelkheir, K. & Blondeau-Patissier, D., (submitted) *Validity of SEADAS water constituent retrieval algorithms in Australian tropical coastal waters*.

Radke, L., Ford, P., Webster, I., Atkinson, I. & Oubelkheir, K. (2006) *Keppel Bay: Physical processes and biogeochemical function.* Technical report 34, Cooperative Research Centre for Coastal Zone, Estuary and Waterway Management, Brisbane.

Robson, B.J., Rosebrock, U., Webster, I.T., Herzfeld, M. & Margvelashvili, N. (2006) *Biogeochemical modelling and nitrogen budgets for the Fitzroy Estuary and Keppel Bay.* Technical report 40, Cooperative Research Centre for the Coastal Zone, Estuary and Waterway Management, Brisbane.

Stevens, A., Brando, V.E., Dekker, A.G., Hodge, J., Farthing, B., Mengersen, K., Oubelkheir, K. & Qin, Y. (submitted) *Remotely-sensed monitoring of chlorophyll and suspended sediment in the coastal waters of the wet tropics region: A demonstration project with national application.* Report to the Department of Environment and Heritage, Canberra.

Webster, I., Atkinson, I., Bostock, H., Brooke, B., Douglas, G., Ford, P., Hancock, G., Herzfeld, M., Leeming, R., Lemckert, C., Margvelashvili, N., Noble, B., Oubelkheir, K., Radke, L., Revill, A., Robson, B., Ryan, D., Schacht, C., Smith, C., Smith, J., Vicente-Beckett. V. & Wild-Allen, K. (2006) *The Fitzroy contaminants project – A study of the nutrient and fine-sediment dynamics of the Fitzroy Estuary and Keppel Bay*. Technical report 42, Cooperative Research Centre for Coastal Zone, Estuary and Waterway Management, Brisbane.

Glossary of terms and acronyms used

Absorption coefficient	Measurement of the amount of sunlight and skylight absorbed per metre depth of water
Air–water interface	Ocean–atmosphere boundary which alters the direction and magnitude of sunlight and skylight
Analytical modelling	Image processing approach used to estimate biophysical properties (e.g. total suspended sediment concentration) by applying radiative transfer equations to image data
Apparent optical properties (AOPs)	Apparent optical properties of water—those dependent on the strength and direction of incident sunlight and skylight, e.g. reflectance
Atmospheric correction	Image processing approach used to remove atmosphere scattering and absorption effects from image data so the signal remaining is that emanating from the air–water interface or from the land surface (thus not from the top of the atmosphere)
Attenuation	Reduction of true reflectance or radiance levels with increasing depth in the water column due to absorption and scattering effects per metre depth of water
Backscattering coefficient	A measure of the proportion of light that will be backscattered—dependent on particle size, composition and shape per metre depth of water
Beam attenuation coefficient	Measurement of the amount of light reduction by a collimated beam of light per metre depth of water
Bio-optical modelling	Application of radiative transfer–based models to calculate light interactions in natural water to estimate water column constituents from remotely sensed data
Biophysical properties	Biological and physical properties of an environment
CDOM	Coloured dissolved organic material
CHL	Chlorophyll
Colour palette	Colour table applied to an image to enhance information visibility
CSIRO	Commonwealth Scientific and Industrial Research Organisation
C-WOMBAT-c	Coastal Waters and Ocean MODTRAN-4 based atmospheric correction software
Diffuse skylight	Sunlight that has been scattered by aerosol, dusts and clouds, and is not in a direct beam from the sun
DIN	Dissolved inorganic nitrogen
DIP	Dissolved inorganic phosphorus
DOC	Dissolved organic carbon
DON	Dissolved organic nitrogen
DOP	Dissolved organic phosphorus

Downwelling irradiance	Sunlight and skylight incident upon a surface from all viewing angles
EOS	Earth Observation Sensor (NASA mission)
FE–KB	Fitzroy Estuary–Keppel Bay
GBR	Great Barrier Reef
Geometric correction or georeferencing	The process of converting an image into a form where each pixel has a projection, datum and coordinate, enabling it to be integrated with other spatial data
GES–DAAC	Global Environmental Services Data Administration and Archiving Center
HDF	Hierarchical data format
Hydroscat-6	Instrument for measuring the backscattering coefficient of water bodies at a six wavelengths
Hyperion	Experimental satellite-borne hyperspectral imaging sensor with 30 m pixels and 196 spectral bands mounted on the EO-1 platform
Hyperspectral	A device is hyperspectral if it records reflected or emitted light using (usually >10), narrow spectral (cf. multispectral) bandwidths covering the entire wavelength range required
Ikonos	Commercially operated high spatial resolution (4 m) multispectral and panchromatic (1 m) satellite imaging sensor
Image pixel	Smallest spatial sampling unit of an imaging sensor to measure reflected or emitted energy from the surface of the earth
Inherent optical domain	An area of water exhibiting similar specific absorption and specific scattering properties
Inherent optical properties (IOPs)	Properties of the water column that do not change with illumination strength and direction, i.e. absorption and (back)scattering coefficients
Irradiance reflectance	A ratio of (upwelling) reflected sunlight and skylight measured over all directions to incident (downwelling) sunlight and skylight
Kd	Vertical diffuse attenuation coefficient—an estimate of the amount of light attenuated by water per metre depth of water
Matrix inversion method (MIM)	A mathematical solution to invert bio-optical model equations to estimate concentrations of water column constituents
MODIS	Moderate resolution imaging spectrometer
Multi-date normalisation	An image correction approach used to remove the distorting effects of different types of atmospheric conditions over an image of the same area collected on different dates
Multi-spectral	An image data collection system where reflected or emitted energy is measured in <10 broad discontinuous spectral bands
Multi-temporal	Data that has been collected for the same area over a series of successive dates
NAPM	Non-algal particulate matter
NASA	(US) National Aeronautics and Space Administration

Near infra red (NIR)	The non-visible 700–1000 nm portion of the electromagnetic radiation (EMR) spectrum
Normalised difference vegetation index	A normalised ratio transformation using the red and NIR pixel values which is related to vegetation cover
Normalised water leaving radiance (nLw)	Atmospheric and air–water interface correction of image data produces the upwelling radiance from the water surface normalised with respect to viewing and illumination angles
NSIDC	National Snow and Ice Data Center
Planimetric projection	A map projection where each map element is at its true location on the ground (cf. aerial photography and some satellite images which have a perspective projection)
PN	Particulate nitrogen
POC	Particulate organic carbon
Point source integrating cavity absorption meter (PSICAM)	A device for measuring absorption properties of water samples based on spectrometer measurements of a water sample within a diffuse light environment
PP	Particulate phosphorus
Pseudo-invariant features (*PIF)*	Landscape features that retain the same reflectance over time and can be used for image calibration
Radiative transfer modelling approach	All radiative transfer numerical models compute radiance distributions and related quantities (irradiance, reflectance, diffuse attenuation functions, etc.) in the water column as a function of the water absorption and scattering properties, the sky and air–water interface conditions and the bottom boundary conditions
Radiometric correction	Conversion of image pixel digital numbers from a relative scale (usually volts in a detector) to an absolute physical units scale (e.g. radiance)
Radio-sonde data	Vertical profile through the atmosphere of temperature and humidity, used for atmospheric correction
Reef Plan	(Great Barrier) Reef Water Quality Protection Plan
*Reflectance **or** spectral signature*	Ratio of upwelling radiance to downwelling irradiance on a target, that is, its characteristic reflectance response
Remote sensing reflectance or R(0-)	Atmospheric and air-water interface correction of image data produces the ratio of upwelling radiance from the water surface to downwelling irradiance just below the water surface
SD	Secchi disk
Secchi depth	Commonly used approach to measure the clarity of a water body by dropping a black/white disk and noting the depth at which the black and white are no longer distinguishable
SIOPs	Specific inherent optical properties
Spatial resolution	A measure of the scale of the smallest feature able to be detected on an image

Spectral angle mapping	An image classification approach used to group pixels with similar reflectance signature
Spectral signature	See *Reflectance*
SST	Sea surface temperature
Striping effects	Artefacts in Landsat images due to scanner or detector variations (in the case of Landsat 5 TM every 16th line)
Substrate types	Types of material found on seafloor: sand, rock, seagrass, algae, etc (the exact terminology is substratum)
Subsurface irradiance reflectance R(0-)	Ratio of upwelling to downwelling irradiance just below the water surface
Suspended sediment	Sediment particles that are floating in suspension (as opposed to dissolved) in the water column
Total suspended material (TSM)	All particulate matter suspended in the water column that does not pass through a 0.7 micron glass fibre filter (effective pore size 0.45 micron)
Tripton	The non-algal part of TSM
Underwater light climate	A physics-based description of how light behaves in a water column
Upwelling irradiance	A measurement taken using a field spectrometer with the sensor head pointing down to capture upwards directed (= reflected from the water column or substrate) direct and diffuse light over all directions
Water quality parameters	Biological and physical properties of the water column that have been adopted by scientific and management agencies as indicative of the condition of a water body, for example, Secchi depth, chlorophyll and total suspended sediment concentration
WQIPs	Water quality improvement plans